INFORMATION TO USERS

This manuscript has been reproduced from the microfilm master. UMI films the text directly from the original or copy submitted. Thus, some thesis and dissertation copies are in typewriter face, while others may be from any type of computer printer.

The quality of this reproduction is dependent upon the quality of the copy submitted. Broken or indistinct print, colored or poor quality illustrations and photographs, print bleedthrough, substandard margins, and improper alignment can adversely affect reproduction.

In the unlikely event that the author did not send UMI a complete manuscript and there are missing pages, these will be noted. Also, if unauthorized copyright material had to be removed, a note will indicate the deletion.

Oversize materials (e.g., maps, drawings, charts) are reproduced by sectioning the original, beginning at the upper left-hand corner and continuing from left to right in equal sections with small overlaps.

Photographs included in the original manuscript have been reproduced xerographically in this copy. Higher quality 6" x 9" black and white photographic prints are available for any photographs or illustrations appearing in this copy for an additional charge. Contact UMI directly to order.

UMI®

NOTE TO USERS

This reproduction is the best copy available.

UMI®

UNIVERSITY OF ALBERTA

Analytical and Numerical Modelling of Transient Convective Transfers
on SAGD Performance

by

Luong T. Doan $\copyright$

A Thesis Submitted To The Faculty of Graduate Studies and Research
in Partial Fulfillment of The Requirements for The Degree of Doctor of Philosophy

in

Petroleum Engineering

Department of Civil and Environmental Engineering

Edmonton, Alberta
Spring 2001

The author has granted a non-exclusive licence allowing the National Library of Canada to reproduce, loan, distribute or sell copies of this thesis in microform, paper or electronic formats.

The author retains ownership of the copyright in this thesis. Neither the thesis nor substantial extracts from it may be printed or otherwise reproduced without the author's permission.

L'auteur a accordé une licence non exclusive permettant à la Bibliothèque nationale du Canada de reproduire, prêter, distribuer ou vendre des copies de cette thèse sous la forme de microfiche/film, de reproduction sur papier ou sur format électronique.

L'auteur conserve la propriété du droit d'auteur qui protège cette thèse. Ni la thèse ni des extraits substantiels de celle-ci ne doivent être imprimés ou autrement reproduits sans son autorisation.

0-612-60286-9

Canada

UNIVERSITY OF ALBERTA

LIBRARY RELEASE FORM

NAME OF AUTHOR   Luong T. Doan

TITLE OF THESIS   Analytical and Numerical Modelling of Transient
Convective Transfers on SAGD Performance

DEGREE   Doctor of Philosophy   ©

YEAR THIS DEGREE GRANTED   2001

Permission is hereby granted to THE UNIVERSITY OF ALBERTA LIBRARY to reproduce single copies of this thesis and to lend or sell such copies for private, scholarly or scientific research purposes only.

The author reserves other publication rights, and neither the thesis nor extensive extracts from it may be printed or otherwise reproduced without the author's written permission.

(SIGNED) _Joantheluong_

PERMANENT ADDRESS:
2933 - 111 B STREET
EDMONTON , AB
_T6J - 4R5_

DATED _NOVEMBER 24th /2000_

UNIVERSITY OF ALBERTA

FACULTY OF GRADUATE STUDIES AND RESEARCH

The undersigned certify that they have read, and recommend to the Faculty of Graduate Studies and Research, for acceptance, a thesis entitled Analytical and Numerical Modelling of Transient Convective Transfers on SAGD Performance submitted by Luong T. Doan in partial fulfillment of the requirements for the degree of Doctor of Philosophy in Petroleum Engineering.

Professor S.M. Farouq Ali (Supervisor)
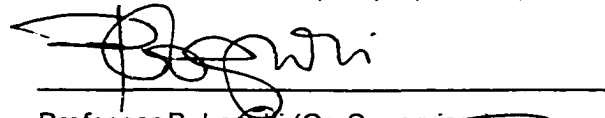
Professor B. Lepski (Co-Supervisor)
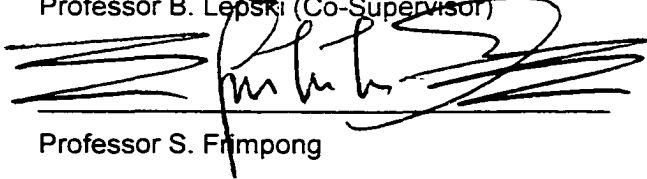
Professor S. Frimpong

Professor M. Pooladi-Darvish
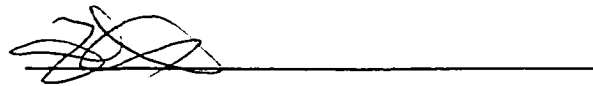
Professor Z. Xu

Professor A. Kantzas (External Examiner)

Date August 15, 2000

Abstract

The steam-assisted gravity drainage (SAGD) method has shown promise for efficiently recovering many heavy oil and oil sand reservoirs in Canada. In this study, a comprehensive review of thermal recovery literature enabled a comparison of different approaches to simulate transport processes in various steam injection recovery processes. Studies by Butler and co-workers on the SAGD subject served to explain the temperature distribution in the reservoir ahead of the steam zone, and how it influenced oil drainage rate.

A new analytical model was developed to simulate the expanding steam zone in the SAGD process. This new model was based mainly on the *Stefan Phase-Change problem*, and incorporated convective transfers taking place in the reservoir. These convective heat transfers included heat losses to the cap and base rock, and heat removed from the reservoir in the produced fluid stream. A rigorous mathematical solution was obtained for this new analytical SAGD model, which enabled the steam zone interface position and velocity to be determined at different times. Results from the new SAGD analytical model agreed mostly with results obtained from CMG's STARS™ thermal simulator, and results calculated from Butler's models. The agreement in the oil production rate between the new analytical model and STARS™ simulator was good for the middle-time period. Difference in the predicted oil production rates in the early-time period was due to the assumption that slope drainage is present from the start of the process by the proposed analytical model. Different external boundary conditions led to the difference in the predicted oil production rates for the new analytical model and the simulator in late-time period.

Results from the new analytical SAGD transient model agreed with corresponding results calculated from Butler's models. The steam zone interface velocity predicted by the new analytical model at different times agreed quite closely with those calculated by Butler's LinDrain (1994) model, with the agreement being closer in later-time periods. Oil production rate predicted by the new analytical model was less than those predicted by the TANDRAIN model, and Butler's 1985 model. The reason was believed to be due to the heat loss to cap rock and base rock, and due to heat removed due to fluid production from the reservoir; these losses are accounted for in the new analytical model.

After the new transient analytical model was validated, it was used to investigate the effects of flow potential and thermal diffusivity on the SAGD process. The results in these cases showed that the steam zone advanced further into the reservoir for low fluid production potential and high thermal diffusivity. In the first case, low fluid production potential resulted in less heat being removed from the reservoir, and hence, more heat accumulated inside the reservoir and contributed to the forward movement of the steam zone. In the second case, high thermal

diffusivity value promoted the expansion of the steam zone into the reservoir. Effects of a water sand in communication with the oil reservoir on SAGD performance were also investigated, using CMG's STARS™ simulator. The presence of a bottom water layer was determined to have a lesser impact on recovery than the overlying water layer case. Oil recovery was determined to decrease with increasing water layer thickness. Increasing the areal coverage of the bottom water layer resulted in only a slightly reduced recovery as compared with the confined bottom water layer. However, increasing the areal coverage of the overlying water layer severely reduced the recovery efficiency of the process, as heat was diverted into the overlying water zone.

Acknowledgments

The author wishes to thank Dr. Quang Doan, his brother, for the guidance and support throughout the course of this study. Thanks are also extended to Dr. Mustafa Oguztoreli for his suggestions and many hours of discussion on the formulation of the problems.

The encouragement and support from his family will always be remembered.

The encouragement by Mr. Brian Weatherill, Mr. Bob Pearson and Mr. Hank Baird at Adams Pearson and Associates Inc. is appreciated. His close friends, Mr. T. Chowdhury and Mr. H. Ho, provided solid moral support during the course of this study.

The author was able to use STARS^{TM} simulator for part of the work in this thesis; this was possible due to the donation of reservoir simulators by the Computer Modelling Group Ltd., Calgary to the Petroleum Engineering program at the University of Alberta for teaching and research purposes.

Finally, the author also wishes to acknowledge the support from his supervisor and co-supervisor.

TABLE OF CONTENTS

List of Tables

List of Figures

Nomenclature

C	rock heat capacity, m/Lt^2T [kJ/kg.K]
g	gravitational acceleration constant, L/t^2 [m/s^2]
h	enthalpy per unit mass, L^2/t^2 [kJ/kg]
H	height of the reservoir, L [m]
k	reservoir permeability, L^2 [m^2]
K	rock thermal conductivity, mL/t^3T [kJ/m.d.K]
L	length of horizontal well, L [m] or
	latent heat of vaporization, L^2/t^2 [kJ/kg]
m	parameter used to define viscosity-temperature relationship
M	volumetric heat capacity, m/Lt^2T [kJ/m^3.K]
q	oil drainage rate, L^3/t [m^3/s]
S	saturation, dimensionless
T	temperature, T [K]
t	time, t [s]
u	velocity, L/t [m/s]
x	x-coordinate, L [m]
X(t)	position of steam zone interface, L [m]
y	y-coordinate, L [m]
z	z-coordinate, L [m]

Greek Symbols

ξ	transformed coordinate for steam zone interface position, L [m]
ϕ	reservoir porosity
α	thermal diffusivity, L^2/t [m^2/d]
γ	parameter relating velocity and steam zone interface velocity, dimensionless or
	heat penetration variable as defined by Butler's 1985 model
μ	oil dynamic viscosity, m/Lt [mPa.s]
ν	oil kinematic viscosity, L^2/t [m^2/s]
θ	angle of steam zone interface with horizontal
ρ	density, m/L^3 [kg/m^3]
Δ	change (for example, change of enthalpy)
λ	parameter in solution
β	ratio of Region 1 density to Region 2 density

Subscripts

1	Region 1 (steam zone)
2	Region 2 (reservoir ahead of steam zone interface)
b	boiling (as in saturation temperature)
i	initial
irr	irreducible water
mf	mobile fluid(s)
o	oil
or	residual oil
r	reservoir (as in reservoir temperature)
s	steam (as in steam temperature)
st	steam
total	total effect, including reservoir and fluids filling pore volume
w	water

Superscripts

*	production

Chapter 1 — Introduction

Horizontal well technology holds promise in the recovery of heavy oil and bitumen resources in Alberta and Saskatchewan, due primarily to the extended contact between the reservoir and a horizontal well. In addition, horizontal wells can be optimally placed to delay gravity segregation and/or minimize heat loss to unwanted zones in steam injection recovery methods. One of the main thermal recovery methods for heavy oil and bitumen recovery is the steam-assisted gravity drainage (SAGD) method. For this method, pairs of parallel horizontal steam injector and producer are drilled near the base of the reservoir. High-pressure and high-temperature steam is injected into the reservoir to reduce the viscosity of the bitumen, and improve its mobility. The mobilized bitumen, along with steam condensate, is produced into the lower-positioned horizontal producer by gravity drainage. Simultaneously, the steam zone expands vertically and laterally. Continuing steam injection leads to expansion of the steam zone, and production of the bitumen from the reservoir. Theoretical and experimental investigation of different aspects of the SAGD method and its variations such as single-well SAGD (SW-SAGD) – especially, its steady-state behaviour – have been performed, and mentioned in the literature. However, unsteady state behaviour of the SAGD method has not been studied as extensively.

This study investigates theoretically the effects of convective heat transfers due to steam injection, heat loss to cap and base rock, and fluid production on the recovery performance of the SAGD process. Analytical solution to the heat transfer process which includes conduction, as well as convection due to state change and heat losses (due to production, and heat loss to cap and base rock), for appropriate boundary conditions and initial condition, is developed. The heat transfer process is coupled with flow in porous media and material balance considerations to produce a mathematically rigorous model for transient reservoir heating and fluid production for the SAGD method.

I

Chapter 2 — Survey of the Literature

2.1. Introduction

The volume of crude oil contained in Canada's heavy oil and oil sand deposits is approximately 2.8 trillion barrels (445 billion m^3), roughly equal to the world's current combined conventional oil in place. However, recovering the viscous crude oil from these heavy oil and oil sand deposits is technically and economically much more challenging than recovering crude oil from conventional light-oil reservoirs. In some cases, the oil is sufficiently mobile under initial reservoir pressure and temperature conditions for it to be recovered using primary production (cold production) and/or by waterflood. In the majority of the cases, oil viscosity under initial reservoir temperature (and pressure) conditions is of the order of hundreds of thousands of centipoise or more, rendering the oil immobile. Thermal energy, in the form of high-pressure and high-temperature steam, is usually injected into these reservoirs to reduce the oil viscosity and make it mobile. A brief review of different thermal recovery methods, and a careful review of the steam-assisted gravity drainage method (SAGD) – in particular, those references discussing fundamental features of the SAGD models – are provided in the following sections.

2.2. Steamflooding and Cyclic Steam Stimulation

2.2.1. Steamflooding

Conceptually, steamflooding is similar to waterflooding (or hot waterflooding): fluid is injected into the reservoir through some injector(s) to displace the oil in the reservoir toward and into separate producer(s). In steamflooding, high-pressure wet steam is injected continuously into the reservoir where it forms a steam zone around the injector. The injected steam gives up its latent heat, which is transferred (by conduction and convection) into the reservoir ahead of the steam zone. Some of the injected heat is lost to the cap rock and base rock. The steam zone expands with time, and in the process continues to heat up the oil-bearing reservoir and displace the mobilized oil along with the condensate towards the producer. It is noted that steam eventually overrides the oil zone (i.e. it migrates to the top of the reservoir, and bypasses the oil below), due to its lower density. Injectors and producers are often arranged in some patterns to improve the sweep efficiency of the flooding process (Prats, 1982). It is important to note that in steamflooding oil production prior to steam breakthrough is due mainly to pressure driving force (Vogel, 1992).

2.2.1.1. Theoretical and Experimental Studies

Lauwerier (1955) considered the heat conduction from a layer of injected hot water to adjacent oil layers. Solving the heat balance equation, made up of three components (heat injected, heat accumulated, and heat loss to the oil layers), Lauwerier obtained the temperature distribution in

2

both the water layer and oil layers as a function of time. This solution formed the basis for performance analysis of the hot waterflood process.

Marx and Langenheim (1959) developed a direct relationship between the growth of the steam zone and the rate of heat loss to the overburden and underburden. As the heat loss to the overburden and underburden increased, the growth rate of the steam zone decreased. In this model, the steam zone front was thought to be vertical and the displacement mechanism was thought to be similar to that of a piston (similar to the displacement assumed in Lauweirer's model). The mode of heat transfer was by conduction and the entire heating and displacement processes, were localized at the condensation front (at the edge of the steam zone, where steam gave up its energy and condensed). As such, the flow of heat from the steam zone into the liquid zone ahead of the condensation front was neglected. This type of model is commonly referred to as frontal drive model.

Mandl and Volek (1969) developed another frontal drive model to predict steam zone expansion with time. They incorporated the heat transfer into and inside the liquid (condensate) zone ahead of the condensation front, as they recognized such transfer would affect both the flow of condensate water and oil and the growth of the steam zone. As such, the condensation front no longer remained vertical with time. Rather, its shape changed as a result of contrasts in the density and viscosity of fluids ahead and behind the condensation front (due to steam override, or example). Analysis of the heat balance and mass balance equations behind and in front of the condensation front led to the introduction of the critical time t_c variable, which marked a change in the mode of heat transfer across the condensation front. For time less than t_c, heat transfer was mainly conductive, while when $t \geq t_c$ the transfer of heat was predominantly convective. As a result, two different expressions for the steam zone volume were proposed: one before the critical time, and one after. It is seen easily that the steam zone volume determined by Mandl-Volek model before the critical time was the same as that given by the Marx-Langenheim model (1959).

Myhill and Stegemeier (1978) developed another frontal drive model. A number of important assumptions were made: no vertical temperature gradient in the reservoir, constant steam injection pressure and quality, conductive heat losses from the steam zone to the overburden and underburden, and convective heat transfer being the main heat transfer inside the reservoir. Also, the displacement of oil by the condensate ahead of the condensation front was assumed to be negligible. In this model, it was not necessary for the front to be vertical. A function describing the thermal efficiency of the steam zone, $E_{h,s}$, was introduced and played a role in the determination of the steam zone volume.

Beside the frontal drive models, there are also gravity drive models to predict steamflood performance. van Lookeren (1977) presented a gravity override model based on segregated flow principles. Equations were developed for approximating the steam zone in both linear and radial

3

steam drives. The shape of this steam zone was found to be dependent on the steam injection rate, pressure, and effective formation permeability to steam. The steam zone tilted interface was a function of the steam viscosity and injection rate, oil viscosity, reservoir height, and a pseudo mobility ratio derived from combination of flow and material balance equations. The steam zone interface was seen to become more vertical with increasing oil viscosity. This model did not incorporate the oil production from the cold and hot water drives from the steam condensate in calculating the oil displaced by the steam zone.

Neuman (1975) presented a comprehensive gravity override model for a steamdrive process. Two important assumptions were made: steam rose quickly to the top of a permeable reservoir, and horizontal pressure gradient in the steam zone was much less than the vertical pressure gradient on liquids resulted from density variations. As such, the time for steam to rise to the reservoir top was negligible compared to the time required to heat the total reservoir area. Continuing steam injection led to the downward growth and areal spread of the steam zone. Overall enthalpy balance equation, along with the mass flow rate of condensate and oil were considered, based on the temperature distribution due to heat conduction inside the infinite reservoir. This model allowed the following parameters to be determined: velocity of the steam-liquid interface, thickness of the steam zone, rate of increase of the steam zone thickness and areal extent, volume of oil displaced from the steam zone and the heated reservoir beneath it, reduced injection rate sufficient to sustain the growth of the steam zone after an area is heated to steam temperature, and additional oil displaced after steam injection is stopped.

Miller and Leung (1985) assumed a complete vertical overlaying steam zone (i.e., 100% areal coverage) in their model. In this model, reservoir heating was assumed to be dominated by conductive heating, and oil production was proportional to the 'depth-integral of oil viscosity inverse'. The temperature distribution of the condensate and the oil zone beneath was found using a 1-D unsteady state heat conduction equation.

Kumar, Patel, and Denbina (1986) presented a model to predict the height of the steam zone. This model was a variation of the Miller and Leung's model (1985). Two important assumptions were made: injected steam overriding to the top of the reservoir from the outset of a steamflood, and conduction being the principal mechanism by which the oil underneath was heated. As heat propagated downward into the oil column, viscosity of the oil was no longer a function of temperature alone. Rather, it also became a function of distance and time of exposure to the heat flux. This model, however, does not require a pre-steam oil production rate. It was found that for cases where steam overrode from the beginning of the flood, effect of convective heat transfer was considered minimal due to counteracting gravitational forces and viscous forces in the reservoir. Hence, conduction of heat remained the dominant effect in heating the oil.

4

As expected, other models which seek to combine features of both frontal and gravity override models have also been developed. Jones' semi-analytical model to predict the growth of the steam zone (1981) was based on the models by van Lookeren (1977) and Myhill and Stegemeier (1978). An advantage with this model was its applicability in accounting for the displacement mechanisms for all production stages normally observed in the life of a steam drive project. Hence, the model predicted quite closely the production rate for the various reported field data. On the other hand, several empirical constants were employed to obtain better match for the displacement process.

Gomaa (1980) used numerical simulation results to develop a set of correlation charts for steamflood recovery performance prediction. The simulation results were matched with field data for the Kern River steamflood in California; however, it was found necessary to lower the relative permeability curve for water in order to match successfully the flow of water and mobilized heavy oils. Using net heat injected into the reservoir, which accounted for the vertical heat losses, led to a single oil recovery curve for different reservoir thicknesses. In addition, Gomaa determined that for constant steam injection rate per unit volume of reservoir the oil recovery performance was independent of pattern shape and size.

Farouq Ali (1982) presented a steamflood performance semi-analytical model which took into account the two dominant displacement mechanisms: frontal displacement and vertical drive/displacement, of steam during a steamflood. It combined the van Lookeren equation to estimate the thickness swept by steam, along with the Mandl and Volek equations to calculate the steam zone volume. Viscosity of the fluids (oil and condensate) along with their relative permeabilities ahead of the steam zone were calculated, based on calculated average temperature in this zone. A correlation was used for fluid relative permeabilities. The volumes of oil and water displaced from the steam zone due to expansion and displacement of fluids were determined from material balance equation. These iterative steps were then repeated until steam breakthrough occurred at the producer. The suggested model accurately predicted the production rate for the Kern A River pilot project. Application of this model to cyclic steam stimulation, however, proved to be problematic due to mainly the re-saturation of the depleted oil zone.

Matthews (1983) suggested a list of screening criteria for successful implementation of the steamflood process. The criteria included oil saturation, sand porosity and thickness, reservoir permeability (including permeability distribution and presence of potential thief zones), presence of fractures, oil viscosity. The ratio of net to gross pay and reservoir continuity between injector and producer were also determined to be important in affecting oil recovery.

Vogel (1984) developed a model for steamflood recovery whereby gravity drainage, and to a lesser extent steam drag were the main production mechanisms. The steam chamber was assumed to override, spreading instantaneously and occupying the top portion of the reservoir.

5

Hence, oil production was due to the downward expansion of the steam chamber. Due to this assumption, heat loss to the cap rock was under-estimated and to the base rock was over-estimated. The model did not provide any equation to determine the oil drainage rate, however.

Closmann and Smith (1983) established the counter-current flow of oil and steam above steam-heated fractures. A steam-oil interface was formed and traveled upwards through the reservoir, while at the same time the oil above the interface was heated and drains downwards to the fracture. This process was called ceiling drainage by Edmunds (1984). Chu (1985) developed a simple correlation for steamflood SOR, based on field data from 20+ steamflood field projects. The correlation is a function of reservoir depth, thickness, permeability, porosity, temperature, oil viscosity and saturations (initial, residual).

Peake (1989) presented a simple analytical model for steamflood performance analysis based on material balance for a two-zone reservoir model. The model included the presence of an initial hydrocarbon gas saturation in the reservoir, change in the pore volume due to compressibility, and material balance for the steam, condensate and oil zones. The following assumptions were invoked: symmetrical fluids flow between the injection well and production well, the fluids were confined within the patterns, no water influx, and no escape of steam from the control volume. In addition, production of steam was assumed insignificant once steam breakthrough occurred. Calculations for the oil and water production, with known saturations, were illustrated.

Chen and Sylvester (1990) slightly modified Farouq Ali's model (1982), mainly by incorporating the fractional flow equation to determine the oil saturation in the unswept zone. The model was found to provide a good prediction of field production, without requiring any empirical factors. However, it should be pointed out that the predictive capability of this model depends strongly on the relative permeability relationships. Hence, the use of appropriate relative permeability functions is important for a good history match.

Palmgren, Bruining, and de Haan (1991) considered steady-state heat balance at a moving sharp interface assumed to exist between the steam zone and the unheated reservoir in their development of a model for steamflood. The fluid flow equations, written in the stream function formulation, were solved using finite element. To describe the penetration of steam condensate ahead of the interface, the authors assumed either a single flowing fluid phase with average properties or an under-running water tongue under steady-state conditions. Experiments were performed, with experimental results showing qualitative agreements with the numerical model. Palmgren and Bruining (1992) extended the above model by assuming segregated flow, and obtained a first order nonlinear hyperbolic equation for the location of the interface. This interface location was determined using the method of characteristics.

The segregated flow theory (Dupuit assumption) neglects flow along the vertical direction; as

6

such, fluids flow horizontally due to potential gradients caused by gravity forces. This segregated flow theory has been shown by Yortsos (1991) to be a reasonable approximation for 2-D flow in homogeneous systems; however, it has yet been shown to be applicable for thermal recovery processes, due to presence of a large viscosity variation over short distances.

Closmann (1995) assumed steady-state temperature distribution ahead of a horizontal interface, and obtained analytical solution for oil drainage rage for mature steamflood projects produced under strong override conditions. Oil was allowed to flow along the horizontal direction only. Kimber, Deemer, Luce, and Sharpe (1995) considered unsteady-state temperature distribution ahead of an advancing steam front to develop a model for calculating oil flow rate by gravity drainage and pressure forces in mature steamfloods. Additionally, the authors assumed the presence of a heated region with a constant viscosity around the producer. When the steam zone was small, the net oil production rate was found to increase marginally by allowing an extra pressure drop by producing steam beyond the heat requirement of the process. In the latter stage of the process, when the steam zone became larger, it was detrimental to the process efficiency to produce extra steam for an additional pressure drop.

The Fracture-Assisted Steamflood Technology (FAST) was developed to overcome typically low steam injectivity in many heavy oil and oil sand reservoirs. The main idea behind this method was to improve communication between injector and producer through the use of hydraulic fracturing. Specifically, the producing well was fractured hydraulically and then thermally stimulated to heat the formation around the wellbore. The injection well was then fractured to create inter-well communication between the injector and producer. Once the inter-well communication was established, the injection rate was lowered to enable distribution of steam over a larger portion of the pay zone. In the last stage of the FAST process, water injection through the horizontal fractures was used to recover additional oil. Britton, Martin, Leibrecht, and Haiman (1983) reported the successful implementation of this process in Street Ranch pilot in Texas, achieving a SOR of less than 12.

Soni and Harman (1986) numerically determined that gravity displacement of the bitumen from the rock matrix to the horizontal fracture was the primary recovery mechanism in the FAST process. The bitumen in the fracture was then pushed towards the production well as an oil-water emulsion.

Pujol and Boberg (1972) examined the scaling groups derived to study a scaled laboratory model of the steamflood process. Accurate scaling of the capillary pressure was found to be not crucial for highly viscous oils, due to small values for the ratio of capillary to viscous forces; as such, unscaled capillary pressures would have little effects on the recovery of oil. For oils having viscosity less than 1000 mPa.s (centipoise), capillary pressure became more important, and unscaled capillary pressure resulted in optimistic recovery for laboratory experiments.

7

Farouq Ali and Redford (1977) reviewed different studies on scaling laboratory thermal recovery processes. A new approach to obtain the scaling criteria for steam and steam-additive injection was thoroughly analyzed by Kimber, Farouq Ali, and Puttagunta (1988). The dimensionless similarity groups were obtained using both the dimensional and inspectional analyses. As it was not possible to satisfy all of the scaling groups, the authors developed different subsets of scaling criteria with each subset seeking to scale some of the scaling criteria (for example, geometric scaling) while relaxing others (gravitational effects). Experiments were carried out to determine the effects of these subsets on oil recovery.

Stegemeier, Laumbach, and Volek (1980) used inspectional analysis to obtain the dimensionless similarity groups for the steamflood process. These scaling groups were utilized in the design and operation of scaled models to study the Mt. Poso and Midway Sunset steamflood projects. A notable feature of this study was its use of vacuum models. As such, the experiments were performed at sub-atmospheric pressures. The main requirement of this approach was the scaling of the Clausius-Clapeyron equation for the appropriate range of experimental pressures. Additionally, the authors suggested scaling criteria for vertical wells based mainly on the size of glass beads used to pack the model reservoir. The authors used the same criteria to scale up experimental results to predict field performance.

Huygen and Black (1982) performed scaled model experiments to investigate the effectiveness of different injection and production strategy using vertical and horizontal well combinations in steamflooding the Athabasca oil sand. Steamflood recovery performance was found to be significantly dependent on the geometry and communication between the injection and production well. The authors concluded that for oil sands, communication between wells was necessary, and the use of horizontal wells (which behaved like a fracture) was an effective method for providing initial injectivity into the reservoir. Two deficiencies in the experiments were noted. First, the oil saturation in the model was higher than field oil saturation; consequently, the recovery obtained from the model was judged to be optimistic. The model horizontal permeability was lower than in the field; as a result, the lateral growth of the steam zone into the reservoir was underestimated.

Chang, Farouq Ali, and George (1991) obtained results from scaled model experiments in a low-pressure model to study steamflooding a heavy oil reservoir having a bottom water layer different, using 4 different combinations of horizontal and vertical wells for injection and production. The experiments were scaled according to criteria suggested by Stegemeier, Laumbach and Volek (1980). Three different types of reservoir were used: homogeneous reservoirs, reservoirs having a thin bottom water layer (10 % of pay thickness), and reservoirs having a thick bottom water layer (50 % of pay thickness). The horizontal injector and producer combination was found to achieve the highest oil recovery, and horizontal wells performed better in thin bottom water reservoir as compared to the case for a homogeneous reservoir.

Doan, Farouq Ali, and George (1991) derived scaling criteria for flow into and inside a steamflood horizontal well, using both dimensional and inspectional analysis. The experimental horizontal well radius was sized according to one of the criteria. Experiments were carried out, and included the measurement of pressure drop across the horizontal producer with time. Other experiments were also performed to evaluate the flow of steam in the vicinity of the horizontal well.

Matthias, Doan, Farouq Ali, and George (1992) looked at different strategies for steamflooding a reservoir having a thick bottom water layer (50 % of pay thickness). The authors also studied the performance of the long and short horizontal wells, and vertical producers. Horizontal well length was measured in relation to the dimension of the flood pattern. The horizontal well radius was scaled according to a criterion relating flow into the well from the reservoir and flow inside the horizontal well (Doan et al., 1991). It was concluded that the long horizontal production well out-performed both the short horizontal production well and the vertical producer, as it provided higher cumulative recovery and a higher oil-steam ratio (OSR).

Doan (1996) developed a correlation between oil recovery and heat utilization from scaled model experiments. Heat utilization was determined from heat balance calculation, which considered heat injected, heat losses to cap rock and base rock, and heat removed from the reservoir due to production. Heat loss to the cap rock and base rock was determined from an analytical solution to the heat conduction from the reservoir to the cap rock and base rock. Experiments were also performed to investigate steamflood recovery using horizontal wells in dipping reservoirs.

2.2.1.2. Numerical Studies and Field Projects

Moughamian, Woo, Dakessian, and Fitzgerald (1982) used a 3-D finite difference, steam injection simulator to study steamflood recovery for a steeply dipping heavy oil reservoir in California. Sensitivity studies were also made to select the best operating parameters. Several important conclusions were made, based on the simulation results. Areal sweep efficiency was the most important parameter affecting the cumulative recovery. For a given injector location, lowest oil recovery was obtained when the producers were aligned in the direct line-drive pattern with respect to the injector. In this work, the energy balance, and the heat loss to the cap rock resulting from injecting steam updip were not mentioned.

Hong (1991) used a compositional steamflood simulator to study different driving mechanisms in steamflooding dipping reservoirs. Some operational strategies studied were shutting in the updip producer once steam breakthrough or high steam-oil ratio (SOR) occurred, reducing injection rate to meet economic constraints, switching injectors and producers during drainage to obtain maximum recovery, and finally injecting a non-condensable gas (such as N_2) to prevent steam cycling in the updip portions of the reservoir. The two models representing the reservoir included the 2-D cross section and 3-D model. It was concluded that gravity drainage of the heated oil is the main production mechanism in steeply dipping reservoirs. The location of the injectors and

9

producers, as such, must be carefully chosen to maximize the oil production. An optimal strategy was suggested for maximizing oil recovery, including a combination of steam injection, selective shutting in of wells updip after steam breakthrough, and later injection of non-condensable gas.

Rial (1984) developed a 3-D, 3-phase reservoir simulator that accounted for distillation effect, temperature-dependent relative permeabilities, gravity, viscous and capillary forces. Using this simulator, he studied the effectiveness of placing a horizontal injector at the bottom of a heavy oil reservoir for steamflooding. The input data for the model were representative of the Kern River Field in California. The horizontal injection well was shown to provide better areal sweep efficiency, as compared to vertical steam injector.

The effectiveness of horizontal wells to reduce steam override in a mature steamflood, along with preventing steam override in new steamflood operations was examined by Huang and Hight (1986). A 3-D, 3-phase thermal simulator accounting for the effect of gravity, viscous and capillary forces, and temperature-dependent relative permeability was developed. In this model, heat transfer was modeled by both the conduction and convection processes. Reservoir properties representing the typical California unconsolidated heavy oil reservoir were used for the study. Simulation results showed that with the use of horizontal wells, the areal sweep efficiency increased significantly, the oil recovered in the region where the over-riding steam bypassed was substantial, and the project life was shortened. In 'blind spots' (i.e., the volume of oil not exposed in the flow pattern), the oil saturation was reduced from 60% to 30%.

Combe, Burger, Renard, and Valentin (1988) numerically investigated the performance of a steamflood when horizontal wells were employed. The authors considered five different case studies: fluid and reservoir characteristics, different spatial distributions for vertical and horizontal wells, different injection and production strategies, layered reservoirs with tight streaks between layers, and reservoirs having initial mobile water saturation. The results showed the efficiency of horizontal wells in exploiting thin, marginal heavy oil reservoirs having low oil mobility.

Gomaa, Duerksen and Woo (1977) used a numerical simulator to carry out a sensitivity study for recovery performance prediction for a steamflood pilot in the Thick Monarch Sand of the Midway-Sunset Field. Some of the main parameters studied included relative permeabilities, bottom-hole pressure, vertical permeability, reservoir thickness, pattern size, steam injection rate, and presence of shale barrier(s). It was found that recovery was negatively affected if pattern size was increased, unless steam injection rate was proportionally increased.

Many studies have been conducted over the years to investigate the effectiveness of chemical additives in alleviating gravity override, and improving steamflood sweep efficiency and recovery. Traverse, Deibert and Sustek (1983) reported some results for Texaco's San Ardo steamflood project. Inverted nine-spot patterns of 20-acres spacing were used, and a recovery of 50% of OOIP was achieved. The use of steam additives, recompletion of wells, and cross-flooding

10

practice (whereby the corner producers in the original pattern were converted to injectors in the infill pattern) together with infill drilling were estimated to be capable of increasing oil recovery from 50% to 70% or more.

Friedmann and Jensen (1986) studied experimentally the use of surfactant-generated foam on steamflood experiments in Berea sandstone cores. Relative permeability to steam was lowered by the surfactant. It was also determined that high oil saturations decreased the formation and propogation of foam. Mohammadi and McCallum (1989) reported results of a pilot steamflood, in which alkyl toluene sulphonate (ATS) and nitrogen were used as steam additive. An incremental oil production of 29400 barrels was achieved after injecting 257000 lb of ATS.

2.2.2. Cyclic Steam Stimulation

Cyclic steam stimulation involves the mobilization and production of bitumen (or heavy oil) on a cyclical basis. This is achieved by first injecting a slug of steam into the reservoir; this injection stage is then followed by the soak period, during which the energy in the steam is transferred into the surrounding reservoir. Once the reservoir around the well is sufficiently heated, the mobilized oil is then produced. The next cycle is implemented when oil production rate from previous cycle declines to low levels. In cyclic steam stimulation, the same well is used for both steam injection and oil production. As such, reservoir heating and oil production tend to occur in a area close to the wellbore. This is in contrast to steamflooding, where steam is injected into the reservoir through one well (injector), and oil production is through a separate well (producer) which is located some distance away from the injector. Also, in cyclic steam stimulation the mobilized oil and steam condensate flow through the heated zone around the well and are produced through it. With steamflooding, the mobilized oil is displaced (i.e., pushed) by the steam zone and steam condensate toward the producer. The size of the steam slug, duration of the soak period and duration of the production period vary, depending on the conditions of the reservoir and characteristics of the oil in consideration.

2.2.2.1. Theoretical and Experimental Studies

Boberg and Lantz (1966) developed a model to predict performance of isolated wells being cyclic steam stimulated. The steam zone was assumed to be cylindrical, with the well being in the centre. The steam zone radius was calculated using the Marx and Langenheim's model (1959), with allowance made for heat loss from the injection tubing. During the soak period, heat losses (both vertically and horizontally) were estimated as function of time from solutions to the heat conduction equation (Fourier's equation). Fluid flow was assumed to be radial. During the production period, heat removed from the reservoir in the (hot) produced fluids was also accounted for in the heat balance analysis. Oil production rate was determined from the combined flow through two concentric cylinders in series (one representing the cold reservoir, and the inner cylinder representing the heated steam zone), with oil viscosity being determined at

11

an average temperature accounted for all the heat losses. For the next cycle, Boberg and Lantz added the heat still remained in the reservoir with the heat injected for the new cycle to determine the new steam zone radius.

Doscher (1966) described the displacement of oil from the steam-heated region by the expanding overriding steam zone, coupled with gravity drainage, to the wellbore in later production cycles. This effect was not included in Boberg and Lantz's model (1966). This gravity drainage occurred due to the density difference between the seam and the heavy oil and condensate. The declining pressure (in the heated zone) associated with fluid production led to flashing of residual water saturation into vapour phase. The vertical heat losses became larger in later cycles, leading to lower cumulative OSR.

Towson and Boberg (1967) extended Boberg and Lantz's model (1966) to include production due to gravity drainage. Heat conduction occurred in both vertical and radial directions. Effects of depletion of the heated zone on steady-state production rate were not considered. Also, the effects of solution gas and water re-vapourization inside the steam zone were not considered. The radial flow equation was defined with the hydrostatic head differential replacing the pressure gradient. It was determined that choking back production pressure helped prevent the flashing of produced water, and hence decrease the heat removed in the produced fluids. Gravity drainage of the heated oil was found to be an important recovery mechanism in thick formations having high vertical permeability.

Nikko and Troost (1971) devised a scaled low-pressure physical model, which utilized a series of resistance and capacitor tubes connected to the sand pack, to simulate the CSS process. This setup ensured the reservoir beyond the model to receive and supply oil during the stimulation and production periods. Also, the experiments were performed under conditions to ensure heat remain inside the model. It was determined that decreasing the cycle length had two contrasting effects: increasing cumulative oil production, but reducing cumulative OSR. Injecting a given steam volume in more slugs (i.e. more cycles) led to higher initial OSR and cumulative oil production, but less oil production later on, compared to larger slugs (i.e. fewer cycles). The cumulative OSR were the same for both cases in later cycles.

Closmann, Ratliff, and Truitt (1970) assumed only vertical heat loss and constant steam-zone radius in their model. Also, effects of heat removed from reservoir in the produced fluids were neglected. Superposition was applied to determine the average oil viscosity at different times, which determined the horizontal oil fluxes from various layers of the reservoir. This model was developed specifically for the first cycle, and would need to be modified to be applicable for subsequent cycles. Hurst and van Evendingen's solution for transient reservoir response (1949) was used to determine the time required to resaturate the steam zone with oil.

12

2.2.2.2. Numerical Studies and Field Projects

de Haan and van Lookeren (1969) reported operational data for different aspects of Shell's CSS project in the Tia Juana field in Western Venezuela. Analyzing the production data the authors determined that the high initial oil production rates were due to transient pressure effects (including the quick depletion of the heated zone). As the heated zone became cooler, its effect on the productivity index was negligible. Compaction drive became more important, however, and typically amounted up to 40% of the total production.

Borregales (1977) reported that the main production mechanisms in CSS operations in the Boliar Coast fields, Venezuela to include solution gas drive (during cold production stage), compaction drive in combination with reactivated solution drive, and then gravity drainage. In this case, the decrease in pore pressure led to increased compressive load on the rock matrix, along with a decrease in overall pore volume and subsidence of the ground surface. When these happened, the fluids were squeezed from the reservoir. Also, water squeezed from the interbedded shale streaks provided additional displacement of the oil.

An important feature of Imperial Oil Resources Ltd.'s CSS operations at Cold Lake is the creation of fractures around the wells due to steam injection. Settari, Kry and Yee (1988) reported the existence of asymmetrical fractures around the wells rather than strictly horizontal fractures (as predicted by conventional theory, based on the depth of the reservoir). Denbina, Boberg and Rotter (1991) established that the fractures were mainly vertical in the early cycles of CSS, but with continued steam injection and production many horizontal fractures formed in later cycles.

Denbina, Boberg and Rotter (1991) numerically simulated the production in the early cycles at Cold Lake. It was necessary to allow for shear failure during the steam injection stage to match production data. The shear failure led to larger pore volume during steam injection, and allowed compaction drive during production. Incorporation of relative permeability hysteresis into the model enabled the steam condensate to flow into the dilated zone, but prevented its back flow during the compaction-drive stage. The authors determined that in the early cycles compaction drive was the main production mechanism for oil production, while gravity drainage became more important in later cycles.

Farouq Ali (1994) reviewed the success of the CSS process in heavy oil and oil sands recovery in Canada. Of importance was the modification to the basic CSS process for various reservoirs, depending on their characteristics. A successful example is the strategy of injecting steam at pressures above the formation fracture pressure in Cold Lake to provide the initial injectivity necessary for bitumen heating and mobilization, as well as to provide compaction-drive effects beneficial to oil displacement.

13

2.3. Steam-Assisted Gravity Drainage (SAGD)

The steam-assisted gravity drainage (SAGD) process was developed (in late 1970's) at about the same time as the introduction of horizontal well in oil and gas operations. It was devised to take advantage of the gravity drainage of mobilized bitumen into a horizontal well placed at the bottom of the bitumen reservoir. In this process, steam moves upward in a direction opposite that of the bitumen which is drained downwards by gravity. In the following sections, a review of the SAGD process is provided.

2.3.1. Theoretical and Experimental Studies

Butler, McNab, and Lo (1981) first reported an analytical model and scaled model experiments for the steam-assisted gravity drainage (SAGD) process. In this model, two horizontal wells were used for the injection-production process, with steam being injected into the reservoir through the upper horizontal well. Heated oil and steam condensate were drained simultaneously downwards around the edge of the steam zone by gravity into the lower horizontal producer, as shown in Figure 2.1. Oil drainage rate due to gravity was described by Darcy's law, for a layer of $d\xi$ ahead of the steam zone interface, per unit length of the horizontal producer (Figure 2.2).

$$dq = \frac{kg\rho Sin\theta}{\mu}d\xi \qquad (2.1)$$

In this model, reservoir heating was assumed to be due to steady-state heat conduction, and the steam zone interface was assumed to move uniformly at a constant velocity U. The temperature distribution between the constant-velocity steam zone interface and unheated reservoir was thus given by,

$$\frac{T-T_s}{T_s-T_r} = \exp\left(-\frac{U\xi}{\alpha}\right) \qquad (2.2)$$

14
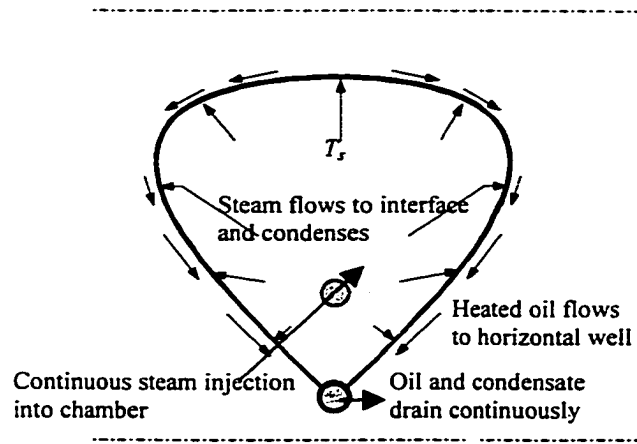
Figure 2.1: Vertical Cross-Section Through Expanding Steam Chamber (after Butler, 1994)
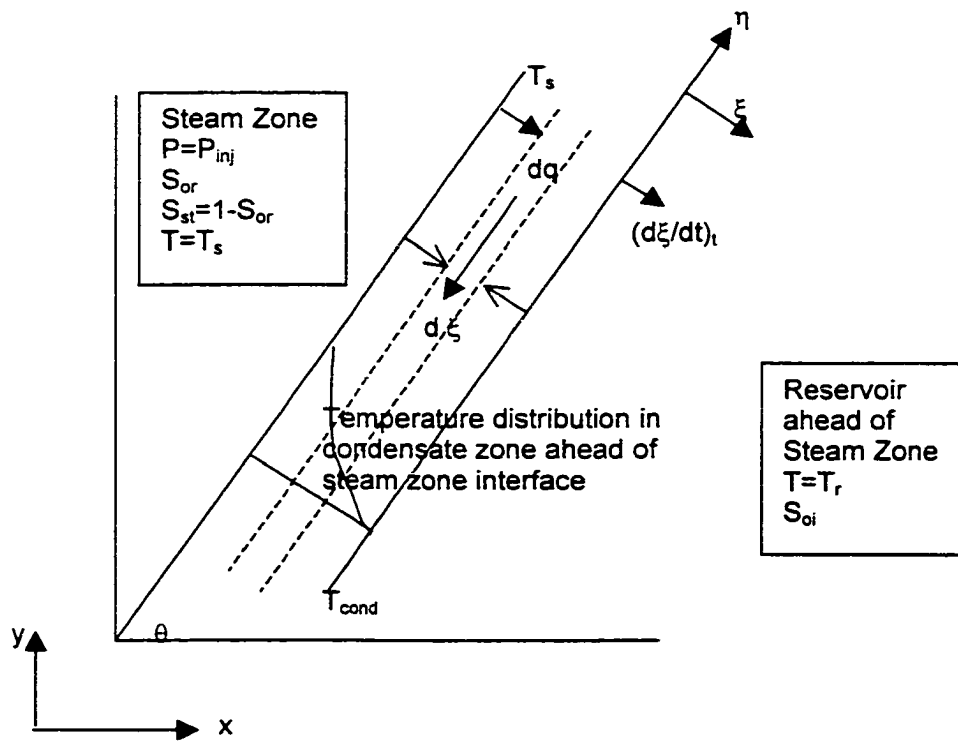
Figure 2.2: Cross-Section Drawing of Flows of Heat and Oil in Reservoir Element Near the Steam Zone Interface.

15

Oil drainage rate was a function of its temperature-dependent kinematic viscosity. Consideration of the material balance in the zone ahead of the steam zone interface led to the following oil drainage rate equation:

$$q = L \sqrt{\frac{2\phi\Delta S_o kg\alpha(h-y)}{m\nu_S}}\Bigg|_{\text{side}}$$

(2.3)

In the above equation, m was a dimensionless parameter having values between 3 and 5. It was seen that oil drainage rate, according to Equation (2.3), was independent of the shape of the steam zone interface or its horizontal extension. Rather, it was a function of the drainage height. Additional equations were also derived to calculate the x- and y-position of the steam zone interface with time, as given below.

$$x = t \sqrt{\frac{kg\alpha}{2\phi\Delta S_o m\nu_s(h-y)}}$$

(2.4)

$$y = h - \frac{kg\alpha}{2\phi\Delta S_o m\nu_s}\left(\frac{t}{x}\right)^2$$

(2.5)

It is important to note that the model assumed conduction as the dominant mode of heat transfer, and the entire process was localized at the interface. Convection of heat ahead of steam zone interface was not considered. One of the major concerns with the analytical model, duly noted by the authors, was the transient profile of the interface curves (calculated from Equations (2.4) and (2.5)), which were seen to move away from the horizontal producer with time. As such, it was possible that oil could eventually move along and below a horizontal stationary interface (i.e., without a significant drainage height). It was implicitly assumed that all the heated oil ahead of the interface was produced once it reached the bottom of the steam zone. As such, no horizontal potential gradient was required for the production of the oil ahead of the steam zone interface, at the bottom of the steam zone. In reality, the pressure gradient between the horizontal injector and producer would provide the driving force for the production of oil in this region. In practice, steam trap is implemented to prevent steam from being significantly produced from the reservoir.

In addition, the recession of steam zone interface away from the horizontal producer was believed to overestimate the oil drainage rate given by Equation (2.3). The authors derived several dimensionless similarity groups, and used the following two groups as scaling criteria for their experiments.

16

$$B_2 = \sqrt{\frac{mkgH}{\phi \alpha S_o V_s}} \tag{2.6}$$

$$t^{'} = \frac{t}{h} \sqrt{\frac{kg\alpha}{\phi \Delta S_o hm V_s}} \tag{2.7}$$

The first scaling criterion, B_2, was used to scale the properties of the reservoir and fluid, and the second criterion was used to scale time. Good agreements were obtained between experimental data and results predicted by the equations.

Butler and Stephens (1981) modified and extended the above study to account for drainage into a series of parallel wells. An important feature in this study included the approximation of the interface curves suggested in the previous study (Butler et al., 1981) by tangentials connected to the horizontal producer. This tangential drainage (TANDRAIN) modification led to the following equation for oil drainage rate:

$$q = L\sqrt{\frac{1.5\phi \Delta S_o kg\alpha h}{m V_S}}\Bigg|_{1-side} \tag{2.8}$$

Another feature of this study was the modification of the theory to account for the effects of no-flow boundary between horizontal wells in adjacent patterns. The steam zone interface curves were only allowed to spread to the vertical no-flow boundary (plane) located halfway between two adjacent wells, rather than to infinity as in the original model (Butler et al., 1981). Photographs of experiments showing the growth of the steam chamber for various injection period were also included.

The growth of the steam zone in the vertical direction, from the base to the top of the reservoir, was not considered in previous studies (Butler et al., 1981), Butler et al., (1981)). Butler, Stevens, and Weiss (1981) combined this problem with the lateral growth rate of the steam zone as it gradually moved upward. In this analysis, the steam zone shape was assumed to be circular, and the horizontal well was located at the center. The growth rate of the steam zone was then postulated to be the rate of increase in its radius. Subsequently, an equation predicting the height of the steam chamber as a function of time was derived. It effectively predicted, with reasonable accuracy, the vertical growth rate of the steam zone in field operation.

Griffin and Trofimenkoff (1986) carried out laboratory experiments to investigate the applicability of the SAGD process for Esso's horizontal well pilot in the Cold Lake reservoir. Two scaled physical models, one being visual and low-pressure and one being high-pressure, were designed

17

according to the scaling groups suggested by Butler et al. (1981). In the visual model experiments, little steam override was observed. This observation differed considerably from theoretical prediction (Butler et al. (1981)). In the high-pressure model experiments, oil production rates were substantially higher than the values predicted theoretically. The 'extra production' was believed by the authors to be due to displacement from the end regions of the steam chamber.

To resolve the problem of steam zone interfaces receding with time from the horizontal producer, Butler (1985a) developed a new semi-analytical approach to predict the advance of a vertical element of the steam zone interface with time. The steam zone interface was divided into a number of sections, and the heat buildup ahead of these sections were determined. Temperature distribution ahead of the moving steam zone interface was approximated by the solution to the problem of 1-D heat conduction ahead of an interface moving at constant velocity (Carslaw and Jaeger, 1959). A new parameter, heat penetration variable, was introduced and had the following form.

$$\gamma = \frac{q_c}{[\rho C (T_S - T_R)]} = \frac{\alpha}{U}$$

(2.9)

The differential equation, incorporating the heat penetration variable, was solved numerically to determine the growth rate of the steam zone and production rate at different times. The temperature gradient along the steam zone interface was dependent on the heat penetration and frontal advance velocity. The temperature-gradient function was determined to be exact at two limits (near the horizontal producer and near the top of the steam zone), and be an approximation for steady state temperature distribution between the two limits. This treatment ensured the desired geometry of the steam zone interface: upper portion of the interface moving away, and lower portion of the interface being anchored at the horizontal producer, with time. In other words, the velocity varied along the vertical direction of the reservoir. However, the steam zone interface was assumed to advance steadily.

A new dimensionless parameter was introduced as a scaling criterion for the experiments.

$$B_3 = \sqrt{\frac{kgh}{\alpha \phi \Delta S_o m v_s}}$$

(2.10)

Values of the B_3 scaling criterion for two different bitumens (approximating Athabasca and Cold Lake oil sands) were computed and used in the experiments. It was seen that this dimensionless group was a measure of convective fluid flow to conductive heat flow. Good agreement was reported between experimental data and theoretical results. The effects of reservoir parameters and steam temperature on B_3 were investigated. The author stated that the presence of non-

18

condensable gases could cause a significant barrier to mass transfer, and hence heat transfer of the SAGD process.

Butler (1985b) tabulated charts showing typical values of m and mv_s for different crude oils. The following expression was derived for the parameter m.

$$m = \left[v_s \int_{T_R}^{T_s} \left(\frac{1}{v} - \frac{1}{v_R} \right) \frac{dT}{T - T_R} \right]^{-1}$$

(2.11)

As such, m is mainly a function the characteristics of the viscosity-temperature relationship for the oil (or bitumen) being considered, between the steam and reservoir temperatures.

Joshi and Threlkeld (1985) experimentally studied the effect of different well configurations on the SAGD process. Three well configurations were considered: a horizontal well pair, a vertical injector located above a horizontal producer and a single vertical well with dual completion used as injector and producer. Of the three well configurations, the horizontal well pair was found to perform the best (i.e. achieved highest oil recovery). Increasing production rate (by lowering production pressure) was found to lead to earlier steam breakthrough.

Chung and Butler (1988) experimentally investigated the effects of several parameters, including well spacing and steam temperature, on SAGD recovery performance. The experiments were scaled using the criteria developed by Butler (1985a) for Cold Lake and Athabasca reservoirs. It was determined that steam could be circulated in a vertical well to create successfully thermal communication between a horizontal injector, which was positioned farther up in the reservoir, and a horizontal producer positioned near the base of the reservoir. Oil drainage rate was increased, and process efficiency improved when steam was first introduced into the upper part of the reservoir. It was observed that this improvement was due to the formation of lesser volume of the water-oil (WO) emulsion. Naturally, under field conditions, the time required for the upward rise of the steam chamber in relation to the duration of its lateral growth is an important factor affecting the location of the injector.

The growth of the steam zone during the initial stage of the SAGD process was studied by Butler and Petela (1989). The steam chamber was observed to grow downward between the horizontal injector and producer initially, with the growth rate being controlled by the pressure gradient and the thermal properties of the reservoirs. The flow of the steam condensate and oil along the stream surfaces were assumed as if they were a single fluid, in the development of an equation for the breakthrough time.

Sugianto and Butler (1990) experimentally investigated the effectiveness of the SAGD process in bottom water reservoir by using a scaled visual 2-D physical model, with an active aquifer layer.

19

The scaling groups used to build the model followed those established by Butler et al. (1981). The displacement mechanism, effects of injection pressure, bottom-water layer thickness, and placement position of the horizontal producer were studied. Thickness of the bottom-water layer, along with the placement-position of the horizontal injector and producer were observed to affect cumulative oil recovery significantly. In many of the experiments, the horizontal producer was kept near the oil-water contact to ensure maximum drainage and recovery of oil. To avoid water coning, the production pressure was maintained slightly higher than the pressure in the aquifer.

Liebe and Butler (1991) also investigated the use of vertical injectors in SAGD process. The model was scaled using scaling groups for linear flow, as suggested by Butler (1985a). Three different producers were used: vertical, horizontal, and planar. They represented a point sink, line sink, and plane sink, respectively. The experiments were scaled for gravitational force as the driving mechanism. However, pressure driving force was also introduced in the experiments. Experiments utilizing two different reservoir oils and at two pressures were carried out. It was determined that the oil production rate was highest for the planar well, and it was about 3 times the rate achieved by the vertical well.

Reis (1992) assumed the steam zone shape to be that of an inverted triangle to develop a simple analytical model for predicting recovery performance for the linear SAGD process. The inverted-triangle steam zone was anchored at the horizontal producer, and its expansion was approximated by the increase in the base of the inverted triangle along the interface between the reservoir and the cap rock. The temperature distribution ahead of the moving steam zone interface was exponential, similar to that for the steady-state solution to 1-D heat conduction ahead of a moving boundary problem (Carslaw and Jaeger, 1959). Due to these simplifying assumptions, the author was able to obtain the closed-form solutions for the energy balance and determine the SOR (as the volume of the steam zone was known). Results from this model were compared to experimental data presented by Butler et al. (1981). There was little agreement between results predicted for the steam zone radius from this model and experimental data.

Reis (1993) employed the same consideration to develop a model for the SAGD process in cylindrical coordinates system. In this case, the steam zone shape around the vertical injector was approximated by an inverted cone. The exponential solution for heat conduction ahead of a moving interface (Carslaw and Jaeger, 1959) was also used to describe the temperature distribution in the reservoir ahead of the steam zone interface. Analogous equations were derived to calculate oil flow rate and heat injection. The main limitation of this model was that the oil production rate was predicted to increase steadily with time, due to its assumptions.

Butler (1994) suggested the following equation to approximate this linear geometrical steam zone interface profile between the base and the top of the reservoir.

$$q_y = q_h\left(1 - \frac{y^2}{h^2}\right)$$

(2.12)

where q_y is the drainage rate at any height h in the reservoir. The total flow was given by,

$$q_h = L\left.\sqrt{\frac{0.5}{\frac{y}{h} - \left(\frac{y}{h}\right)^3}}\sqrt{\frac{kg\alpha\phi\Delta S_o h}{mv_s}}\right|_{1-side}$$

(2.13)

It was seen that when the value of the dimensionless height (y/h) was equal to ($1/\sqrt{3}$) the heat ahead of the interface approximated that determined from steady-state temperature distribution (as given by Butler et al. (1981)). Above and below this critical point, there was less heat ahead of the steam zone interface than that given by the steady-state temperature distribution. As such, this critical point corresponded to maximum drainage rate; with this consideration, Equation (2.13) assumed the following form.

$$q = L\left.\sqrt{\frac{1.3kg\alpha\phi\Delta S_o h}{mv_s}}\right|_{1-side}$$

(2.14)

Hamm and Ong (1995) reported improvements in oil recovery for the Enhanced Steam-Assisted Gravity Drainage (ESAGD) process, in which a pressure differential was created between the steam zones of two adjacent horizontal patterns once the bitumen away from the steam zone interface became sufficiently mobilized. The authors stated that this pressure differential enabled the steam zone growth to be accelerated.

Farouq Ali (1997) provided a discussion of the SAGD process, including its experimental and numerical studies, and field implementation. He pointed out the importance of convection (as expressed in the flow of steam condensate), which was not included in the analytical solutions. In addition, steam and fluid flow behaviour inside the horizontal wells and geomechanical effects were stated to have significant impacts on the process, including the formation of separate steam zones due to uneven steam distribution along the injector.

Zhou, Zhang, Shen and Pu (1995) experimentally investigated the effects of injection and production well configurations in a heavy oil reservoir (oil viscosity of 11000 mPa.s at initial reservoir conditions). They used the scaling criteria suggested by Pujol and Boberg (1972) to scale gravitational and pressure forces. It was determined from experimental results that steamflooding with horizontal wells arranged in a line-drive pattern was most effective in recovering oil, even more than the well-pair SAGD configuration. The following was conjectured

as an explanation for this observation. In a process controlled by gravity drainage, such as SAGD, reservoir heating takes place at a slower pace, and there was, thus, more heat loss to cap and base rock than in a process controlled by pressure drive (such as steamflooding). It was unknown, however, if the experiments had been scaled to consider effects of heat loss to cap and base rock. In addition, steam injectivity is usually low in oil sand reservoirs (at least in initial stage) due to high bitumen viscosity. Pressure driving force does not take place until the reservoir has sufficiently been heated up. A horizontal steam injector, with its large contact area with the reservoir, improves steam injectivity. It also enables a large steam zone to be created in a stable manner and in a relatively short period of time due to small pressure gradients existing around it.

Butler and Jiang (1996) looked at the effect of gravity on the movement of water oil interface towards a horizontal well for reservoir having a bottom water sand. Analytical solutions were developed to track the movement of the interface and predict oil recovery at breakthrough. Comparisons between analytical solutions and experimental results were reported to be good.

Sasaki, Akibayashi, Yazawa, Doan and Farouq Ali (1999) experimentally examined the steam zone behaviour in the early stage of the SAGD process. The experiments were scaled using the B_3 dimensionless group suggested by Butler (1985b). Temperature distribution inside the model reservoir was determined both by thermocouple readings and thermal video system. From this, it was estimated that heat losses from the reservoir were about 60-70% of the total heat injected. Larger vertical spacing between the horizontal injector and producer was found to lead to earlier creation of the steam zone. The authors showed that selectively injecting steam intermittently into the reservoir through the producer (simultaneously with steam injection through the injector) in the earlier stage of the SAGD process led to quicker oil production, enhanced steam zone growth rate and oil production. This SAGD-ISSLW (intermittent steam stimulation of lower well) process was effective in accelerating the instability of the steam zone interface near the steam zone ceiling, and leading to larger steam zone, compared to the conventional SAGD process.

Butler and Mokrys (1989) discussed an analog to the SAGD process for reservoirs unsuitable for steam recovery processes. In this VAPEX (Vapour Extraction) process, a hydrocarbon solvent near its dew point was injected simultaneously with hot water into the top of a thin heavy oil or oil sands reservoir. As the solvent chamber expanded, the solvent diffused into the surrounding oil and diluted it. The mobilized oil drained downwards by gravity, and came into contact with the hot water which vapourized the dissolved solvent out of the draining oil. The warm solvent vapour rose counter-currently upwards, and became warmer as it interacted with the hot water near the top of the reservoir. Once it reached the top, the solvent chamber spread laterally. In this process, the solvent served to dilute the viscous oil, as well as to act as heat carrier for even heat distribution around the vapour chamber. The hot water served to heat the oil, as well as to leach the dissolved solvent from the draining oil for re-use at the top of the chamber. Experimental

22

results showed that the success of the VAPEX process depended on proper selection of the solvent, and the ability to raise reservoir temperature to a suitable range for the optimum recovery and recycling of the solvent.

Das and Butler (1996) considered the countercurrent extraction of solvent in the VAPEX process in a subsequent study. It was determined that using horizontal injector and producer provided a larger contact area for mass transfer, which also enabled more and faster solvent extraction rate. Das (1998) pointed out that the oil produced by the VAPEX process was of higher quality than the reservoir oil, due to the de-asphaltene of the reservoir oil by the solvent. Suggestions were provided to investigate further the effects of capillarity, asphaltene deposition, and reservoir heterogeneity on VAPEX performance.

2.3.2. Numerical Studies and Field Projects

A number of numerical studies of the SAGD process and its variations have been presented in the literature. These studies are often performed in connection to design studies of SAGD pilots and/or field operations.

The first horizontal well drilled in Canada (1978) for thermal recovery of heavy oil and oil sands resources was by Esso Resources Canada Ltd. (ERCL). Adegbesan, Leaute and Courtnage (1991) discussed various aspects of ERCL's Horizontal Well Pilot 1 project in Cold Lake. The pilot consisted of one vertical steam injector, a horizontal producer (length of completed interval being 245 meters), and three vertical observation wells. Different production strategies were tested, including CSS for the horizontal well (i.e. injection and production through the horizontal well), and using the horizontal well as a producer and the vertical well for steam injection. Data such as temperature, bottom-hole pressure, and seismic monitoring data were used in the analysis of reservoir behaviour. The authors established that in the early stage of the pilot pressure drive was the main production mechanism. In the middle stage, the main production mechanisms included solution gas drive and fluid expansion drive (including steam flashing) and compaction drive. Only in the later stage of the pilot did gravity drainage become the main mechanism for oil production. As Farouq Ali (1997) noted, it was difficult to characterize this pilot as a SAGD process due to two main reasons: steam injection was at formation parting pressure, and complex operation due to different production strategies. In addition, the authors determined from history match simulation that approximately 40% of the horizontal producer was contributing to oil production. Presence of non-condensable gas was found to have significant influence on temperature distribution inside the steam zone.

Jain and Khosla (1985) used a commercial simulator to predict the performance of three different combinations of horizontal and vertical wells for an Athabasca oil sand reservoir. In the first combination two 150 m-long parallel wells separated by a distance of 60 m were used. The second combination had a 300 m-long horizontal steam injector in communication with a vertical

23

producer. The last combination had a 400 m-long horizontal producer in communication with 2 vertical steam injectors to create a heated plane over a horizontal well. The first two configurations modeled the steamflood process, while the last configuration simulated a SAGD process. Simulation results showed the last well configuration (SAGD process) had the highest oil production rate along with the highest cumulative oil recovery.

Edmunds, Haston, and Best (1989) described the implementation of the SAGD process at AOSTRA's Underground Test Facility (UTF) in Fort McMurray. The authors analyzed the growth rate of the steam zone in terms of ceiling and slope drainage. Ceiling drainage occurred at the top of a rising steam zone, while slope drainage occurred at the side of the steam zone as it spread sideways. The authors examined the effects of reservoir anisotropy, heterogeneity, solution gas, capillary pressure on the steam zone shape and growth rate. A detailed description was also provided of the UTF, including the drilling and completion practice for the three pairs of horizontal wells. Satisfactory production results were reported.

Siu, Nghiem, Gittins, Nzekwu and Redford (1991) used a coupled reservoir-wellbore simulator to history match injection and production data of UTF's first well pair. The wellbore flow equation accounted for frictional and hydrostatic pressures drops, and heat transfer between flow in the tubing and annulus. It was found necessary to have a pressure drop of 650 kPa over the 150-m horizontal injector to match successfully production pressure data. As such, pressure drop calculations should be determined and incorporated in commercial SAGD operations which utilize long horizontal wells.

Jespersen and Fontaine (1991) discussed Sceptre's operations at the Tangleflags field in Saskatchewan, which demonstrated that the top-drive and gravity-flow principle can be used in reservoirs having bottom water, without excessive water production and without excessive consumption of steam. In this case, vertical steam injectors were used; oil was produced by pressure drive and gravity drainage into the horizontal producer. This was realized by balancing the pressure of the production well against that of the aquifer.

Edmunds and Gittins (1993) used simulation results to examine the effects of wellbore flow on steam distribution and formation of steam zone in SAGD process for long horizontal wells. A semi-empirical correlation was developed for the breakthrough time, which was dependent on reservoir permeability, interwell spacing, pressure differential, wellbore size, etc. Wellbore pressure gradients, particularly those in the horizontal injector, were determined to be an important factor affecting steam zone formation and hence oil recovery. It was found that even small pressure gradients would accumulate over the length of a commercially long horizontal well, and could affect the gravity stabilization of the SAGD process. A simplified analysis was employed to estimate the optimum horizontal well length for the SAGD process.

Kamath, Sinha, and Hatzignatiou (1993) numerically investigated SAGD performance in the heterogeneous, layered Ugnu reservoir in Alaska. Oil viscosity under initial reservoir conditions ranged between 50000 to 10×10^6 mPa.s. The authors modified the SAGD model (Butler, 1985a) for a layered, anisotropic and heterogeneous reservoir. The dimensionless heat and mass balance equations were solved numerically to determine the effects of reservoir characteristics (including presence of shale barriers), horizontal well length, injector-producer spacing, etc. The solutions were compared with Butler's model (1985a) for homogeneous reservoirs, as well as with CMG's STARS^{TM} simulator for heterogeneous reservoirs. There was good agreement in all cases. It was determined that recovery performance was improved with high steam injectivities, high vertical permeability, and optimum spacing between horizontal injector and producer.

Edmunds, Kovalsky, Gittins and Pennacchiloli (1994) reviewed different aspects of AOSTRA's Phase A operation at UTF. Numerical simulation was used in trying to analyze the performance of the pilot, including determining the mechanisms for steam zone growth and oil production, for different reservoir properties and operational parameters. It was observed that solution gas did not accumulate inside the steam zone, and hence did not impact its expansion significantly. Discussion was also provided with a view of planning Phase B commercial operation of the SAGD process at UTF.

Kisman and Yeung (1995) used STARS^{TM} simulator to predict SAGD performance in the Burnt Lake oil sands reservoir. The authors utilized data to construct a geological model prior to setting up their simulation runs. Effects of parameters such as relative permeability, wettability changes, oil viscosity, thermal conductivity, shale barriers, solution gas, operating pressure and placement of the horizontal producer were investigated. Horizontal well length was 1000 meters. It was found that oil viscosity and relative permeability ahead of the steam zone, rather than inside the steam zone, had a large impact on oil recovery.

Donnelly and Chmilar (1995) considered geological screening criteria in evaluating the potential for application of SAGD to McMurray oil sand deposits. The geological screening criteria included thickness of overburden, net pay of oil sand, presence of continuous shale streaks in oil sand pay, etc. Bitumen production rate was estimated using linear and cylindrical geometric steam chamber models as proposed by Reis (1992, 1993) and semi-elliptical steam zone geometry (as observed at UTF). From the analysis, maps of analytical performance contours were prepared.

Hamm and Ong (1995) performed simulation studies on the application of ESAGD process to Shell Canada's Peace River oil sand reservoirs. Different factors were considered, including magnitude of the pressure differentials to promote steam zone growth between two adjacent patterns, pattern spacing, and presence and accumulation of non-condensable gases in the steam zone. It was determined that a relatively small pressure differential (approximately 500 kPa) was required for enhancing steam zone growth between two adjacent patterns.

Accumulation of non-condensable gases were deemed to have negligible effects on steam zone temperature and temperature distribution, as long as these gases were also produced with steam through the producer. Up to 50% increase in oil recovery compared to that obtained by conventional SAGD process was observed after 10 years of operation.

Oballa and Buchanan (1996) discussed the application of hybrid grid surrounding a discretized wellbore to simulate the interaction between the wellbore and reservoir for the SW-SAGD process. Altogether, two different operating strategies, consisted of four different scenarios, were considered. The scenarios included no production of reservoir fluid, reservoir heating due to conduction by steam circulation, co-injection of steam and co-production of oil, and counter-current flow along the wellbore. To model accurately fluid and heat flow inside the wellbore, it was divided into grid blocks in connection with the adjacent reservoir blocks and other wellbore blocks. As such, it was possible to model frictional pressure drop, liquid holdup inside the wellbore. Two different oils were used. It was determined that for the SW-SAGD process balance must be established and maintained between injection and production along the wellbore length.

Ito and Suzuki (1996) carried out an extensive numerical study of the SAGD process performance for the Hangingstone oil sands reservoir in Fort McMurray. Reservoir parameters used in the study were obtained from successfully matched simulation studies performed previously for the CSS process in the same reservoir. Analysis of the temperature distribution at and ahead of the steam zone interface, along with steam zone shape, established that convective heat transfer played the main role in reservoir heating, more so than conductive transfer. Water (steam condensate) flow ahead of the steam zone provided the energy for convective heating of the oil, as well as displaced it. Effects of geomechanical changes introduced into the reservoir (such as changes in reservoir porosity and permeability) on production mechanisms were qualitatively evaluated.

The effects of wells placement on SAGD recovery performance in a marginal reservoir (with gas cap and/or underlying aquifer) were investigated numerically by Chan, Fong, and Leshchyshyn (1997). The aquifer was assumed to be inactive, and only the effects of its thickness was studied. SAGD recovery was found to be reduced by up to 25% by the presence of a gas cap, 50% by the presence of an underlying aquifer. In this type of marginal reservoir, the study revealed that offsetting the horizontal producer from its injector could alleviate the reduction in oil recovery by up to 15%. Similarly, placing the horizontal wells in a repeated pattern such that a horizontal injector supports two horizontal producers could improve oil recovery by another 10%. However, the thermal efficiency of the process was still lowered, in the form of higher SOR.

Kasraie, Singhal and Ito (1997), using CMG's STARS^{TM} simulator, attempted to develop screening criteria for Tangleflags-type reservoirs. Some of the parameters studied included steam-trap operating strategy, oil viscosity, oil pay thickness, and effectiveness and spacing of

vertical injectors from horizontal producer. The authors concluded that the gas cap was beneficial in providing a more even heating of the reservoir. On the other hand, a thin bottom water layer was judged to have little impact on steam injection and oil recovery; an active aquifer, on the other hand, was judged to lead to severe water coning and significant increase in SOR. Increasing the spacing between vertical steam injectors led to higher cumulative oil recovery, but also higher SOR.

Luft, Pelensky, and Williams (1997) detailed a study of the thermal performance of insulated concentric coiled tubing used in SW-SAGD process. The study included experimental measurement of internal and external coiled tubing wall temperature, local heat flux, steam quality, pressure drop, and thermal expansion using a field-scaled 200-ft long ICCT™ spool. Some of these results were also compared with thermal conductivities measured from heat loss test cell. Additionally, the measured temperature profiles were compared with predictions from two-phase flow computer program HOWSCAT™. Agreement between experimental and field measurements of the temperature profiles, and numerical results were within 10% for the case of single-phase liquid flowing inside the annulus.

Dusseault, Geilikman, and Spanos (1998) discussed qualitatively production strategies of combining cold production with sand production in enhancing SAGD production. In these strategies, the SAGD horizontal wells are drilled between rows of cold-production vertical wells. As cold-production rate declined with time, solid (sand) production increased until economic limits, when the vertical wells were converted to inert gas injectors, steam injectors with a view of maintaining reservoir pressure for SAGD operations. These wells could also be converted to sand disposal wells.

Mendoza, Finol and Butler (1999) reported the SAGD pilot test carried out in the Tia Juana field in Western Venezuela. Two different pairs of horizontal wells were drilled. The horizontal well length was approximately 400 meters. One of the most important tasks of this pilot was to evaluate the applicability of tools used to monitor the distribution steam along the injector, and growth of the steam zone in the reservoir with time. Thermocouples and pressure transducers were installed along the horizontal injector, enabling measurement of well temperature profile in real time. First-year production performance was history-matched using CMG's STARS™ simulator, with absolute vertical and horizontal permeabilities being the main adjusted parameters to achieve history match. Simulation results predicted ultimate recovery of 50-60%, compared to 10% recovery achieved by cyclic steam stimulation.

A numerical study of the early-time response for the single-well (SW) SAGD process was reported by Elliot and Kovscek (1999). CMG's STARS™ simulator was used. Three different early-time processes were considered: cyclic steaming, steam circulating, and extreme differential pressure between injection and production sections of the horizontal well. It was found

27

that cyclic steaming was most effective in accelerating early-time heating of the reservoir. A uniform temperature distribution along the entire wellbore was achieved; additionally, all of the injected steam entered the reservoir and heated the near wellbore area. Another finding was that the ultimate oil recovery was similar in all three cases, irrespective of the efficiency of reservoir heating in early time periods.

Donnelly (1999) reported field production data and the simulation study to history match such data for the Hilda Lake pilot. The 950-m (horizontal section) horizontal producer was placed approximately 6 meters below the 900-m horizontal steam injector. There were four observation wells spaced along the horizontal wells. The horizontal producer produced into a wellhead gas-liquid separator, which helped maintain the production pressure constant. Solvent and then steam was injected to create thermal communication between the horizontal injector and producer. There was good agreement between field production data and simulation results. However, it was observed that the steam zone temperature (as measured at the observation wells) was 20-30 $^{\circ}$C lower than that predicted by the simulator. The author believed that pressure drop and presence of non-condensable gases in the steam zone was the cause for this difference.

Doan, Baird, Doan and Farouq Ali (1999) studied the heating efficiency in heavy oil reservoirs underlain and overlain by a contiguous water zone. The authors used CMG's STARS^{TM} simulator to study reservoir heating and oil production for different types of reservoirs (including effects of fluid flow for the contiguous water zone). It was determined that the presence of a bottom water layer had a lesser impact on recovery than the overlying water layer case. Increasing the areal coverage of the bottom water layer (akin to an active water zone) resulted in only a slightly reduced recovery as compared with the confined bottom water layer. However, increasing the areal coverage of the overlying water layer severely reduced the recovery efficiency of the process, as heat was diverted into the overlying water zone.

Ito, Ichikawa, and Hirata (2000) presented new simulation results of the SAGD performance at UTF Phase B and for the Hangingstone project. The authors achieved good matches between simulation results with field data, particularly regarding the location of various temperature contours. It was determined that for UFT Phase B the steam zone growth was detoured by the shale layers in the sand; however, as time went on, the impermeable shale layers became permeable, and bitumen production was still possible. At Hangingstone, the steam was able to pass through some of the shale layers, and there was no significant detouring of the steam zone. In addition, it appeared that the flow took place through were dendritic flow channels which were created due to high steam injection pressure.

Chapter 3 – Statement of the Problem

The research undertaken in this study examines the effects of convective transfers on the performance of the steam-assisted gravity drainage (SAGD) process, which has come to be seen as a promising recovery method for the heavy oil and oil sands resources in Canada. The overall objective is to develop a new analytical 1-D model to describe the transient SAGD process, incorporating the convective transfers such as bulk transfer from the steam zone to the reservoir, heat losses to cap and base rock, and heat loss due to fluid production. The specific objectives of the study are as follows:

1. To investigate the applicability of the Stefan problem in describing the transient expansion of the steam zone, and the transfer of heat from this zone to the reservoir ahead of the steam zone encountered in the SAGD process.

2. To formulate a simplified transient mathematical model to describe the heat and mass transfer processes between the steam zone and the reservoir ahead of the steam zone for the SAGD process.

3. To obtain solution for this model, and compare the solution to other solutions derived for evaluation of the SAGD process performance.

4. To draw conclusions about the utility of the new analytical model of the SAGD process, and provide recommendations for future studies in this area.

29

Chapter 4 – Development of Mathematical Model

4.1. Introduction

The development of a new analytical model for the Steam-Assisted Gravity-Drainage (SAGD) Process is presented in this chapter. First, a review of the "phase change problem" is given, and explanation is provided to illustrate the applicability of the Stefan problem for several steam injection recovery processes. The development of a simplified, transient SAGD analytical model incorporating convective transfers is then shown. Also, assumptions behind the model are stated. Finally, solution to the analytical model is provided.

4.2. Stefan Phase Change Problem

The "phase change problem" (also "moving boundary problem") has important applications in many areas of engineering and science. Typically, in this type of problem, a substance exists near its phase transformation point. As such, it undergoes a phase change, and either emits (releases) or absorbs energy during the phase transformation process. It is readily seen that solidification and melting processes of substances follow this problem. Stefan (circa 1889) first studied this type of problem associated with the freezing of polar ice cap[*]. This study, and other subsequent investigations into the crystallization of liquids, evaporation of liquids and condensation of gases by Stefan led these types of phase change problem being called the Stefan problem.

As Carslaw and Jaeger (1959) pointed out, in some versions of the Stefan problem, the two phases existing in the two regions of the phase envelope of the substance might have different densities, heat capacities, thermal conductivities, and (obviously) temperature distributions. In other cases, the differences in some of the properties might not be significant. The solution of such problems, particularly when the properties of the two phases are different, is inherently difficult because the interface between the two phases is moving as the latent heat is absorbed or released at the interface of the two phases. As a result, the location of the solid-liquid interface is not known a priori, and must form part of the solution (Ozisik, 1980).

An important feature of the Stefan problem is the boundary conditions at the boundary between the two phases (or at the interface, when the two phases occupy two different regions). One boundary condition describes the temperature continuity at the interface. The second boundary condition describes the heat flux across the interface, which is associated with the emission or absorption of heat. The following simple problem, modified from an example provided by Carslaw and Jaeger (1959) illustrates this point more clearly.

---

[*] Carslaw, H.S. and J.C. Jaeger: Conduction of Heat in Solids, Oxford Clarendon Press, 1959, pp. 282-3.

30

A solid substance existing in Region 1 (extending between $x = 0$ and $x = X(t)$) has the following properties: specific heat capacity C_1, thermal conductivity K_1, and thermal diffusivity α_1. Across the interface separating the two phases, the properties of the liquid in Region 2 ($x > X(t)$) are specific heat capacity C_2, thermal conductivity K_2, and thermal diffusivity α_2. It is assumed that the densities of the solid and the liquid phases are the same. This assumption implies there exist negligible change of volume on melting (or solidification). Hence, there is no net motion of the bulk liquid (i.e. no convection). The melting point of the substance is T_b. The temperature distribution in both regions is governed by Fourier's linear heat conduction equation, as follows:

$$\frac{\partial^2 T_1}{\partial x^2} - \frac{1}{\alpha_1}\frac{\partial T_1}{\partial t} = 0 \qquad 0 < x < X(t) \qquad (4.1)$$

$$\frac{\partial^2 T_2}{\partial x^2} - \frac{1}{\alpha_2}\frac{\partial T_2}{\partial t} = 0 \qquad X(t) < x \qquad (4.2)$$

At the interface $X(t)$, temperature continuity dictates that one of the boundary conditions is:

$$T_1 = T_2 = T_b \qquad (4.3)$$

The second boundary condition at this $X(t)$ interface deals with the absorption or emission of latent heat of the substance at this surface. If over a time increment dt, the interface moves a distance $dX(t)$, and if the temperatures in Region 1 and Region 2 are maintained at T_1 and T_2, respectively, then a quantity of $\{L\rho[dX(t)/dt]\}$ of energy is liberated per unit area, where L is the latent heat (per unit mass) of the substance. This emitted heat is removed by conduction. As such,

$$K_1\frac{\partial T_1}{\partial x} - K_2\frac{\partial T_2}{\partial x} = L\rho\frac{dX}{dt} \qquad (4.4)$$

The general solutions to problem posed by Equations (4.1) – (4.4) are:

$$T_1 = A * erf\left(\frac{x}{2(\alpha_1 t)^{0.5}}\right) \qquad (4.5)$$

$$T_2 = T - B * erfc\left(\frac{x}{2(\alpha_2 t)^{0.5}}\right) \qquad (4.6)$$

31

In Equations (4.5) and (4.6) A and B are constants, and are to be determined by the boundary conditions specific to the problem under consideration. These boundary conditions include those at the extremes of the domain, as well as those at the interface separating the domain into Region 1 and Region 2.

The particular solution to the problem requires two additional boundary conditions. Carslaw and Jaeger (1959), Rubenstein (1971) and Ozisik (1980) pointed out that exact solutions (i.e., analytical solutions) are only available to the following cases of the *Stefan problem*: i) semi-infinite region $x > 0$ initially at constant temperature T greater than the melting point, and surface $x = 0$ subsequently maintained at zero temperature, ii) infinite region in which $x < 0$ is initially solid at constant temperature and region $x > 0$ is initially liquid at constant temperature, iii) supply or removal of heat by a continuous line source for cylindrical coordinates. It should be noted that closed form solution does NOT exist for either finite system or systems having radiation condition at $x = 0$. Approximate solutions for all other *Stefan-problem* problems, including multi-dimensional problems, can only be obtained by numerical techniques.

In oil recovery processes utilizing steam injection into the reservoir, the injected steam typically forms a steam zone (or chamber), which expands with time. Inside this steam zone, the pressure is the steam injection pressure, and temperature is the steam (saturation) temperature T_s. Fluid saturations inside this zone typically include residual oil saturation (S_{or}), irreducible water saturation (S_{wir}), and steam saturation (S_{st}). At the steam zone interface, the injected steam condenses and gives up its latent heat of vaporization. This heat is transferred away from the interface by conductive and convective transport to heat up the reservoir and mobilize the viscous crude. The reservoir ahead of the steam zone interface is usually described as having a initial reservoir temperature T_r, and saturations of S_{oi} (initial oil saturation) and irreducible water saturation (S_{wir}). The reservoir pressure p_r might be equal to or less than the steam injection pressure, and the reservoir might also have some initial gas saturation (such as a gas cap) or a bottom-water layer. As steam injection begins and continues, the steam zone expands, steam condenses and gives up its latent heat at the steam zone interface. In order for the steam interface to advance, the injected heat must overcome the heat loss to the cap and base rock. Depending on the recovery process, the steam zone either displaces the fluids ahead of the steam zone interface toward the producer (as in steamflooding), or rises upward in opposite direction of the downward draining of heated oil and condensate (as in SAGD). While the oil production mechanism differs in some aspects between different recovery processes, the reservoir heating and fluid mobilization mechanisms remain similar for all recovery processes. Furthermore, from the discussion provided above, it is clear that the *Stefan problem* provides a good basis for the development of a transient, simplified model for SAGD process performance, with incorporation of convective transfers.

32

4.3. Framework of New Analytical Model for SAGD Process Performance Prediction

A few comments are in order prior to the development of the model. As explained above, the physics of steam injection recovery processes for viscous crude oils is similar to that for the *Stefan problem*. As the injected steam condenses at the boundary of the steam zone, its latent heat is liberated and the steam undergoes a phase change from vapour phase to liquid phase. This phase change results in a change in the density of the substance, and consequently gives rise to convective transport across the steam zone interface (Carslaw and Jaeger (1959), Rubenstein (1971) and Ozisik (1980)). Rubenstein (1971) demonstrated clearly the applicability of the *Stefan problem* to a variety of problems of fluid displacement in porous media, including waterflooding.

The SAGD process, like steamflooding or CSS, is in reality a 3-D flow problem. Figures 4.1 a-b show the 2-D cross-sectional view of the horizontal well pair (injector above, and producer below) and steam zone at two different times. Figure 4.2 shows the 3-D view of the steam zone, with the effects of wellbore hydraulics on its growth (including profile) depicted. As seen clearly in Figure 4.1, the location of the horizontal injector and producer in the SAGD process promotes the steam chamber to grow initially in the vertical plane until the it reaches the cap rock. This stage is known as ceiling drainage stage. The rate at which the steam zone grows, and oil drains, is controlled mainly by the vertical permeability (k_v). Once the steam zone reaches the cap rock, the steam zone spreads sideways. The drainage of oil at this stage is commonly referred to as slope drainage. It is observed that near the top of the reservoir, the steam zone expands sideways (away from the well pair), while at the bottom, oil and steam condensate flow toward the producer. The flow streamlines associated with the SAGD process are, quite clearly, different than those in steamflooding or CSS.

When the flow in the horizontal wellbore is coupled to the flow in the reservoir, the pressure drop (due to friction) and temperature drop (heat loss) inside the well have to be accounted for, as they have an impact on the steam quality distribution along the well length (between the heel and toe of the horizontal well). As a result, the amount of latent heat, which affects the growth of the steam zone, varies along the well length. This, in turns, leads to uneven growth of the steam chamber along the well length and affects oil recovery. Experimental work, conducted by Doan (1996) in a visual model, showed clearly larger steam zone near the heel, and smaller steam zone near the toe of the horizontal injection well. The uneven growth of the steam chamber may be mitigated by increasing the steam flow rate. Coupling of wellbore flow with reservoir flow is not considered in this work. The 3-D flow problem is, therefore, reduced to a 2-D flow problem.

33
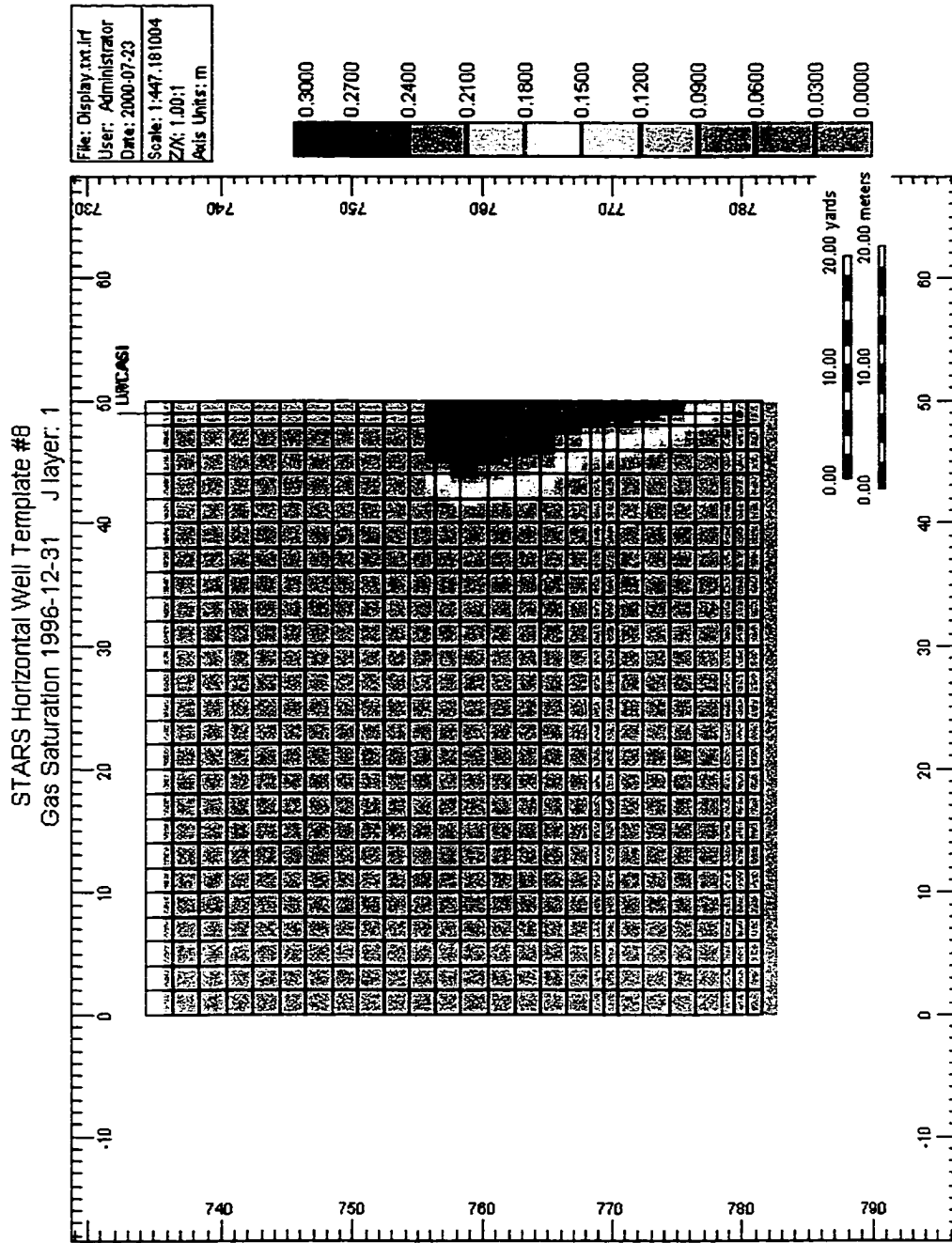
Figure 4.1a: Steam Zone at Early Stages of SAGD Process – Illustrating "Ceiling" Drainage, STARS™ Simulator.

34
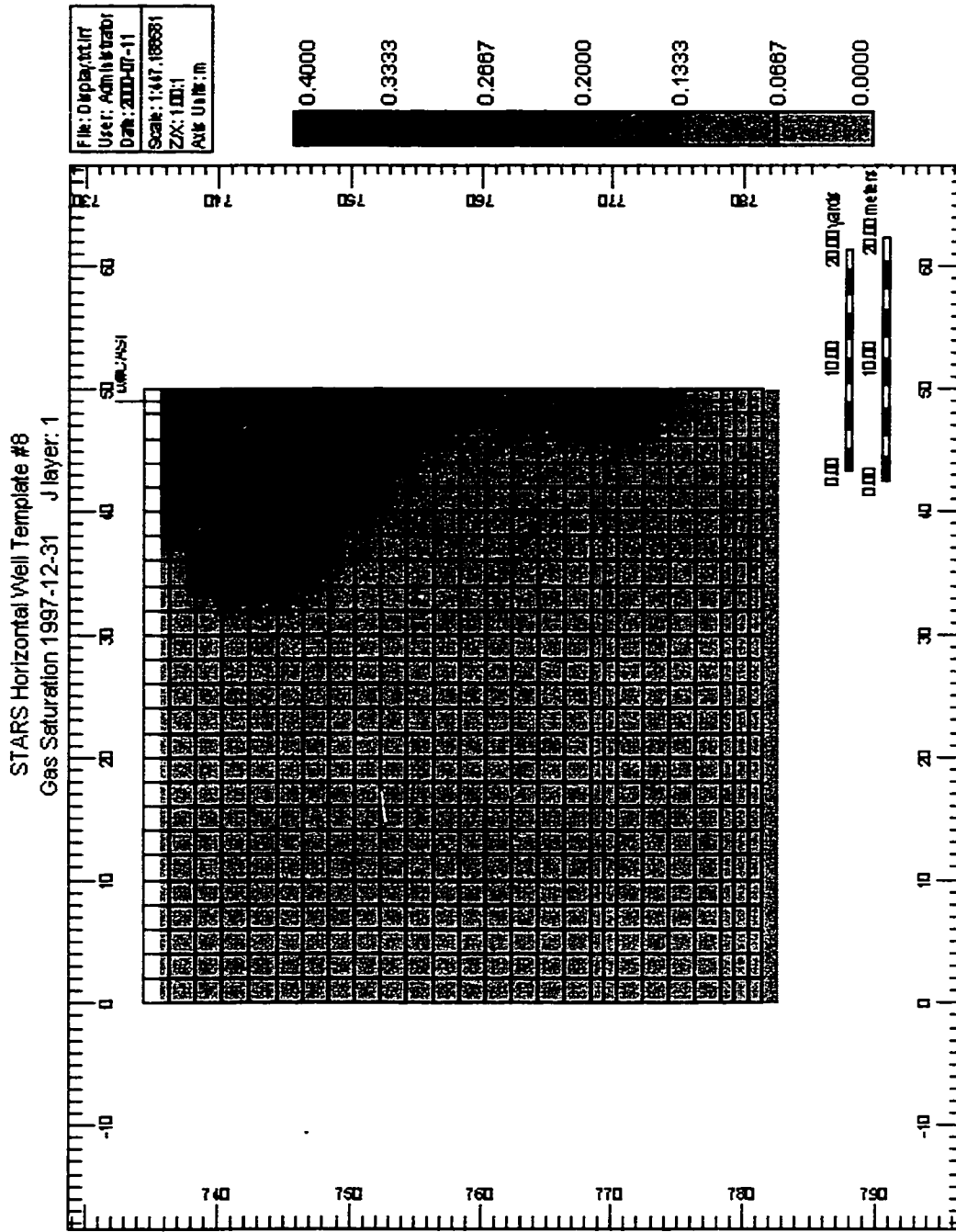
Figure 4.1b: Steam Zone at Late Stages of SAGD Process – Illustrating "Slope" Drainage, STARS™ Simulator.

35

STARS Horizontal Well Template #8
Gas Saturation 1997-12-31

File: Display.txt.in
User: Administrator
Date: 2000-07-11

Z/X: 100:1

0.3000

0.2500

0.2000

0.1500

0.1000

0.0500

0.0000
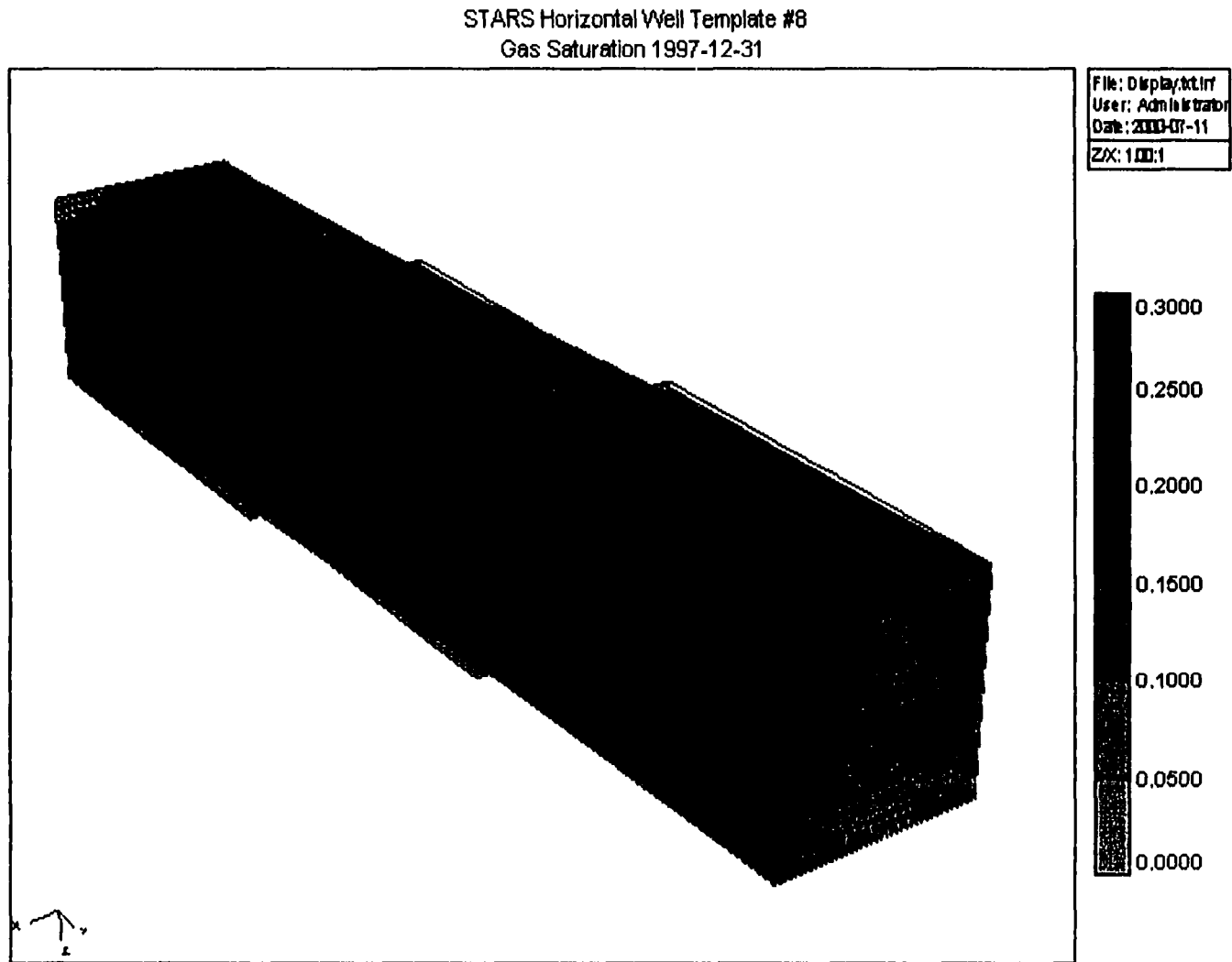
Figure 4.2: 3-D View of Steam Zone, Effects of Wellbore Hydraulics on Steam Zone Growth Depicted, STARS™ Simulator.

Analytical solutions of the *Stefan problem* in "actual" 2-D problems do not exist, however, as Carslaw and Jaeger (1959), Rubenstein (1971) and Ozisik (1980) had already pointed out. In consideration of these facts, the development of the SAGD model in this thesis is simplified to be 1-D. The development of this analytical model does not take into account the initial "cylindrical" growth of the steam chamber. It assumes slope drainage is present instantly. Depending on the vertical permeability of the reservoir, reservoir pay thickness and/or operating conditions (i.e. inject at sufficiently high pressure to enhance vertical permeability). Figure 4.3 is a cross-sectional drawing of the expanding steam zone, along the well axis, typically encountered in a SAGD process, subsequent to the initial growth of the chamber. It is also the basis for the development of the new analytical model for transient SAGD process performance with convective transfers. The interface has a "conical" profile along the vertical plane of the reservoir. It is seen that the steam zone interface separates two regions. Inside the steam zone (Region 1) the pressure is p_s (steam injection pressure), temperature is T_s the steam temperature, S_{or} (residual oil saturation), S_{wir} (irreducible water saturation), and S_{st} (steam saturation). Region 2 is on the other side of the steam zone interface (where the temperature is T_s), and has S_{oi} (initial oil saturation) and irreducible water saturation (S_{wir}). Temperature in Region 2 is less than T_s, and its distribution is a function of the heat transfer mechanisms taking place in this region. Heat losses to the cap and base rock, along with heat removed from the reservoir in the produced fluid, also affect the heat distribution in Region 2. The interface velocity varies at different positions along the vertical plane, at different times.

Given these considerations, the new analytical model is developed as a 1-D model (mainly). The temperature distribution is determined from solution to the 1-D transient transport equation (also known as the Burger's equation), with both conductive and convective transports incorporated. It is noted that this equation is derived from the energy balance equation and then incorporating the definition for conductive and convective transport. This temperature distribution is strictly a function of the spatial and temporal variables x and t. Additionally, in order to describe the non-vertical profile of the steam zone interface with time the reservoir is divided into several sections (or layers). Within each of these sections, the temperature distribution is found, and the solution to the *Stefan problem* is obtained to determine the position of the steam zone interface. This approach, as suggested by Rubenstein (1971), has the effect of approximating an actual 2-D flow problem (involving both heat and mass transfers) into a pseudo 2-D problem. Its main advantage is that solution to the *Stefan problem* is feasible.

4.4. Development of New Analytical Model for SAGD Process Performance Prediction

4.4.1 Development of New Analytical Model for SAGD Process

Figure 4.3 shows the growth of the steam chamber during slope drainage, which is established after ceiling drainage. Prior to developing the analytical model for SAGD process, a brief general

discussion of the SAGD process is provided below. Steam injection results in the existence of two regions in the reservoir at any time. The pressure and temperature in the steam zone (Region 1) are p_s and T_s throughout the zone. Oil saturation inside the steam zone is at S_{or} (residual oil saturation) level. The remaining pore volume inside the steam zone is filled up with steam (saturation S_{st}) and water (saturation S_w) (which might be equal to, or larger than the irreducible water saturation, S_{wir}). As the steam zone expands with time, these conditions remain, and the only variable is the volume (size) of the steam zone. This is manifested by the fact that the position of the steam zone interface $X(t)$ is calculated at different times from the model.

Overburden

Heat Losses to Cap Rock
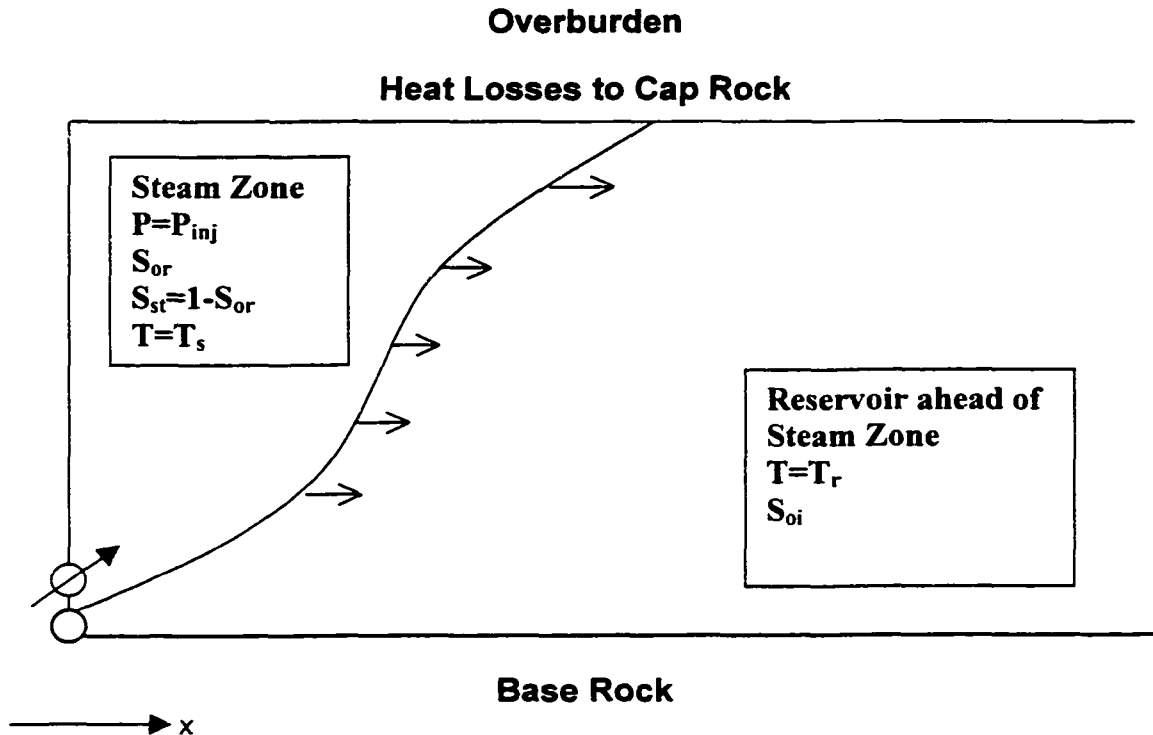
Figure 4.3: Cross-Section Drawing of Expanding Steam Zone in SAGD, with Flows of Heat and Oil in Reservoir Element near the Steam Zone Interface.

1) steam chamber spreads along the top and downward from the start of the process, i.e. slope drainage is present from the start. Ceiling drainage, which takes place in the initial stage of the actual SAGD process is not considered,

2) steam injection rate is high enough to overcome heat losses, and simultaneously provide sufficient energy for the steam zone interface to move forward into the reservoir. A more mathematically rigorous description of the dynamics associated with steam zone expansion requires incorporation of heat loss to cap rock and base rock, as a function of the volume of the expanding steam zone (or more correctly, the

38

contact area between the heated reservoir and its adjacent rock layers), temperature gradients along this contact area, conductive and convective heat fluxes and mass fluxes along the steam zone interface. The features, if incorporated, would render the model intractable, and analytical solution impossible. In view of these considerations, the development of the new analytical SAGD model considers only the dynamics of heat and mass transfers at, and ahead of the moving interface (i.e., in Region 2),

3) single-phase steam flow takes place in Region 1, and single-phase oil flow takes place in Region 2,

4) fluid saturations (S_{oi}, S_{wir}), pressure (p_i), temperature (T_r) are initially uniform throughout the reservoir. Initially, the reservoir temperature T_r is equal to temperature of the cap and base rock (i.e., there is no temperature gradient between the reservoir and its cap and base rock),

5) rock properties such as permeability, porosity, density, and thermal conductivity are uniform within each of the adjoining sections (layers) in the reservoir,

6) the oil is assumed to be dead oil (i.e., there is no gas dissolved in solution); as such, there is no gas cap (or gas pockets) formed in the reservoir due to liberation of solution gas, with steam injection,

7) fluid saturation distribution in Region 2 includes the irreducible water saturation (S_{wir}) and oil saturation (S_o) which is larger than S_{or} (residual oil saturation),

8) fluid properties such as density and viscosity are functions of temperature only. Similarly, rock properties such as density, heat capacity, and thermal conductivity are functions of temperature only,

9) there is no initial gas cap in the reservoir,

10) steam injection does not create fractures in the reservoir rock, as the steam injection pressure is less than formation frac pressure. Neither does it change fluid wettability in the reservoir rock.

The formulation of this analytical model, and derivation of the governing equations start from first principle, including the mass and energy balance equations. Consideration of the volume element for derivation of energy balance (as shown in Figure A1) leads to the following equation,

$$\frac{\partial u_{e,x}}{\partial x} + \frac{\partial u_{e,y}}{\partial y} + \frac{\partial u_{e,z}}{\partial z} = -\frac{\partial \rho_e}{\partial t} \tag{4.7}$$

Assuming 1-D flow along the x-direction, and incorporating conductive and convective energy flux give,

39

$$u_{e,x} = -k\frac{\partial T}{\partial x} + u_f \rho_f h_f \qquad (4.8)$$

where h_f is the enthalpy of the mobile fluids, leads to Equation (4.9),

$$\rho C^* \frac{\partial T}{\partial t} + u_f \rho_f C_f \frac{\partial T}{\partial x} - k\frac{\partial^2 T}{\partial x^2} = 0 \qquad (4.9)$$

The above equation forms the basis for energy transport in Region 2. The first term appearing in Equation (4.9) represents the accumulation (or depletion) in the internal energy of the overall system (including the rock matrix and the fluids stored in the pore space). The velocity u_f in the convective term represents the bulk velocity of the (collective) mobile fluid. The third term in this equation represents the conductive transport. Appendix A provides the derivation of the above equation. It is noted that Equation (4.9) has the form similar to Burger's 1-D transport equation:

$$\frac{\partial T}{\partial t} + u\frac{\partial T}{\partial x} - \alpha\frac{\partial^2 T}{\partial x^2} = 0 \qquad (4.10)$$

Many engineering books discussing the transport equation, its solutions and applications are available in the literature (for example, Patankar (1980), Fletcher (1988)).

Since energy is associated with mass, it is convenient at this stage to define different densities present and are used in the model. The total density in Regions 1 and 2 are defined by,

$$\rho_{1,total} = (1 - \phi)\rho_{r,1} + \phi(\rho_o S_o + \rho_w S_w)_1 \qquad (4.11)$$

$$\rho_{2,total} = (1 - \phi)\rho_{r,2} + \phi(\rho_o S_o + \rho_w S_w)_2 \qquad (4.12)$$

The density of the mobile fluids moving in Region 1 and Region 2 are given by Equations (4.13) and (4.14), respectively. The movement of these mobile fluids from Region 1 to Region 2, across the steam zone interface, constitutes the convective transfer in the overall transport.

$$\rho_{1,mf} = \phi[\rho_{st}S_{st} + \rho_o(S_{o,1} - S_{or}) + \rho_w(S_{w,1} - S_{wc})]_1 \qquad (4.13)$$

$$\rho_{2,mf} = \phi[\rho_o(S_{o,2} - S_{or}) + \rho_w(S_{w,2} - S_{wc})]_2 \qquad (4.14)$$

The density of the mobile fluid that is produced from the reservoir is given by,

40

$$\dot{\rho_{mf}} = \phi \left[\rho_o \dot{S_o} + \rho_w \dot{S_w} + \rho_{st} \dot{S_{st}} \right]$$

$$(4.15)$$

Rubenstein (1971) had considered mass balance at the interface separating two zones of different densities, and obtained an expression for the mass flux associated with the moving interface. Following this consideration, the mass balance across the steam zone interface for the SAGD process is obtained. This mass flux is given by the following equation,

$$\left(\rho_{2,total} - \rho_{1,total} \right) \frac{dX}{dt} = \left(\rho_{2,mf} u_2 - \rho_{1,mf} u_1 + \dot{\rho_{mf}} \dot{u} \right)$$

$$(4.16)$$

The derivation of the mass balance at the interface is further discussed and illustrated in Appendix B. The terms on the left hand side represent the difference in the total mass accumulation between Region 1 (steam zone) and Region 2 (which contains oil and steam condensate) as the interface moves. The first and second terms on the right hand side represent the difference in the mobile mass flux in Region 2 and Region 1, respectively. The third term represents the mass produced from the reservoir. Given assumption 2, the velocity for Region 1 is given by Equation (4.17), which shows that the convective velocity from the steam zone is coupled to the moving steam zone interface.

$$u_1 = \gamma_1 \frac{dX}{dt}$$

$$(4.17)$$

Also, fluid production is assumed to take place along the moving steam zone interface. As such, the production flux is coupled to the velocity of the steam zone interface, as given by Equation (4.18),

$$\dot{u} = \gamma \cdot \frac{dX}{dt}$$

$$(4.18)$$

Substituting Equations (4.17)-(4.18) into Equation (4.16), and solving the resulting equation for the bulk convective velocity in Region 2 gives,

$$u_2 = \frac{1}{\rho_{2,mf}} \left[\left(\rho_{2,total} - \rho_{1,total} \right) + \gamma_1 \rho_{1,mf} - \gamma \cdot \dot{\rho_{mf}} \right] \frac{dX}{dt}$$

$$(4.19)$$

The bulk convective velocity in Region 2 is also related to the steam zone interface velocity $\{d(X(t)/dt\}$ as follows,

$$u_2(y) = \gamma_2(y) \frac{dX}{dt}$$

$$(4.20)$$

41

Recalling Rubenstein's suggestion for simplifying 2-D problems (as discussed in Section 4.3), it is seen that in Equation (4.20) the bulk convective velocity in Region 2 is a function of the vertical position of the steam zone interface, which is moving at different velocities in different layers.

In problems where convective transport is present, the mass flux moving ahead of the interface must be associated with the energy (conductive and convective) flux. It should be clearly understood that mass and energy "goes hand in hand". Following the argument developed by Rubenstein (1971), an energy balance at the interface was derived for the SAGD process. The development of this equation is illustrated in Appendix B, and is given by Equation (4.21),

$$
(\rho_2 h_2 - \rho_1 h_1)\frac{dX}{dt} = \rho_{1,mf} u_1 h_1 - \left(\rho_{2,mf} u_2 h_2 - K_2 \frac{\partial T_2}{\partial x}\right) + (\Delta H)_{loss} \frac{dX}{dt}
$$

$$(4.21)$$

Rearranging the above equation gives the following expression,

$$
-k_2 \frac{\partial T_2}{\partial x} = (\rho_1 h_1 - \rho_2 h_2)\frac{dX}{dt} + (\Delta H)_{loss} \frac{dX}{dt} - (\rho_{2,mf} u_2 h_2 - \rho_{1,mf} u_1 h_1)
$$

$$(4.22)$$

From Equation (4.22), it is seen that the net heat flux into Region 2 is equal to the sum of the change in the enthalpy associated with the change in the position of the steam zone interface over a time step dt, total heat loss (which is composed of heat loss to cap and base rock, and the heat transfer associated with the net bulk convective transport from Region 1 to Region 2 (as given by last two terms on the right hand side of Equation (4.22)). The transport of this net heat flux in Region 2 is governed by both conductive and convective heat transfers. The total heat loss term $(\Delta H)_{loss}$ is composed of the heat losses to cap and base rock. Due to the previously stated assumption regarding conditions for Region 1 (i.e., non-changing conditions inside the expanding steam zone, with only changing parameter is its volume due to moving steam zone interface), the heat losses to cap and base rock are considered as sink term.

The heat transfer within Region 2, but some distance away from the moving steam zone interface, is conductive. The steam zone interface moves due to convection from Region 1 to Region 2, as a result of phase change and fluid production, and not due to pressure driving force (along the x-direction) which may exist between the injector and producer. The magnitude of convective transport is determined by how much fluid has accumulated or been withdrawn from the interface.

42

Having established the energy balance condition and mass balance at the interface, the partial differential equation representative of the conductive and convective transport in Region 2 is rewritten below,

$$k_2 \frac{\partial^2 T_2}{\partial x^2} - \left(\rho_{2,mf} C_{2,mf}\right) u_2 \frac{\partial T_2}{\partial x} = \left(\rho_{2,total} C_{2,total}\right) \frac{\partial T_2}{\partial t}$$

(4.23)

The following parameters are defined to simplify the expression in Equation (4.23),

$$\alpha_2 = \frac{k_2}{\rho_{2,total} C_{2,total}}$$

(4.24)

$$\beta = \frac{\rho_1}{\rho_2}$$

(4.25)

Also, the bulk convective velocity in Region 2, u_2, is given by Equation (4.19). Combining these expressions with Equation (4.23) gives Equation (4.26).

$$\alpha_2 \frac{\partial^2 T_2}{\partial x^2} - \Gamma \left(\frac{dX}{dt}\right) \frac{\partial T_2}{\partial x} = \frac{\partial T_2}{\partial t}$$

(4.26)

where,

$$\Gamma = \left[1 + \beta(\gamma_1 - 1) - \frac{\rho_{mf}^{\bullet} \gamma^{\bullet}}{\rho_{2,mf}}\right] \frac{\left(\rho_{2,mf} C_{2,mf}\right)}{\left(\rho_{2,total} C_{2,total}\right)}$$

(4.27)

Equation (4.26) describes the temperature distribution in Region 2 ahead of the steam zone interface, which is moving at the velocity (dX/dt). As such, this temperature distribution is valid at the interface and ahead of it. The term $\Gamma(dX/dt)$ is the net bulk convective movement of fluid into Region 2.

Mathematically, for this type of moving-boundary problem, the solution of the partial differential equation is associated with the following boundary conditions at the interface:

$$\left\{-K_2 \frac{\partial T_2}{\partial x} = \left(h_1 - h_2\right)\frac{dX}{dt} + (\Delta H)_{loss} \frac{dX}{dt} - \left(\rho_{2,mf} u_2 h_2 - \rho_{1,mf} u_1 h_1\right)\right\}\Big|_{\frac{dX}{dt}}$$

(4.28a)

$$T_2 = T_s$$

(4.28b)

43

At the outer boundary condition:

$$T_2 = T_r \qquad , x \to \infty \qquad (4.29)$$

The initial condition is given by,

$$T_2(x, t = 0) = T_r \qquad (4.30)$$

4.4.2 Heat Loss to Cap Rock and Base Rock

The flow of heat to the cap rock and base rock is perpendicular to the 1-D energy transport considered in this work. As such, the partial differential equation describing this heat loss cannot be directly incorporated into the governing 1-D conductive-convective transport equation. However, the heat loss to the cap and base rock definitely has an influence on the position of the steam zone interface and its velocity (especially at the top of the reservoir). For this reason, the heat loss to the cap rock and base rock would be incorporated in an explicit manner. This approach had been discussed by Neuman (1985), and is given below,

$$\alpha \frac{\partial^2 T}{\partial y^2} = \frac{\partial T}{\partial t} \qquad (4.31)$$

Equation (4.31) describes the conductive heat transfer in the y-direction (or more accurately, direction perpendicular to the x-direction, along with the steam zone interface moves), from the reservoir to the cap rock and base rock. It is subjected to the following initial condition and boundary conditions,

$$T(y, t = 0) = T_r\big|_{y=0} \qquad (4.32a)$$

$$T(y, t) = T_s\big|_{y=0} \qquad (4.32b)$$

$$T(y, t) = T_r\big|_{y=\infty} \qquad (4.32c)$$

The solution to the above conductive heat loss equation, subject to its initial condition and boundary conditions is given by,

$$\Delta T(y, t) = \Delta T_s erfc\left(\frac{y}{2\sqrt{\alpha t}}\right) \qquad (4.33)$$

The heat flow to the cap rock and base rock is, therefore,

$$\dot{q} = -k_h \frac{\partial T}{\partial y} \qquad (4.34)$$

44

4.4.3 Drainage Rate

The treatment of fluid production from the reservoir in the new analytical model follows mostly the approach utilized by Butler et al. (1981). Oil drainage rate is approximated by Darcy's law for gravity drainage, and is given by Equation (4.35),

$$dq = L\frac{kg}{v}dX$$

$$(4.35)$$

Following Butler et al.'s formulation (1981), material balance is considered for the mobile fluid as the steam zone interface moves and fluid production takes place. This consideration leads to the following equation,

$$\left(\frac{\partial x}{\partial t}\right)_y = -\frac{1}{L\phi\Delta S_o}\left(\frac{\partial q}{\partial y}\right)_t$$

$$(4.36)$$

In Equation (4.36) the drainage rate is related to the position of the steam zone interface. Oil drainage rate is time dependent, and is a function of the drainage potential, since the drainage velocity u^* is coupled to the position of the interface and its velocity (dX/dt). Appendix B contains the derivation of Equation (4.36). The overall oil drainage rate is given by Equation (4.37),

$$q = \int_0^h \frac{dq}{dy}dy = L\int_0^h u^* dy$$

$$(4.37)$$

It is seen in Equation (4.37) that the drainage rates at different elevations in the reservoir contribute to the overall fluid production rate. It is noted that Butler et al. (1981) were able to obtain a closed form expression for the incremental drainage rate, from their assumption of constant interface velocity. In this work, the steam zone interface velocity is changing with time.

Having completed the above formulation, it is clear that the proposed analytical SAGD model in this work is significantly different from existing SAGD analytical models in that the heat loss to the cap and rock and heat produced are accounted. In this "pseudo" 2-D model, the position of the steam interface, hence the speed at which it moves come directly from the governing equations.

4.4.4. Convective Transport vs. Conductive Transport

The formulation of the new analytical model for the SAGD process is given in Section 4.4. As seen from Equations (4.16) and (4.19), the net convective transport of mass across the steam zone interface into Region 2 is composed of the convection due to phase change (i.e., condensation of steam) (as discussed by Carslaw and Jaeger, 1959, and Rubenstein, 1971), the

45

convection due to movement of the mobile fluids out of Region 1 into Region 2, and the convection due to the production of mobilized fluids (along the steam zone interface) from the reservoir.

Part of the heat transfer into Region 2 is coupled with the convective mass flux across the steam zone interface, as seen from Equations (4.21)-(4.22). In addition to the convective heat flux due to the transport of heat-carrying fluids (i.e., the various mobile fluids have their own "energy levels" associated with their temperatures) from Region 1 into Region 2, the condensation of steam at the steam zone interface provides a source of energy (equal to the latent heat of vaporization) which also contributes to the heat transport into Region 2. On the other hand, part of the energy is lost from the reservoir due to the heat conducted into the cap rock and base rock. Also, the production of hot fluids from the reservoir entails the convective removal of some energy from the reservoir. The net heat transported into Region 2 is then transferred inside the unheated reservoir by conduction, due to the temperature gradients existing at different parts of the reservoir ahead of the steam zone interface.

It is seen quite clearly that the convective transfers modeled in this work for the SAGD process are quite different from those typically considered for the steamflood process. In steamflooding, the steam front propagates from the higher-pressure injector (source) to the lower-pressure producer (sink). As this steam front propagation takes place, mobilized fluids (condensate, oil and maybe gas) are pushed toward the producer (pressure sink). Also, heat is conducted from the reservoir into the cap rock and base rock. Pressure gradients, which exist in the reservoir between the injector and producer, are quite high in the steamflood process – particularly near the steam zone interface, due to the low mobility of the unheated oil in the reservoir ahead of the steam zone. On the other hand, fluid movement in the SAGD process is mainly due to gravity differences. This gravity-driven fluid flow is true for both the vertical rise of the steam, and the downward drainage of mobilized oil and condensate.

In summary, it is seen quite clearly that this formulation of the new analytical model for the SAGD process, which is based on the formulation of a moving-boundary problem (Stefan problem), is significantly different from existing SAGD analytical models. It accounts for the heat loss (to the cap rock and base rock), as well as heat produced. In this "pseudo" 2-D model, the position of the steam zone interface, and hence, the speed at which it moves at different times come directly from the governing equations. As the equations are derived in progression, discussion on the strength and weakness of this model is provided.

4.5. Solution of Analytical Model for SAGD Process Performance Prediction

The solution to the new analytical model for the SAGD Process – subject to appropriate boundary conditions and initial condition, as described in the preceding section – is given by,

46

$$T_2 = T_r + B * erfc\left[\frac{x}{2\sqrt{\alpha_2 t}} - \lambda\Gamma\right] \qquad , \qquad X(t) < x < \infty \qquad (4.38)$$

$$X(t) = 2\lambda\sqrt{\alpha_2 t} \qquad (4.39)$$

Equation (4.38) describes the temperature distribution at and ahead the moving steam zone interface, i.e. region 2. There are two unknowns in the above solution: B and λ. The particular solution is obtained by utilizing the boundary conditions and the initial conditions. The value B is given by,

$$B = \frac{T_s - T_r}{erfc[\lambda - (1 - \Gamma)]} \qquad (4.40)$$

The value of λ is the root of the following equation,

$$k_2\left\{\frac{T_s - T_R}{erfc[\lambda(1-\Gamma)]}\frac{2}{\sqrt{\pi}}e^{-\left\{\frac{x}{2\sqrt{\kappa_2 t}}-\lambda\Gamma\right\}^2} \bullet \frac{1}{2\sqrt{\kappa_2 t}}\right\} = \{\rho_1 h_1 + \rho_2 h_2 + \Delta H_{loss} - \rho_2\Gamma h_2 + \rho_1\gamma_1 h_2\}\lambda\sqrt{\frac{\kappa_2}{t}}$$

$$(4.41)$$

It can be seen that the solution depends on the parameter λ, as it couples the temperature distribution and the position of the interface. It is noted that λ is a single-value parameter; hence, the solution to the formulated problem is unique (Rubenstein, 1971).

As stated previously, the reservoir is divided into a number of layers. Within each layer the position of the steam zone interface at any time $X(t)$ is determined. As such, the position of the steam zone interface is also a function of the vertical height of the layer in consideration, i.e.

$$u_1(y) = \gamma_1(y)\frac{dX(y)}{dt} \qquad (4.42)$$

$$u^\bullet(y) = \gamma^\bullet(y)\frac{dX(y)}{dt} \qquad (4.43)$$

$$u_2(y) = \gamma_2(y)\frac{dX(y)}{dt} \qquad (4.44)$$

The solution procedure to the formulated problem is straightforward, and consists of a number of steps. The solution requires first the calculation for fluid density. Next, the production potentials is calculated. The total heat loss is an input parameter. The magnitude of the heat loss to cap and

47

base rock is calculated from solution to the vertical heat conduction problem between the reservoir and its adjacent cap rock and base rock (as presented by Neuman 1981). The most difficult step in the solution procedure is the determination of λ, the root of Equation (4.41). This variable couples the temperature distribution to the position of the steam interface and its velocity. An Excel™ macro was used to find λ. Once λ is found and a time value input into the model, the temperature distribution, the position of the interface along with its velocity, and oil production rate and cumulative production are calculated by the model. As this is an analytical model, there is no iteration required in the calculation for the solution.

48

5.1. Introduction

Results from the new analytical model to investigate the transient SAGD process performance, with incorporation of convective transfers are presented in this chapter. In addition, these results are compared against solutions offered by Butler et al. (1981a, 1985a), and results obtained from a commercial reservoir simulator.

5.2. Solutions Offered in Other Analytical Models

The following two examples are reproduced from several previously presented works. These examples have been carefully reviewed, and selected for this work mainly to illustrate how Butler utilized his models to determine different parameters associated with SAGD performance, including the velocity of the steam zone front, taking into account the assumptions behind these models. From these examples, comparison is made between the results predicted by the new analytical model developed in this work and results obtained by Butler.

5.2.1. Example 1 from Butler's Monograph (1994)

In this example, performance parameters for the SAGD process are determined for an oil sand reservoir containing Cold-Lake-type bitumen. The reservoir has the following characteristics: thickness of 34 meters, porosity of 0.31, permeability of 1.3 darcies. Reservoir thermal diffusivity is 0.0465 m^2/d. Initial oil saturation is 0.77, and irreducible water saturation in the reservoir is 0.23. Residual oil saturation to steam is estimated to be 0.15. Initial reservoir temperature is determined to be 14 °C. The length of the horizontal producer for this SAGD operation is 500 meters. It is planned to inject steam at a pressure of 1.9 MPa. From laboratory measurements, oil density is determined to be 940 kg/m^3, and oil viscosity is 120 cp at a temperature of 100 °C.

Numerically, the conditions are given as follows.

H = 34 meters

k = 1.28×10^{-12} m^2 (1.3 darcies)

ϕ = 0.31

α = 0.0465 m^2/d (0.5 ft^2/d)

S_{oi} = 0.77

T_i = 14 °C

S_{or} = 0.15 (estimated)

p_s = 1.9 MPa (275 psia)

ρ_o = 940 kg/m^3 at 100 °C

μ_o = 120 mPa.s at 100 °C

49

L = 500 m

The saturation temperature for steam injection pressure of 1.9 MPa is calculated to be 210 °C (i.e., T_s = 210 °C). Kinematic viscosity of the crude as a function of temperature is approximated using Walther's correlation,

$$log_{10}(log_{10}(v+0.7)) = a^* log_{10}(T+273) + b$$

where v is in cs or mm^2/sec, and T is in °C; Butler (1991) suggested the following correlation to describe the relationship between the parameters a and b,

$$a = 0.3249 - 0.4106b$$

Given data for oil viscosity and density at 100 °C, its kinematic viscosity is easily determined,

$$\rightarrow v = \mu/\rho = 120/0.940 = 127.7 \text{ cs at } 100 °C$$

This data enables the values for a and b to be determined; solving for a and b:

$$a = -3.4294,$$

$$b = 9.1435$$

Therefore, the oil kinematic viscosity at saturation temperature is: v_s = 6.7 cs. Similarly, the values of kinematic viscosity at different temperatures within the 14-210 °C range are determined, as shown below. These values are needed to evaluate the parameter m in the oil drainage equation.

T (°C)	14	50	100	150	200	210
v (cs)	151814	2850	128	22.7	7.9	6.7

Table 5.1: Kinematic Viscosity vs. Temperature for Example 1

The next step is to determine

$$\frac{1}{mv_s} = \int_{T_{r+\delta}}^{T_s} \frac{dT}{v(T-T_r)} \tag{5.1}$$

Using numerical integration technique gives the following set of values for the integral:

δ (°C)	1	6	11	16
Integral (s/m^2)	43844	43819	43807	43792

Table 5.2: Kinematic Viscosity Integral vs. Temperature for Example 1

Using the first point in Table 5.2: $m = 1/(43844 \times 6.7 \times 10^{-6}) = 3.40$

Oil production rate is calculated using the following equation (similar to Equation (2.12)):

$$q = 2L \sqrt{\frac{1.3 kg \alpha \phi \Delta S_o h}{m v_s}}$$

(5.2)

with

$k = 1.3$ darcies $\times 0.9869 \times 10^{-12}$ m^2/darcy $\times 0.4 = 5.13 \times 10^{-13}$ m^2

(with the value of 0.4 being the estimated average relative permeability for oil)

$\alpha = 0.5 \times (0.3048)^2$ m^2/d $\times 86400$ s/day $= 5.38 \times 10^{-7}$ m^2/s

$\Delta S_o = 0.77 - 0.15 = 0.62$ (mobile oil saturation)

$\rightarrow$ q = 1.004×10^{-3} m^3/s = 86.76 m^3/d (or 546 b/d)

The steam front advance rate is next calculated. Butler (1994) had suggested Equation (5.3) to determine the steam front velocity at $(y/h) = (1/\sqrt{3})$.

$$U = \frac{h}{\sqrt{3(t^2 + t_c^2)}}$$

(5.3)

where the characteristic time t_c is defined by the following,

$$t_c = 0.5h \sqrt{\frac{m v_s \phi \Delta S_o h}{1.3 kg \alpha}}$$

(5.4)

In early time (when $t < t_c$), then:

$$U = \frac{1}{\sqrt{3}} \frac{h}{t_c}$$

(5.5)

The temperature ahead of the moving steam front is given by Equation (5.6),

$$T^* = \frac{T - T_r}{T_s - T_r} = e^{-(U\xi/\alpha)}$$

(5.6)

51

Using the above equations, $t_c = 1.11 \times 10^8$ sec = 1281 days

$$U = 1.77 \times 10^{-7} \text{ m/sec} = 0.015 \text{ m/d}$$

Solving Equation (5.6) for a value of $T^* = 0.5$ gives:

$$\xi \text{ (for } T^* = 0.5) = 2.1 \text{ m}$$

In summary, it is seen that for the given reservoir conditions and injection pressure of 1.9 MPa, the steam front moves at a velocity of 0.015 m/d after 1281 days (3.5 years). Oil production rate is 86.7 m³/d (approximately 550 b/d) for the 500-m horizontal producer.

5.2.2. Example 2 from Butler's Monograph (1994)

In this example, Butler utilized the same procedure as that illustrated above to evaluate SAGD performance for Esso's HWP1 Horizontal Well Pilot. Reservoir characteristics and bitumen properties are given below.

$H = 27.4$ m

$\phi = 0.33$

$k = 0.62 \; \mu m^2$ (based on permeability of 1.6 darcies and $K_{ro} = 0.4$)

$\Delta S_o = 0.482$

$\alpha = 5.00 \times 10^{-7} \; m^2/s$ (0.465 ft²/d)

$m = 3.1$

$v_s = 3.00 \times 10^{-7} \; m^2/s$ (3 cs)

Table 5.3 provides the results in this case, including the "depth of heat penetration". These values are calculated at $t_c = 505$ days.

Days:	0	100	300	1000
U (m/d) [§]:	0.031	0.031	0.027	0.014
Values of ξ (m):				
$T^* = 0.5$	0.996	0.97	1.11	2.12
$T^* = 0.1$	3.17	3.24	3.69	7.04

– – – – –

[§] calculated rate of advance of front at a height of $(1/\sqrt{3})$ of total, i.e. at 15.8 m.

Table 5.3: Results of Example 2, for Esso's HWP1 Horizontal Well Pilot.

It is important to note that in this example, the steam front velocity was calculated at different times. It clearly changed with time: the steam front velocity declined with time, from 0.031 m/d after 100 days to 0.014 m/d after 1000 days.

52

5.3. Selected Simulation Results by CMG's STARS™

In this section, results from a numerical model are presented. Specifically, the STARS™ thermal simulator from the Computer Modelling Group (CMG) Ltd. of Calgary, Canada is used. It is a comprehensive numerical model, with full features of 3-D reservoir flow and comprehensive mass and heat transfer mechanisms incorporated. It was initially developed for the steamflood process, but has proved versatile and easily adaptable in simulating other recovery processes including steamflood with chemical additives, dry and wet in-situ combustion, SAGD. Detailed information of the formulation and solution of the numerical model (including chemical reactions, complex phase changes, etc.), its features, and its algorithm are given in the CMG's STARS™ User Manual (1999). Within the last 10 years, various investigators around the world have extensively used the STARS™ thermal simulator to simulate the SAGD process for field applications.

At the present, there are a number of SAGD operations in Alberta, with some being commercial projects, and others being pilot projects with potential of being converted to commercial operations. Some of these projects include the UTF operation by Northstar Energy in Fort McMurray, project by Alberta Energy Company (AEC) at Pelican Lake, Suncor Energy's project at Burnt Lake, project at Hangingstone by Japan Canada Oil Sand (JCOS), BlackRock Ventures Ltd.'s project at Hilda Lake, and PanCanadian Petroleum's projects at Senlac and Christina Lake. Little data, including production performance data, are published for many of these projects. Ito et al. (1999, 2000) reported some reservoir properties for the Hangingstone reservoir, along with predicted production results from simulation studies; some (actual) injection data and simulated production forecast were reported by BlackRock Ventures Ltd. for the Hilda Lake project. It should also be noted that Esso's HWP1 project at Cold Lake has been operated from time to time as a SAGD process (in its conventional configuration). What is important about this project is the extensive volume of data, particular reservoir characteristics data, published over the years for the CSS operations and (to a lesser extent) for the HWP1 pilot. As seen in the previous section, Butler had extensively presented data for the Cold Lake reservoir in his investigations. Given this fact, the simulation runs performed in this work are made on the basis of the data available for the Cold Lake reservoir. Another reason for this decision is to provide appropriate comparison of results from the STARS™ thermal simulator and those from the new analytical model in this thesis.

It should be noted that results generated by a reservoir simulator usually are much more numerous and comprehensive than results available from an analytical model. This is due to many reasons, including especially the "number-crunching" capability of modern computers in processing the calculations associated with a numerical model. At the same time, a tremendously large amount of data is required in setting up an appropriate model prior to the actual simulation. The data set includes typically formation tops, reservoir rock properties (such as its thermal

properties, petrophysical properties), fluid properties (such as density, viscosity, solubility, etc.), relative permeability for different flowing fluids, presence and extent of reservoir discontinuity, well completion data, along with injection and production constraints. The amount of data required to build a reservoir model, and the interpretation of the simulation results, however, means that a simulation study could take weeks to complete. As a result, there is still a need for analytical models which have the capability of estimating and predicting some key performance parameters (relatively) quickly and accurately.

In this work, results are first generated for a base case for different reservoir configurations. Sensitivity studies are then conducted to determine the effects of different pamaters on the SAGD recovery perfcrmance. Some of the parameters studied include thermal diffusivity of reservoir rock, heat loss, and fluid production rate. The performance of the SAGD process in oil sand reservoirs in communication with a bottom-water sand is also investigated. It is designed mainly to illustrate the limitation of both analytical and numerical simulations.

5.3.1. Reservoir Model

When wellbore hydraulics is ignored and the reservoir is assumed to be homogeneous, the performance of the SAGD process for the whole reservoir can be modelled as that for an element of symmetry. The grid used to represent the element of symmetry is illustrated in Figure 5.1. The element of symmetry was represented by a 32 x 2 x 35 grid matrix. The dimensions for each block were 1.45 m along the x- direction grid block, 250 m along the y-direction (which was along the length of the horizontal well), and 1 m along the z-direction. Hence, the overall dimension of the element of symmetry were 43.5 m x 500 m x 35 m. A nine-point finite difference scheme was applied in the i,k (x- and z-) directions to account for the diagonal transmissibility (or movement of fluids). Several simulation runs were also made to study the effect of grid block sizes.

The horizontal producer was positioned 1 m from the base of the model, and the injector was located 4 m above it. The drainage height was, therefore, 34 m. This drainage distance was similar to Butler's Example 1 listed in Section 5.2. The model reservoir was assumed to be homogeneous and the permeability was isotropic ($k_v = k_h$) at 1.3 darcies. The sandstone reservoir was assumed to have a porosity of 30%; the irreducible water saturation was 23%, and initial oil saturation was 77%. As a result, initial oil in place was 175850 m^3 for the half element of symmetry. Thermal properties used in this study are summarized in Table 5.4. The viscosity of the oil at different temperatures is illustrated on Figure 5.2, and it is also summarized in Table 5.5. At the initial reservoir temperature of 13 °C, the viscosity of oil is approximately 150,000 cp. The relative permeability for the oil water along liquid gas are illustrated on Figures 5.3 a-b. The residual oil saturation, as illustrated on Figure 5.3 a, is 15% and the critical gas saturation is 5%.

As high-temperature high-pressure steam is injected continuously into a bitumen reservoir thermal stresses are usually created. In such cases, reservoir parameters such as porosity and

BASE CASE SIMULATION RUN
Net Pay (m) 2000-01-01   J layer: 1

File: coldlake2title.txt.irf
User: Administrator
Date: 2000-09-07

Scale: 1:276.635897
Z/X: 1.00:1
Axis Units: m
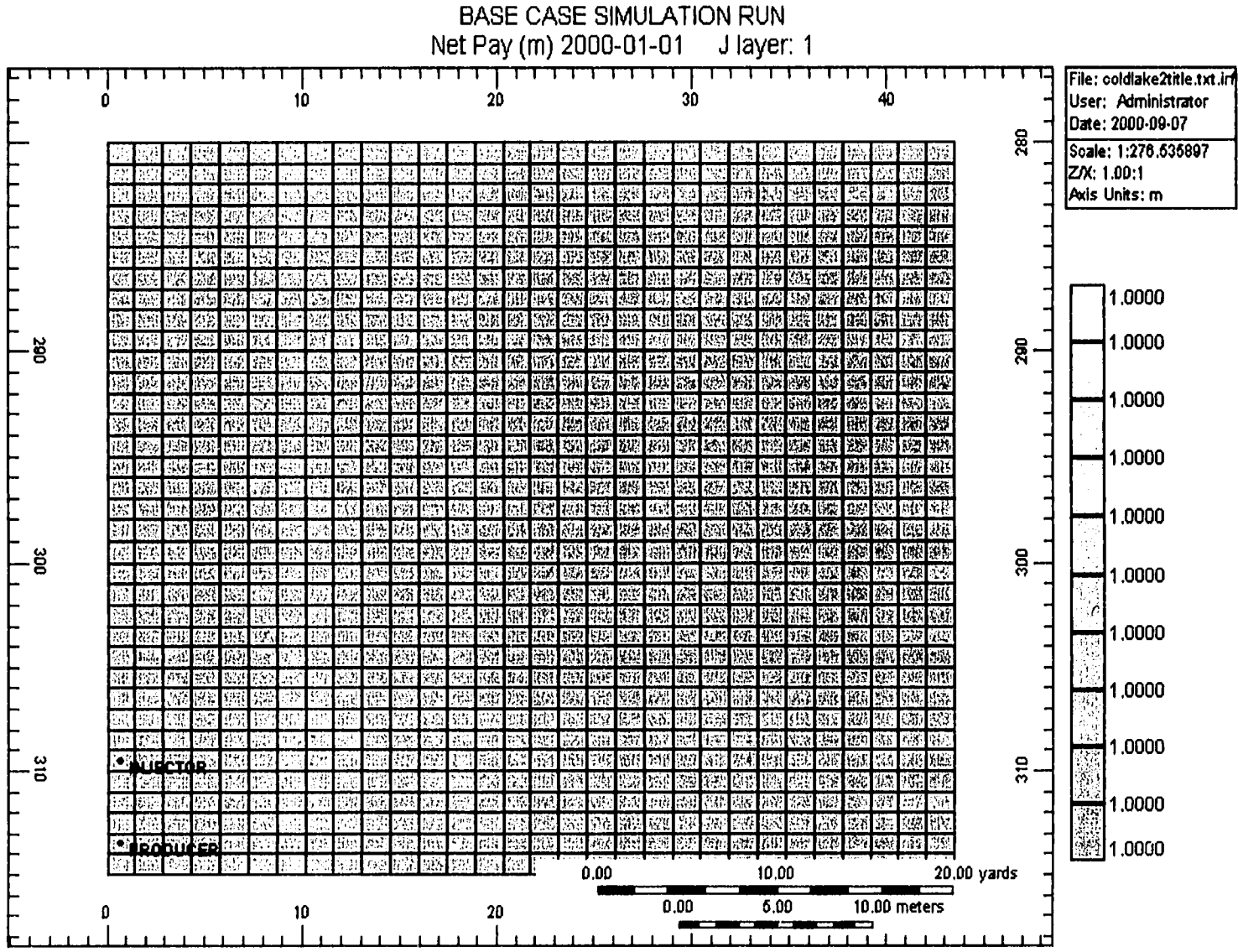
Figure 5.1: 2-D View of the Reservoir Grid Setup Utilized in the Simulation Study, STARS^{TM} Simulator.

Viscosity Temperature Relationship
Cold Lake Reservoir
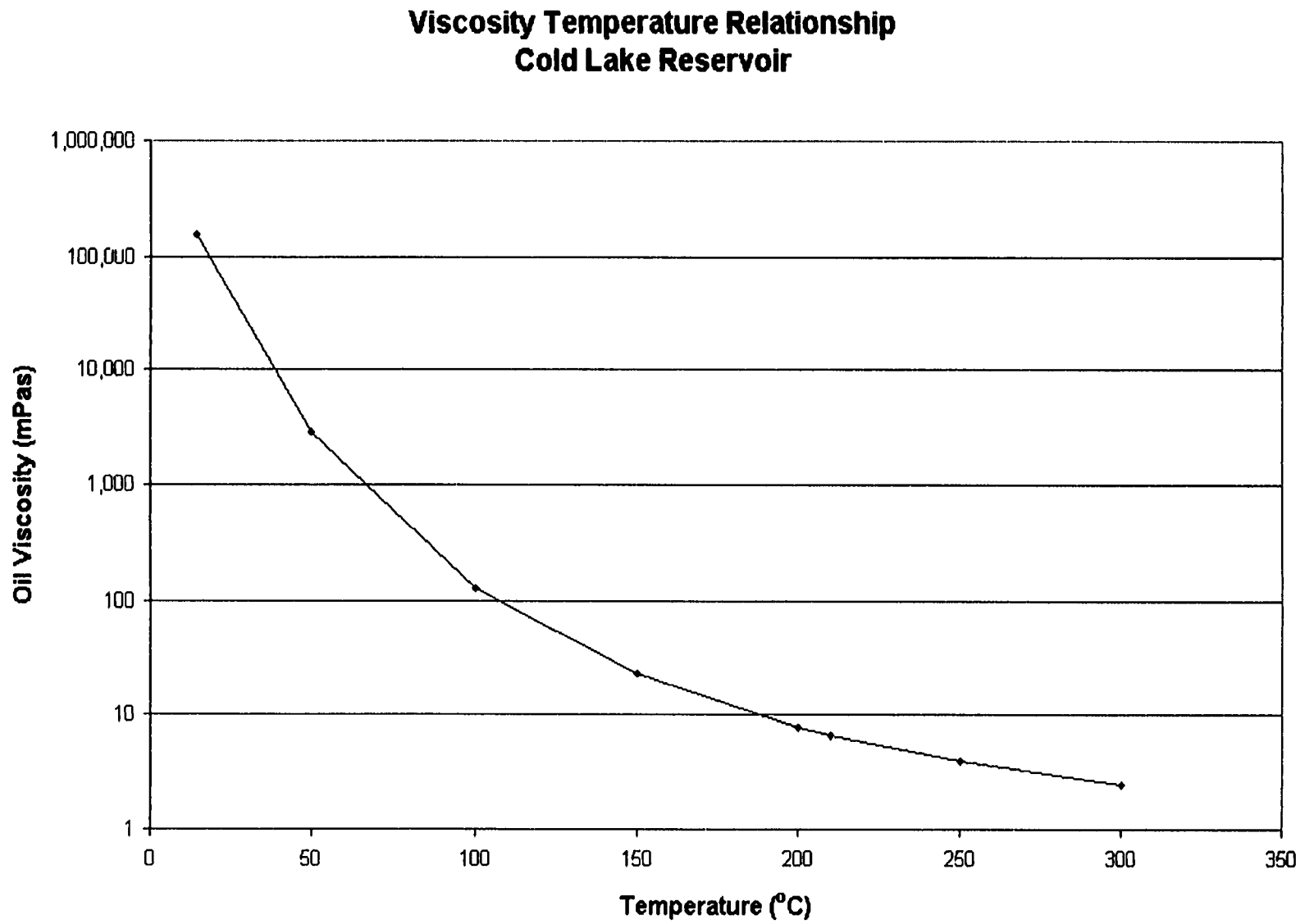
Figure 5.2: Viscosity – Temperature Relationship for Cold Lake Bitumen, Used in Simulation Study, STARS[TM] Simulator.

Properties	Value
Water Compressibility (kPa^{-1})	5.80E-07
Oil compressibility (kPa^{-1})	8.18E-07
Thermal expansion of oil (K^{-1})	7.00E-04
Thermal expansion of Water (K^{-1})	1.90E-03
Thermal expansion of rock (K^{-1})	3.50E-05
Density of water (kg/m^3)	999.1
Density of oil (kg/m^3)	997.5
Heat capacity of rock (kJ/m^{3}K)	1882.6
Specific heat of oil (kJ/kgK)	2.1
Thermal conductivity of rock (kJ/mdayK)	150.0
Thermal conductivity of overburden rock (kJ/mdayK)	150.0
Initial reservoir temperature (°C)	13.0
Initial reservoir pressure (kPa)	3000.0

Table 5.4: Selected Properties of Cold Lake Reservoir Used in the Simulation Study.

TEMP (°C)	VISCOSITY (cp)
14.0	151814
50.0	2850
100.0	128
150.0	22.7
200.0	7.9
210.0	6.7
250.0	4
300.0	2.5

Table 5.5: Selected Values of Viscosity – Temperature Relationship for Cold Lake Bitumen, Used in Simulation Study.

Liquid Gas Relative Permeability
Cold Lake Reservoir
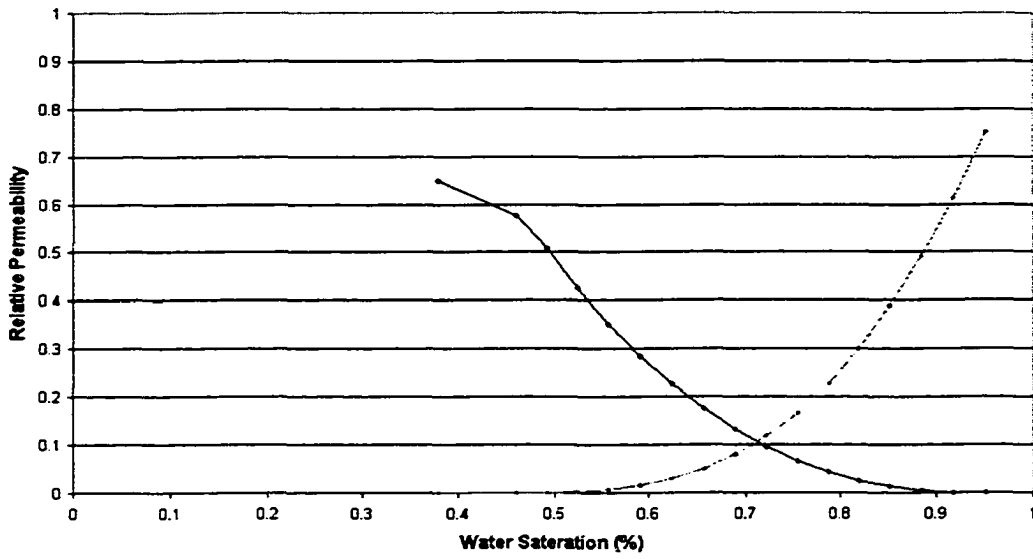
a) Liquid – Gas relative permeability

Oil Water Relative Permeability
Cold Lake Reservoir
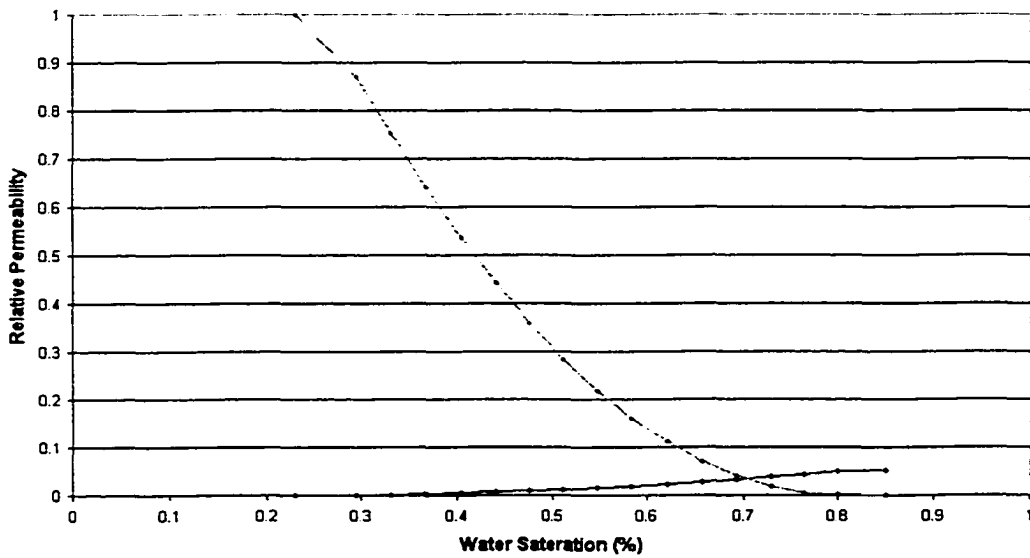
b) Oil – Water Relative Permeability

Figure 5.3: Relative Permeabilities Used in Simulation Study, a) Liquid – Gas Relative Permeability, b) Oil – Water Relative Permeability

58

permeability could be altered substantially during the steam injection recovery process. Due to the limitations of existing analytical models to incorporate these effects, and for direct-comparison purposes in this work, geomechanical effects were not included in the simulation model.

For this study steam injection rate was constrained at a bottom-hole pressure of 1.9 MPa, with a steam temperature of 210.0 °C and at 95% steam quality. The steam trap was operated at 20 °C below the saturation temperature (i.e., at 190.0 °C), with a maximum steam production rate set at of 5 m^3/d.

5.3.2. Simulation Results

Figure 5.4 shows the oil production rate and the instantaneous steam-oil ratio (SOR) for the base case. It should be noted that the rate shown in this figure represents the rate for the full pattern (i.e., the production rate obtained from the simulator is multiplied by a factor of 2, as the simulation model represents an element of symmetry). The pre-heating period lasted approximately 15 days before thermal communication was established between the horizontal injector and producer. The relatively short pre-heating period was due to the fact that the oil viscosity at initial condition was relatively low, and readily mobile with little thermal stimulation. The oil production rate during the heating period was zero. As the temperature around the vicinity of the horizontal well increased, the viscosity of the bitumen decreased, leading to an increase in the oil production rate. Steam injectivity also increased significantly as the viscosity of oil decreased. An average fluid production rate of 70 m^3/d was maintained for 5 years (or 1825 days), before the rate started to level off. The steam-oil ratio (SOR) averaged at approximately 4 m^3/m^3 during the first five years of steam injection. {This ratio appears to be quite high compared to other SAGD projects.} After 5 years of steaming, the SOR increased significantly, and rapidly approached the economic cut-off. The increasing SOR was due to substantial heat loss to the cap rock (especially), and heat produced from the reservoir.

The reported SOR from several operating SAGD projects ranged between 1.9 to 2.7 m^3/m^3. The SOR obtained from the base case run appeared high, compared to these values. The high SOR from the base case is correlated directly to the permeability of the reservoir. In the base case, the permeability was only 1.3 darcies; this value seemed to be relatively low for a "clean" sandstone reservoir. For a clean sandstone reservoir the permeability typically is in the 3-8 darcies range. {It is possible that the relatively low permeability used in Butler's examples (1994) was representative of an inter-bedded sandstone reservoir.}

59

Production Forecast From Cold Lake Reservoir
Base Case - Full Pattern
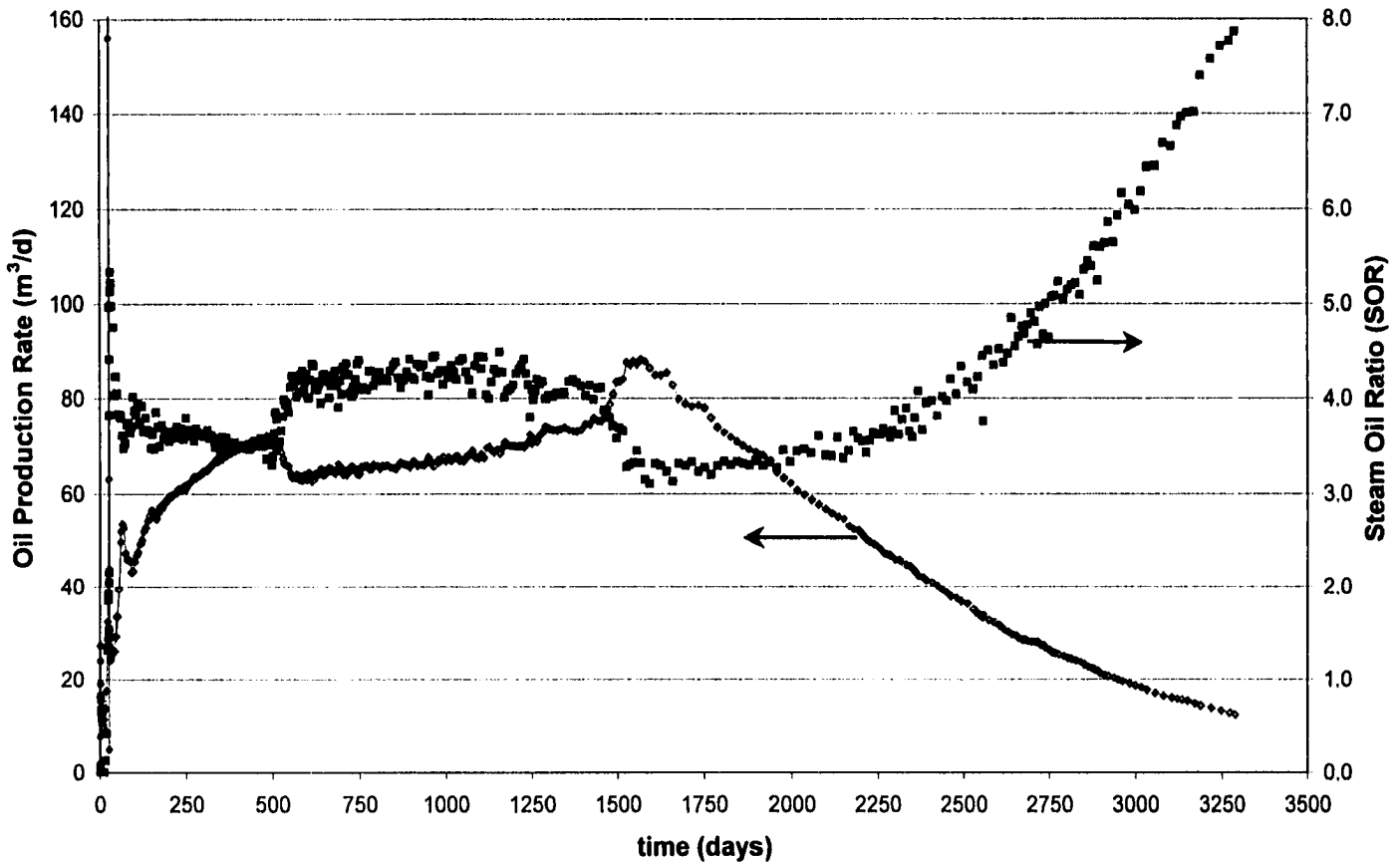
Figure 5.4: Oil Production Rate and Steam-Oil Ratio vs. Time, Base Case of Cold Lake Reservoir, STARS[TM] Simulator.

Figure 5.5 shows the cumulative oil production and the cumulative volume of steam (CWE) injected into the half element of symmetry against time. With approximately 349000 m³ (CWE) of steam injected, cumulative oil production was approximately 88900 m³ for the (half) element of symmetry. Hence, the cumulative steam oil ratio was 3.9, and cumulative oil recovery was 50.6%.

Figure 5.6 shows the oil saturation in 3-D view after three years of steam injection. The relatively even oil saturation distribution profile along the length of the horizontal well was probably due the assumption of negligible wellbore hydraulics in the base case model. Figures 5.7 a-b show the oil saturation at two different time intervals during the SAGD operation, while Figures 5.8 a-b show the temperature distribution at the same time intervals. Initially, the expansion of the steam chamber was circular – representing ceiling drainage period. Once the steam chamber had reached the overburden, it spread sideways – representing slope drainage mechanism. The shape of the steam chamber during the slope drainage period has been well documented.

With more mobile fluids present in the reservoir with time, the effect of convective transport was expected to be more significant. To further understand the process, an energy balance was performed. Applying the heat conservation principle, the heat accumulated in the formation is given by

$$Q_{accumulated} = Q_{inj} - Q_{loss} - Q_{produced}$$ (5.7)

The heat injected into the formation was determined from volume of steam injected (CWE) along with temperature and steam quality, which included both sensible heat and latent heat of vaporization. The amount of heat injected at the sand face may be less due to wellbore heat loss (this effect was not, however, considered in this study). Heat loss to the cap and base rock was typically estimated by the heat conduction equation. The amount of heat produced was associated with the volume and temperature of the produced fluid stream. Finally, the heat accumulated in the reservoir – often difficult to account for – was the heat stored in the fluid-saturated reservoir.

For a fluid saturated rock, the volumetric heat capacity (M) is given by,

$$M = \phi S_o \rho_o C_o + \phi S_w \rho_w C_w + \phi S_g \rho_g C_g + (1 - \phi)\rho_r C_r$$ (5.8)

The heat capacity of water is typically 2-5 times greater than that of oil (Prats, 1982); therefore, its contribution to the total reservoir heat capacity is much greater than that due to oil. The reservoir rock, due to its high heat capacity and mass, contributes the largest percentage to the overall reservoir heat capacity. The heat accumulated in the reservoir determines the role of heat conduction and/or convection in the reservoir. The equations used to calculate the heat injected

61

Production Forecast From Cold Lake Reservoir
Base Case - Full Pattern
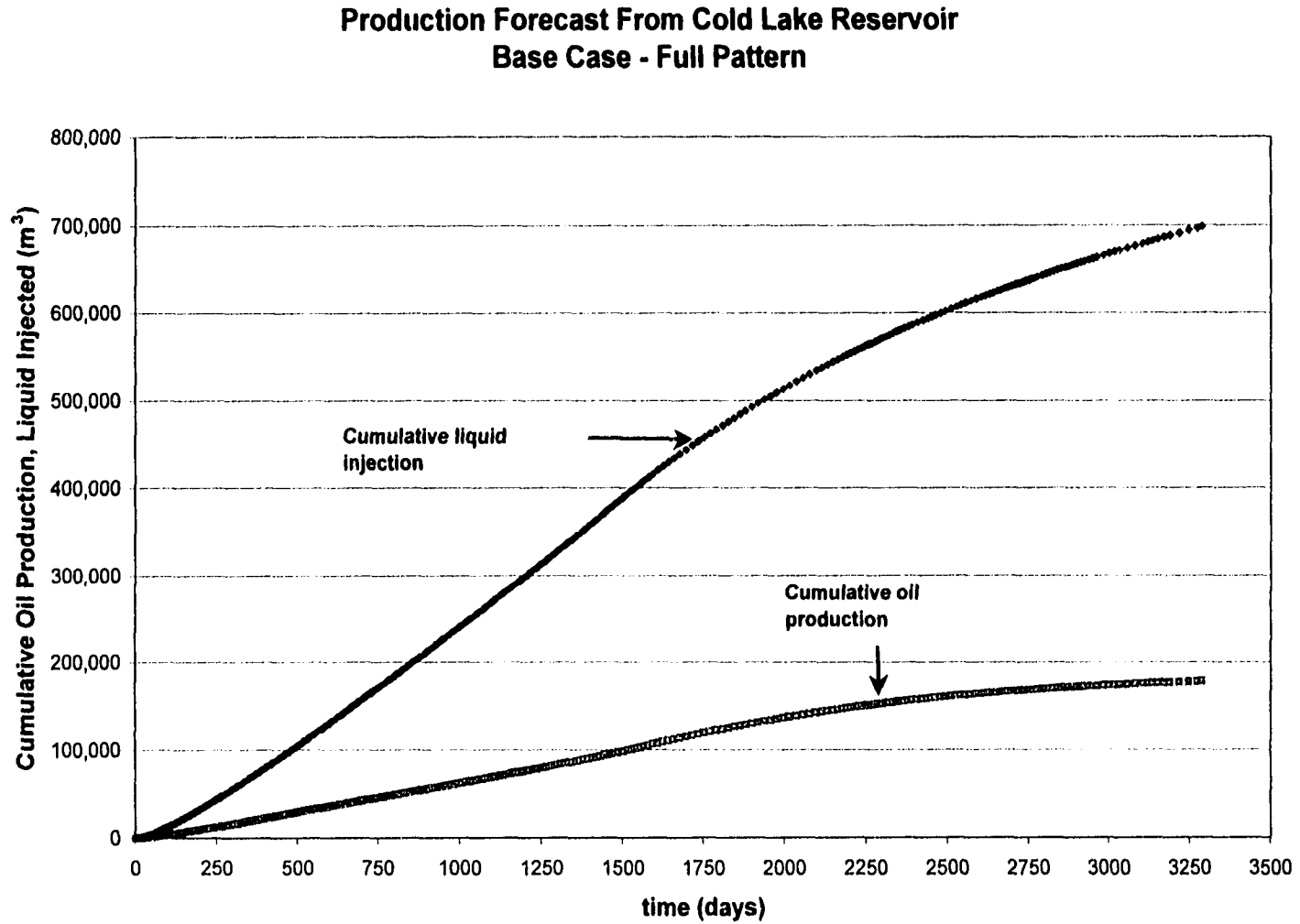
Figure 5.5: Cumulative Oil Production and Steam Volume Injected (CWE) vs. Time, Base Case of Cold Lake Reservoir, STARS[TM] Simulator.

BASE CASE SIMULATION RUN
Oil Saturation 2003-01-01

File : ooldstare2006.txt.in
User : Administrator
Date : 2003-09-07
Z/X: 1.00:1

0.8000
0.7200
0.6400
0.5600
0.4800
0.4000
0.3200
0.2400
0.1600
0.0800
0.0000
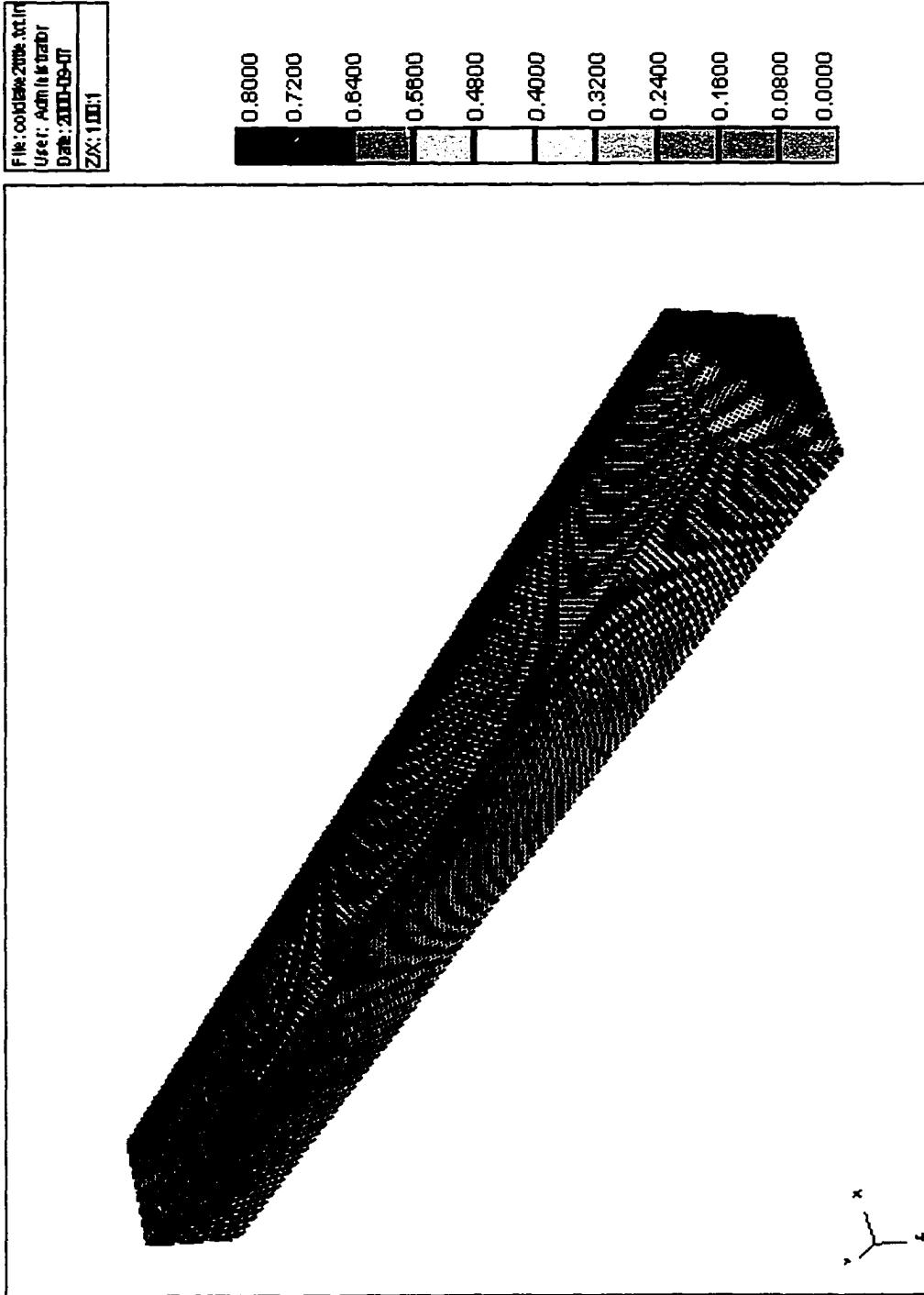
Figure 5.6: 3-D View of Oil Saturation Profile, STARS™ Simulator.

63

BASE CASE SIMULATION RUN
Oil Saturation 2001-01-01   J layer: 1
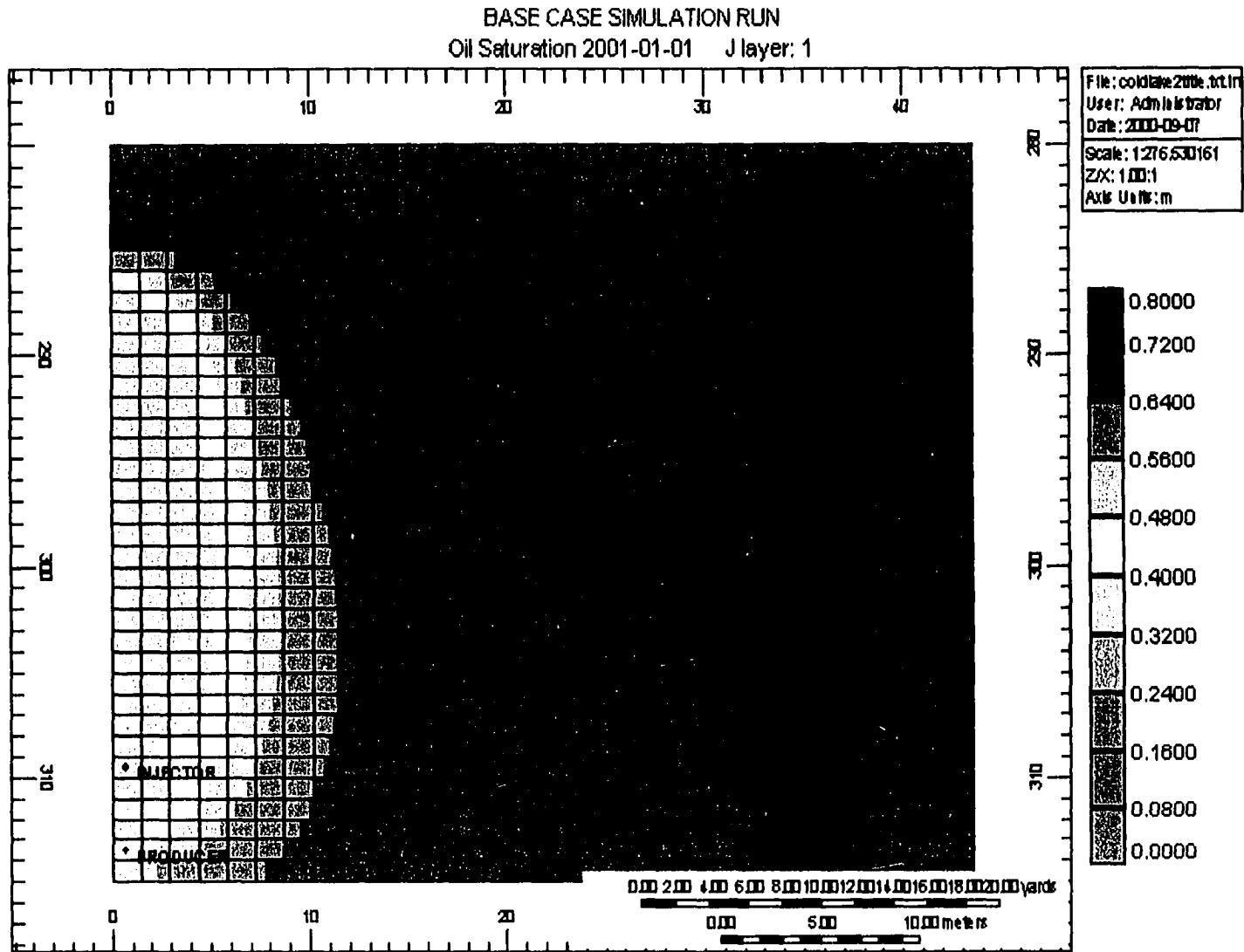
Figure 5.7a: 2-D Cross-Sectional View of Oil Saturation Profile after 1 Year, STARS™ Simulator.

BASE CASE SIMULATION RUN
Oil Saturation 2003-01-01   J layer: 1
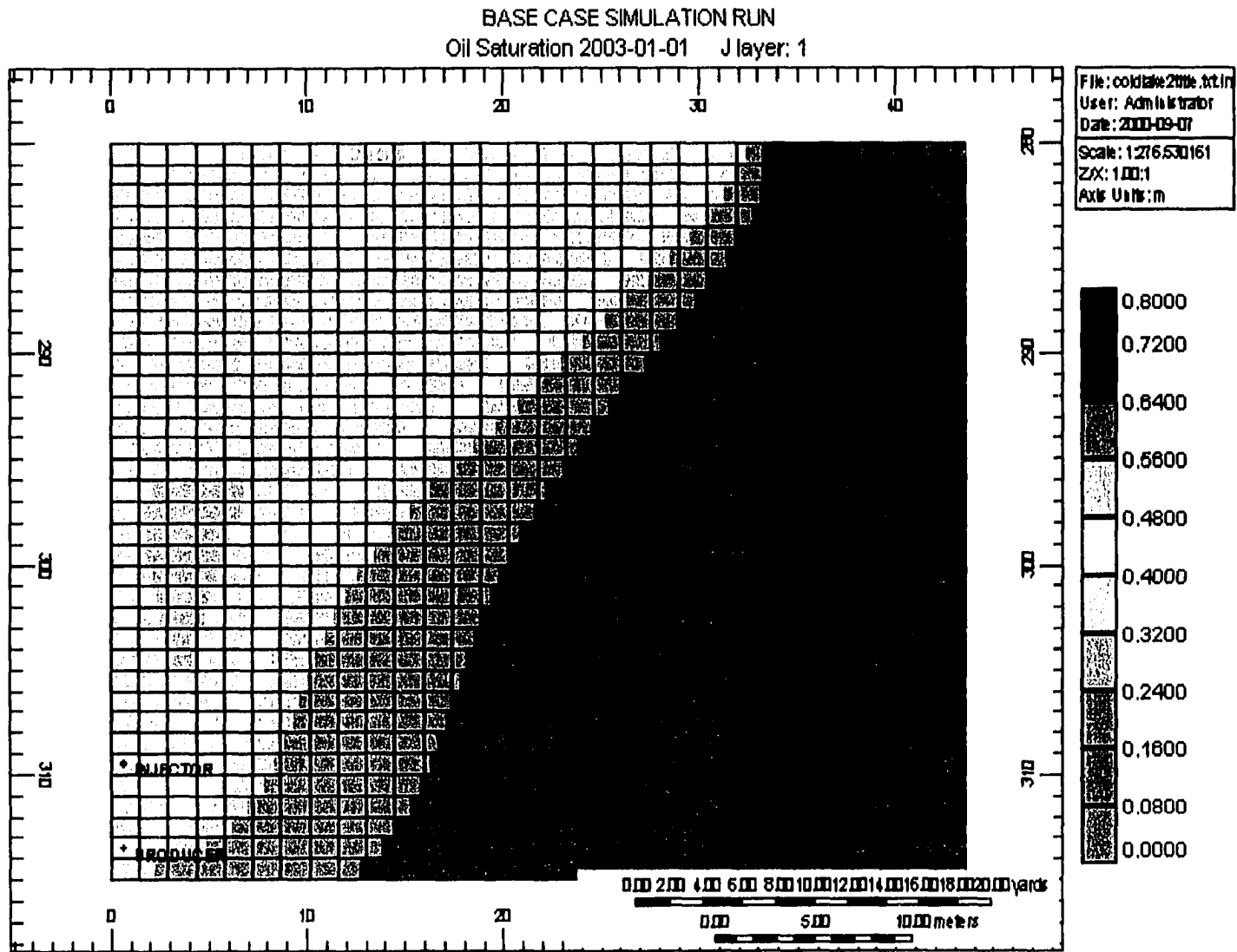
Figure 5.7b: 2-D Cross-Sectional View of Oil Saturation Profile after 5 Years, STARS™ Simulator.
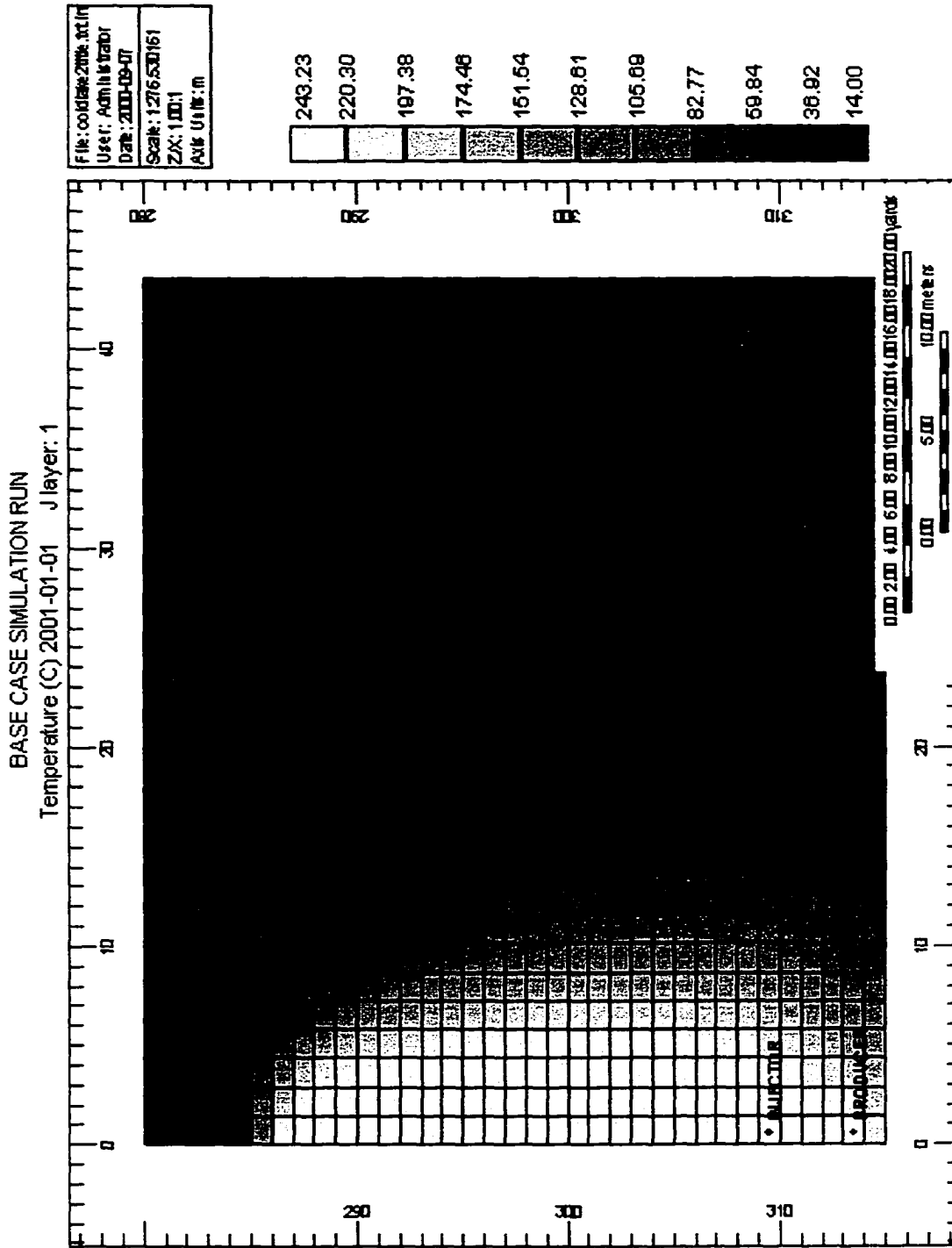
Figure 5.8 a: Temperature Distribution Profile after 1 Year, STARS™ Simulator.

66
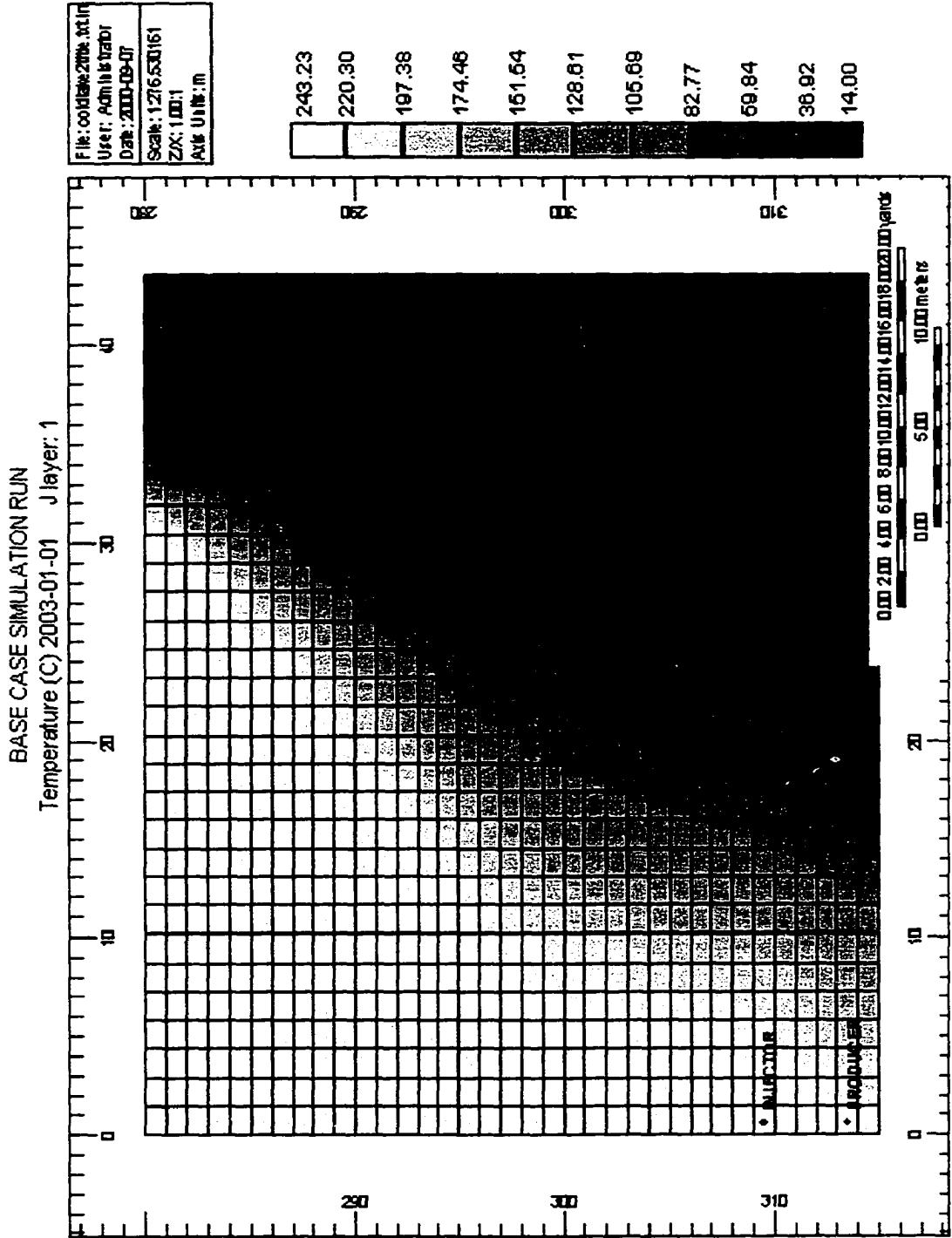
Figure 5.8 b: Temperature Distribution Profile after 5 Years, STARS™ Simulator.

67

into the formation, heat produced from the reservoir and heat loss to the cap and base rock are given in Appendix B.

Figure 5.9 shows the cumulative heat injected, produced, loss and accumulated during the SAGD operation. During the preheating period, approximately 1.20×10^7 kJ of energy was injected. Due to the relatively low in-situ bitumen viscosity, the preheating period only took approximately 15 days before steam injectivity of steam began to increase, and oil production initiated. Average oil viscosity around the vicinity of the horizontal wellbore, at this time, was approximately 6 mPa.s.

Cumulative heat loss to the cap and base rock, after 9 years (3288 days) of steam injection, was approximately 2.20×10^{11} kJ (12% of the total heat injected). The rate of heat loss to the cap rock was larger than that to the base rock due to the larger temperature gradient present, and larger spread of the steam zone near the top of the reservoir. Figure 5.10 shows the cumulative heat loss to the cap and base rock. Initially, there was no heat loss to the cap rock because the steam chamber had not yet reached the overburden. The heat loss to the base rock was steadily increasing, and was associated with the fluid production from the reservoir via the horizontal producer. As the steam zone rose and reached the overburden, the heat loss to cap rock increased exponentially.

Given the cumulative oil and water volumes produced along with their heat capacities, densities and temperatures, the heat produced from the reservoir was determined to be 7.56×10^{11} kJ. After 9 years (3288 days), the heat injected into the reservoir was 1.82×10^{12} kJ. From the heat balance equation (i.e., Equation (5.7)), the heat accumulated in the reservoir was determined to be 8.46×10^{11} kJ. Figure 5.11 shows the heat accumulated in the reservoir, heat loss and heat produced as ratios of the total heat injected. The SAGD process was fairly efficient as 46% of the injected energy accumulated in the reservoir, with 12% lost to the cap and base rock and 42% produced from the reservoir.

The heat balance calculation discussed above represents the balance of the overall system. The heat accumulated in the reservoir was obtained from Equation 5.7; it did not differentiate sensible heat from latent heat in the overall amount. Detailed analysis could be performed to determine the saturation of the fluid and the state of the fluid – only then that differentiation could be made between sensible heat and latent heat of vaporization. This analysis has bot been undertaken in this thesis.

As seen from Chapter 4, the transport equation was derived from first principles. The derivation of these equations showed the increasing accumulation of fluid at the interface lead to increasing influence of convective transport of heat in the reservoir. This is evident from Figures 5.7 a-b and Figure 5.11. As steam was continuously injected into the reservoir, the ratio of heat accumulated to total heat injected in the reservoir decreased, leading to the formation of more condensate

Production Forecast From Cold Lake Reservoir
Base Case - Full Pattern
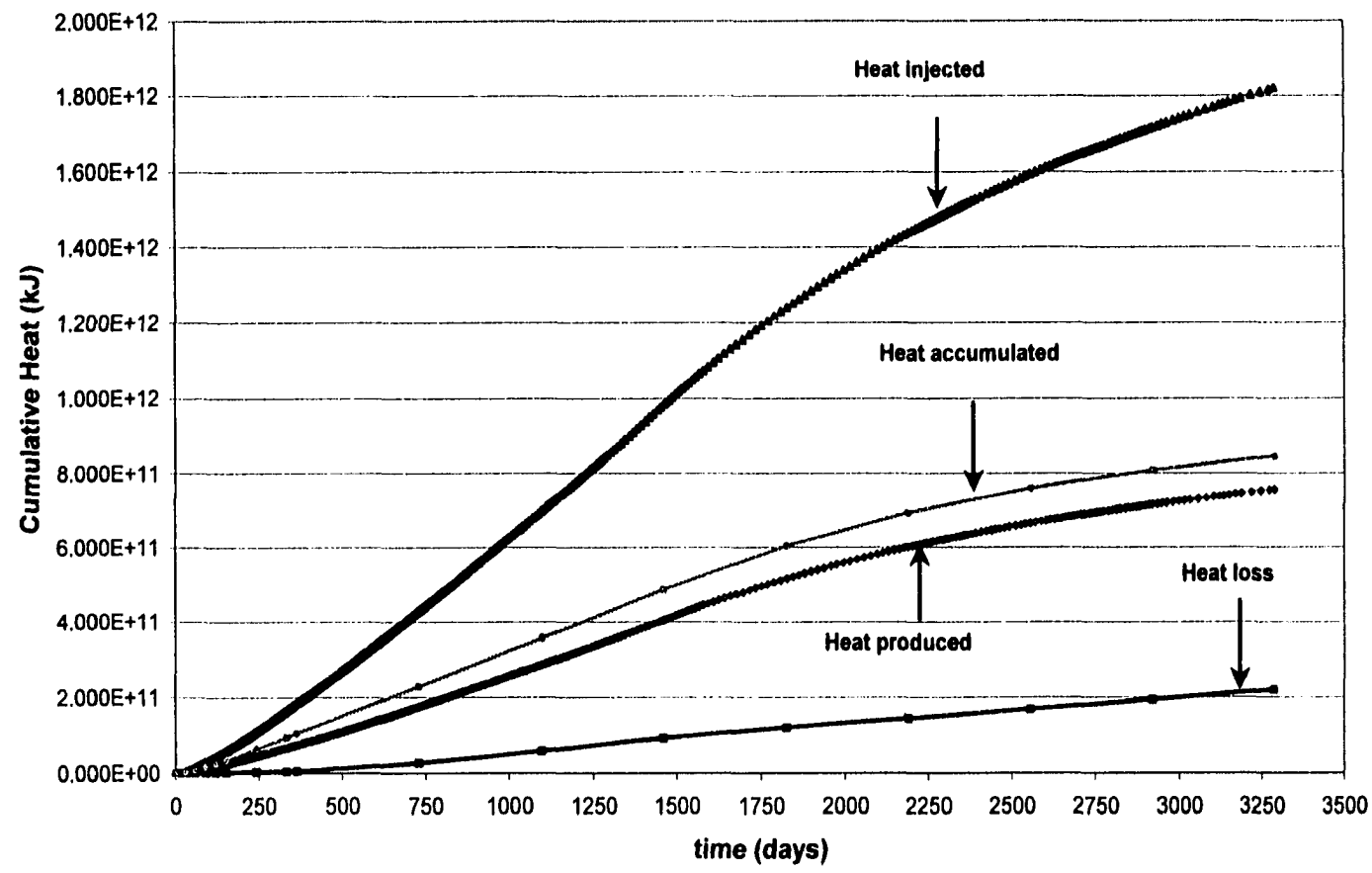
Figure 5.9: Heat Balance Calculations for Base Case Simulation, Cold Lake Reservoir, STARS™ Simulator.

Production Forecast From Cold Lake Reservoir
Base Case - Full Pattern
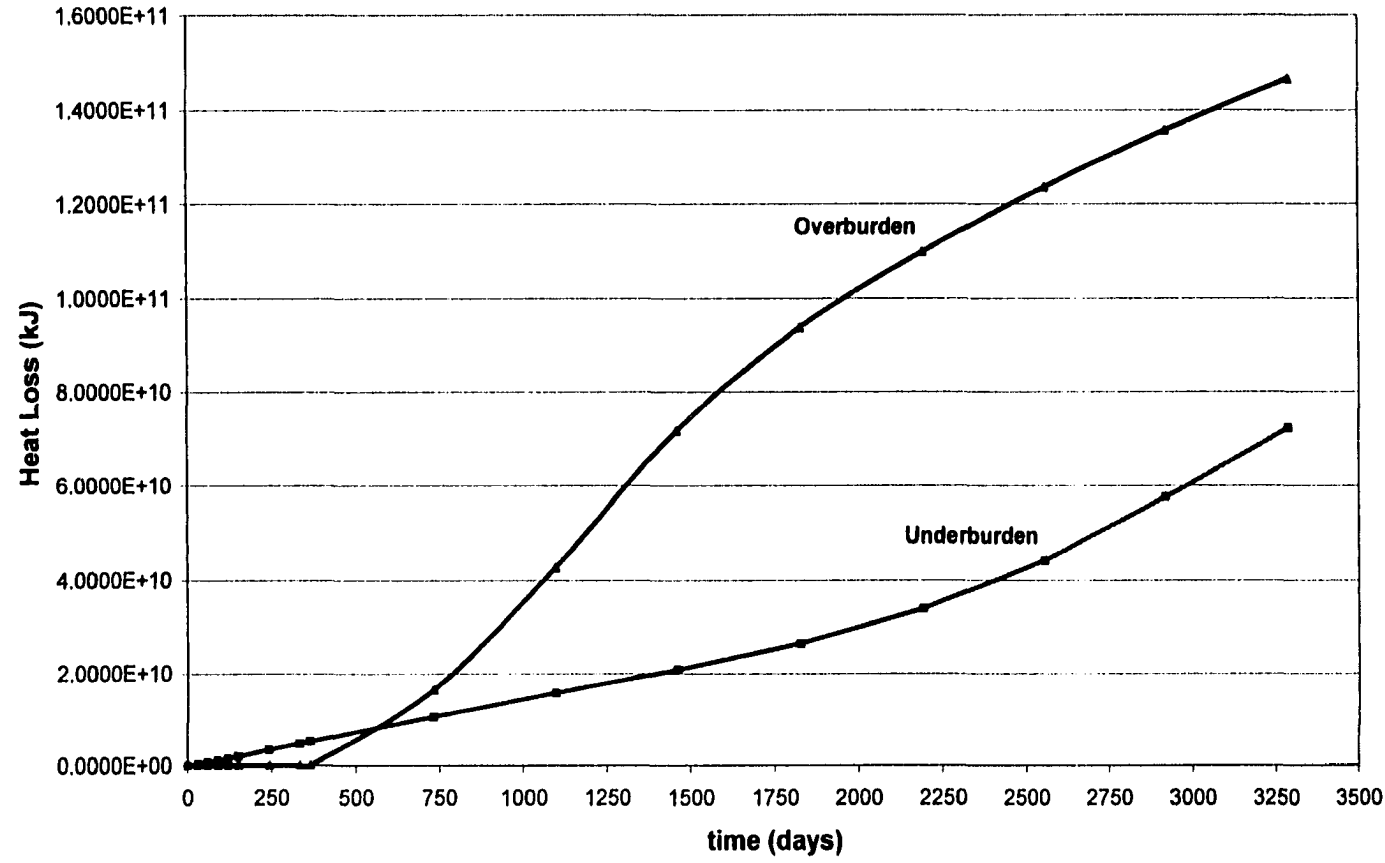
Figure 5.10: Heat Loss to Cap and Base Rock for Base Case Simulation, Cold Lake Reservoir, STARS[TM] Simulator.

Production Forecast From Cold Lake Reservoir
Base Case - Full Pattern
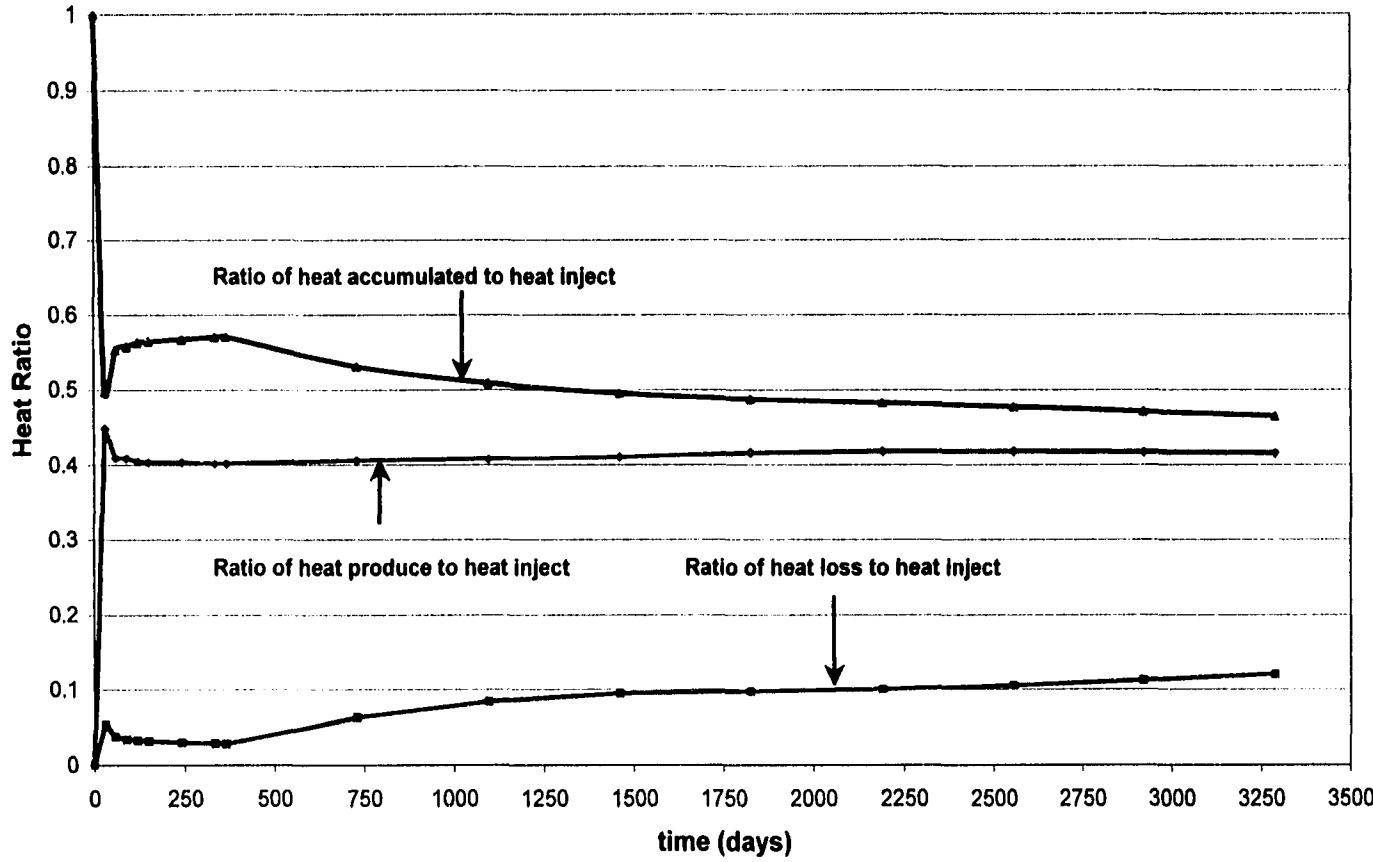
Figure 5.11: Ratio of Heat Accumulated, Heat Loss, and Produced to Heat Injected for Base Case Simulation, Cold Lake Reservoir, STARS™ Simulator.

volumes within the reservoir ahead of the steam zone interface. This increase in the condensate volume, in turn, caused the convective transport component to become more important in the transfer of heat and mass in the reservoir.

It is not possible, at this stage, to conclude which type of heat transport mechanism is more dominant because the volume of fluids stored or accumulate at the interface is not known with certainty. However, detailed simulation studies conducted by Ito (1999, 2000) strongly suggest the dominance of convective transport in reservoir heating. On the other hand, studies conducted by other authors (for example, Butler (1994), Donnelly (1999)) suggest conduction as being dominant. Field data, to date, have not provided conclusive evidence to support either one of these contentions.

5.4. Results of New Analytical Model Incorporating Convective Transport

The analytical model developed in this study includes both conductive and convective transfer of mass and heat present in the SAGD process. The unique solution to the formulated problem gives temperature distribution, position and velocity of the steam zone interface, and flow rate, all being functions of time. In this section the validity of this model is tested. Using the same set of input parameters, the solutions are compared against simulation results from STARS^{TM} and results from Butler's models, discussed in Sections 5.2 and 5.3, respectively.

As part of obtaining the solutions to the formulated problem, Excel^{TM} was used to obtain the root of Equation (4.26). Values for reservoir properties were required in the determination of the solution. These values are given in Table 5.6 a-b. It is noted that the one of the assumptions for the model was fluid production taking place at the steam zone interface. As such, oil viscosity is that evaluated at the steam temperature. This assumption was made to relate the effect of production rate on the position and shape of the interface.

Irreducible Water Saturation (S_{wc})	0.23
Residual Oil Saturation (S_{or})	0.15
ϕ (Porosity)	0.31
H (Reservoir Thickness)	34 m
L (Horizontal Well Length)	500 m
α (Thermal Diffusivity)	0.0465 m^2/d

Table 5.6a: Summary of Reservoir Parameters.

72

	Region 1	Region 2
T (K)	483	286
ρ_r (kg/m³)	2650	2650
ρ_o (kg/m³)	881	940
ρ_w (kg/m³)	852.9	999.5
ρ_{st} (kg/m³)	9.59	0.00
C_r (kJ/kg.K)	1.09	1.09
C_o (kJ/kg.K)	2.34	1.67
C_w (kJ/kg.K)	4.55	4.19
C_{st} (kJ/kg.K)	2.98	0.00
h_r (kJ/kg.K)	352.34	138.00
h_o (kJ/kg.K)	494.99	100.00
h_w (kJ/kg.K)	897.8	53.6
h_{st} (kJ/kg.K)	2796.1	0.000
S_o	0.15	0.77
S_w	0.23	0.23
S_{st}	0.62	0.00

Table 5.6b: Summary of Reservoir Parameters.

Enthalpies of Region 1 and Region 2 were calculated. Their values are given in Table 5.7. It can be seen that the enthalpies for Regions 1 and 2 are different from those for their mobile fluids.

	Region 1					Region 2				
	ρ kg/m³	C kJ/kgK	ρC kJ/m³K	h kJ/kgK	ρh kJ/m³K	ρ kg/m³	C kJ/kgK	ρC kJ/m³K	h kJ/kgK	ρh kJ/m³K
Mobile Fluid	1.844	2.981	5.496	2796.1	5155.5	180.7	1.670	301.7	100.0	18066.
Static Fluid	101.8	3.659	372.4	735.7	74878.	114.9	3.230	371.4	71.6	8193.1
Total Fluid	103.6	3.647	377.8	772.3	80034.	295.6	2.277	673.1	88.8	26259.
Rock	1828.5	1.088	1989.4	352.4	644246	1828.5	1.088	1989.4	138.0	252333
Total Medium	1932.1	1.225	2367.3	374.9	724280	2124.1	1.253	2662.5	131.2	278592

Table 5.7: Calculation of Static and Mobile Fluids in Region 1 and Region 2.

5.4.1. Comparison of Results of New Analytical Model and Results from STARS™ Simulator and Butler's LinDrain Model (1994)

Figure 5.12 shows a comparison between the oil flow rate predicted by the STARS™ simulator, Butler's models and this model. The production rate given by Butler et al.'s model (1981) was independent of time (as the models had assumed steady state heat transfer, and steady state drainage rate as determined by Darcy's law); as such, the rate of 86.76 m³/d (calculated in Section 5.2) was assumed to be the average rate over the entire life of the SAGD production forecast. The oil production rate predicted by the TANDRAIN model (1981) and Butler's 1985 model changed with time. Their profiles track one another quite closely: they both started with

Production Forecast
Comparison
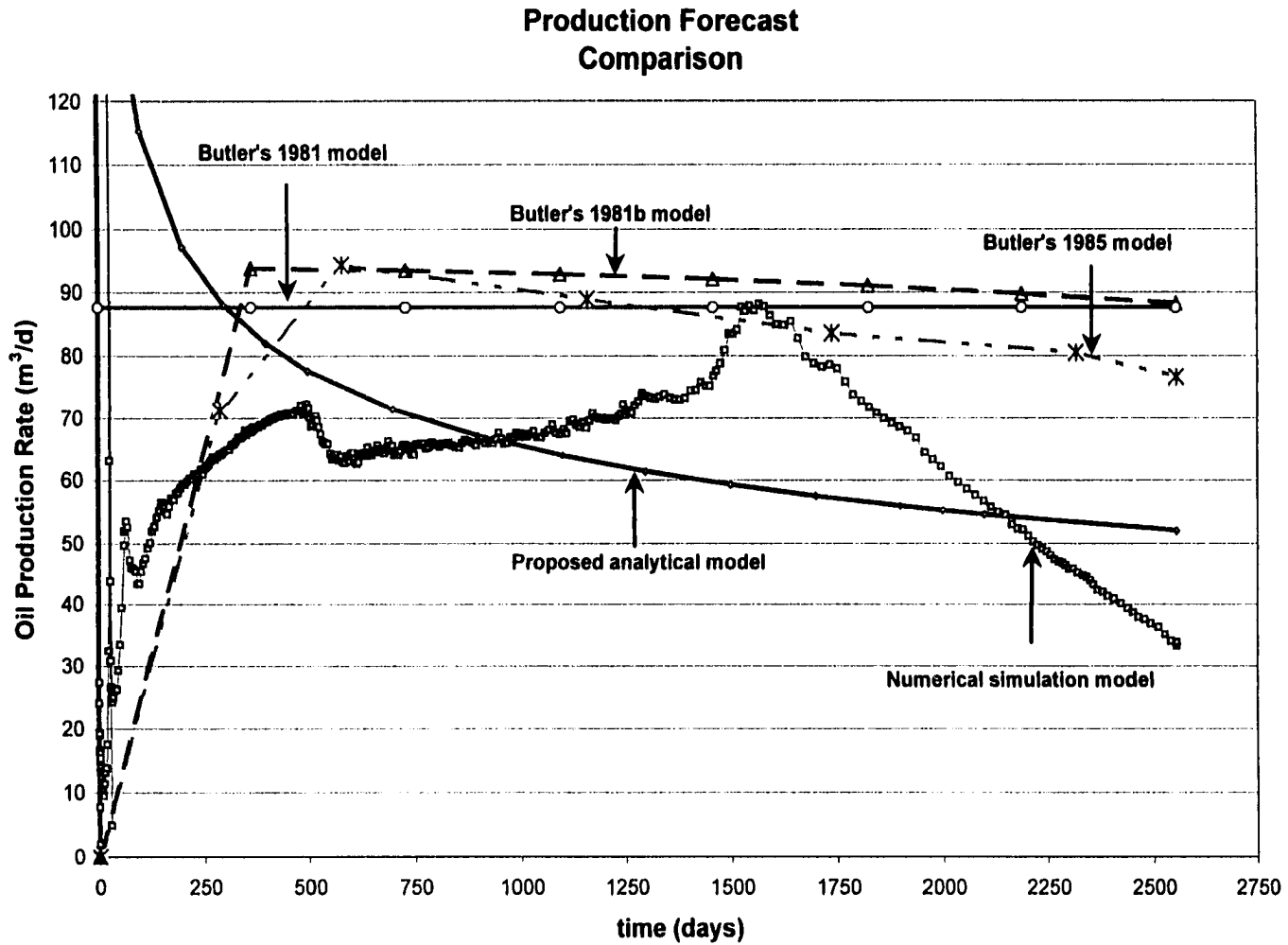
Figure 5.12: Comparison of Oil Production Rate Predicted by Butler et al.'s model (1981), TANDRAIN model, Butler's model (1985), STARS[TM] Simulator and New Analytical Model.

zero oil production rate, with the rate rammed up to reach a maximum value after approximately 300 days for the TANDRAIN model, or 500 days for Butler's 1985 model. It must be pointed out that these two profiles incorporated implicitly the production rate occurring during the ceiling drainage stage, as evidenced by the increasing trend mentioned above. The production rate predicted by the new analytical model also declined with time. At the end of 500 days the oil production rate for the TANDRAIN model, Butler's 1985 model, and new analytical model were 94 m^3/d, 88 m^3/d and 77 m^3/d, respectively. At the end of 1000 days, these three rates became 93 m^3/d, 91 m^3/d, and 67 m^3/d. At the end of 1500 days, these rates were 92 m^3/d, 86 m^3/d, and 59 m^3/d, respectively. From 1500 days to 2000 days, the three rates declined to 91 m^3/d, 83 m^3/d, and 56 m^3/d. The rate of decline in the production rate for the new analytical model was steeper than those for the TANDRAIN model and Butler's 1985 model. The steeper decline in the rate profile predicted by the new analytical model led to larger difference between it and the rates predicted by the TANDRAIN model and Butler's 1985 model widened with time. This was caused, probably, by the heat losses (to cap rock, base rock, and fluid production from the reservoir) accounted for in the new analytical model. The TANDRAIN model and Butler's 1985 model did not account for these heat losses from the reservoir. It is noted that the oil production rate calculated by the STARS™ simulator was less than those predicted by the TANDRAIN model and Butler's 1985 model for practically the whole time period. The oil production rate calculated by the STARS™ simulator was 74 m^3/d, 68 m^3/d, 84 m^3/d and 62 m^3/d at 500 days, 1000 days, 1500 days, and 2000 days.

As seen quite clearly, the oil production rate predicted by the new analytical model matches closely with the rate predicted by the STARS™ simulator, particularly during the middle time period (between 450 days and 1000 days). The average production rate during this period was 71 m^3/d and 67 m^3/d for the new analytical model and STARS™ simulator, respectively. The match was poor, however, at the start and near the end of the entire forecast period. The following reasons are offered for the matches between the results for the new analytical model and the STARS™ simulator.

For the SAGD process, there are two very distinctive flow profiles, with each corresponding to different flow mechanisms in the reservoir. Initially, at the startup of the SAGD process, steam injectivity was low, and steam circulation was required in both the horizontal injector and the horizontal producer. Once thermal communication was established between the wells, then steam injection was initiated. When steam was first injected into the reservoir, it tended to rise to the reservoir top, due to difference in fluid densities and difference between injection pressure and reservoir pressure. As the injected steam came into contact with the cold reservoir, it underwent a phase change whereby its heat was transferred into the fluid saturated reservoir. The reservoir temperature was increased and the oil mobilized. The mobilized oil near the steam zone interface was drained by gravity force. The flow during this period is known as ceiling

75

drainage, and its flow profile was previously illustrated in Figure 5.7a. During this period, the oil rate increased gradually, as more bitumen became mobile with increasing reservoir temperature. The development of the new analytical model in this work assumed slope drainage to be present at the start of the SAGD process. For this reason, discrepancy in forecasted oil production rate exists between simulation results and results from the new analytical model.

During ceiling drainage period, the rate at which the steam chamber rises and the rate at which the oil drains toward the producer are dependent on the vertical permeability (k_v). In relatively clean reservoir, i.e., there exist little or no interbedded mudstone, the permeability usually ranges between 3-5 darcies. In this case, the rate at which the steam zone rises typically is between 10 to 15 cm/d (i.e., 0.010 to 0.015 m/d), and could be as high as 25 cm/d (i.e., 0.025 m/d), depending on the operating condition (such as steam injection pressure). For a reservoir of 25-m thickness, the time taken for the steam to rise to the top of the formation is about 100-150 days. It is believed that discrepancy in the predicted production rate for the first 100 days – while of some importance – was not substantial, in terms of the overall process performance prediction over a 4-6 years period (depending on the SOR and reservoir quality) for the pattern. As mentioned earlier, the flow mechanism associated with ceiling drainage was significantly different from that associated with slope drainage, as counter current flow and re-saturation of fluids would have to be accounted for. It would be possible to formulate a separate problem to describe the flow mechanism specific to this ceiling drainage flow period. When reservoir sand is interbedded with mudstone, the vertical permeability is much lower. In this instance, the time taken for the steam zone to rise to the top of the reservoir is longer (perhaps years). The assumption of ignoring ceiling drainage would be questionable in this case.

Once the steam zone reaches the cap rock, it is forced to spread laterally, and slope drainage becomes dominant. As stated previously, the forecasted oil production rate during this slope-drainage period matches well with STARS™ simulation results. The new analytical model predicts an average rate of approximately 74 m^3/d, compared to the average rate of approximately 69 m^3/d predicted by the STARS™ simulator.

The difference in the two predicted oil production rates near the end of the forecast is probably due to the different boundary conditions considered by the two models. For the analytical model, the boundary was assumed to be semi-infinite. In the numerical simulation model, an element of symmetry was chosen; as such, the condition for the outer boundary of the element of symmetry is no-flow (or closed) boundary condition.

Physically, it is important to note that as the steam zone interface moves laterally further away from the source (injector), oil production rate should taper off quite rapidly, due to significant heat loss to the cap rock and the presence of steam condensate in the system. As such, the energy injected could no longer promote steam zone growth. Therefore, a heat balance could be

performed to determine the physical feasibility of steam injection to maintain steam zone expansion for an indefinite time period. Such heat balance would also help to validate the oil production trend of the analytical model

It is also noted that field development using the SAGD process typically involves many horizontal well pairs. Depending on various factors, especially reservoir geology and economic profitability (as indicated by parameters such as cumulative SOR), many of these well pairs could be in communication with each other in the latter stages of the operation. Hence, the boundary condition which represents the "reality" is believe to be between the boundary condition assumed by the analytical model and that represented in the numerical simulation model.

It is also important to consider another distinction between the analytical model and the STARS™ simulator: constraint placed on fluid production. In the numerical simulation study, pressure constraints were implemented for both the injection and production wells to mimic the actual operational strategies. These constraints controlled the volume of fluid injected and volume of fluid produced. On the other hand, in this analytical model (as in all analytical models), fluid production was governed by the flow potential. Incorporation of pressure constraint(s) into the analytical model was not considered, as it would have required additional relationships between pressure and rates, which would render the problem intractable.

In Section 5.2.2, another example of Butler's models is also provided. In this case, the calculated interface velocity was shown. The steam zone interface velocity at different times was summarized in Table 5.3. Table 5.8, illustrated below, is a summary of the results for the steam zone interface velocity, calculated from the new analytical model at different reservoir heights. Several comments are warranted for the results shown in Table 5.8. First, the steam zone interface velocity increased away from the bottom of the reservoir. What this means is that the forward convection of the steam zone was highest at the top of the reservoir, and lowest at the bottom of the reservoir. Clearly, as seen in numerical simulation results and transparent-model experimental data (Butler, 1991, 1994), fluid drainage and production into the horizontal producer had an impact on how far the steam zone interface advanced in the lower sections (i.e., layers) of the reservoir. Given that the interface velocity values given in Table 5.3 were calculated for a height of 15.8 m in the 27.4-m reservoir, values of the steam zone interface velocity for (y/h) = 0.6 were used for comparison. It is noted that, for Butler's models, the steam zone interface velocity was the same at time t = 0 days and t = 100 days (Table 5.3).

77

	t=100 days (dX/dt), m/d	t=300 days (dX/dt), m/d	t=1000 days (dX/dt), m/d
y/h = 0.0	0.0305	0.0176	0.0097
y/h = 0.1	0.0332	0.0192	0.0105
y/h = 0.2	0.0356	0.0206	0.0113
y/h = 0.3	0.0376	0.0217	0.0119
y/h = 0.4	0.0391	0.0226	0.0124
y/h = 0.5	0.0402	0.0232	0.0127
y/h = 0.6	0.0409	0.0236	0.0129
y/h = 0.7	0.0413	0.0239	0.0131
y/h = 0.8	0.0418	0.0242	0.0132
y/h = 0.9	0.0426	0.0246	0.0135
y/h = 1.0	0.0439	0.0253	0.0139

Table 5.8: Calculated Velocity of Steam Zone Interface at Different Times.

Table 5.9 provides a comparison of the steam zone interface velocity predicted by the new analytical model, and by Butler's LinDrain model (1994). It is seen that at the end of 100 days, a velocity of 0.031 m/d was calculated with Butler's model, compared with a value of 0.041 m/d calculated with the new analytical model. At the end of 300 days, the values were 0.027 m/d and 0.024 m/d for Butler's models and the new model, respectively. Similarly, at the end of 1000 days, the respective values were 0.014 m/d and 0.013 m/d. For both models, the steam zone interface velocity slowed down with time. These results for both models are quite closely in agreement, especially given the differences in their treatment of the heat transfer mechanism in the reservoir. It could also be surmised from the results of the new analytical model that the effects of convective transport on steam zone expansion into the unheated reservoir (Region 2) were more significant in early time period. As such, the steam zone interface velocity from this model at the end of 100 days was more than that determined from Butler's models. However, heat transfer inside the reservoir became more conductive dominated in later time periods, as convective transfers became less important. As a result, the values calculated for the steam zone interface velocity from both models approached one another at later times. It must be noted, however, that the new analytical model in this thesis did not have to rely on many simplifying assumptions.

78

Time, days	100	300	1000
Velocity Calc. from Butler's LinDrain Model (1994), m/d T	0.031	0.027	0.014
Velocity Calc. from New Analytical Model in Thesis, m/d ε	0.041	0.024	0.013

Table 5.9: Comparison of Steam Zone Interface Velocity Predicted by Butler's LinDrain Model (1994) and New Analytical Model, at Different Times.
T velocity calculated at height of 15.8 meters in reservoir of 27.4-meters thickness.
ε velocity calculated at position of 0.6*(y/H)

Figure 5.13 shows a comparison of the cumulative oil recovery between the STARS™ simulator, Butler's models, and the new analytical model. The results from the STARS™ simulator and the new analytical model agreed reasonably with one another, after 2555 days of steam injection. The cumulative oil production predicted by the analytical model and the STARS™ simulator were 173,000 m^3 and 162,000 m^3, respectively. It is noted that usually cumulative recovery provides a good overall indicator for comparison between models. It does not, however, show clearly the mechanisms associated with the recovery process (in this case, SAGD process) at different times.

Figure 5.14 illustrates the position of the steam zone interface at different times during the SAGD process calculated with the new analytical model. The interface position and, hence, the velocity of the steam zone front are both determined by Equation (4.33). It is seen that the steam zone interface position is dependent on the thermal diffusivity (α), time (t) and the parameter λ. It is seen that the steam zone interface was also moving away from the horizontal producer at the base of the reservoir. This profile was also present in Butler's original SAGD model (1981). The following comments are offered for this result. In SAGD operation, the horizontal producer behaves as a sink, compared to the horizontal injector above it (which acts as a source). As a result, steam condensate and mobilized oil converge toward this sink. Therefore, the profile shown in Figure 5.14 shows that the new analytical model (despite its approach of representing flow inside the reservoir in a pseudo 2-D manner) could not model 2-D flow completely and precisely. Having said this, it is important to examine the flow around the horizontal producer.

In a SAGD process, the vertical spacing between the horizontal injector and producer is typically 4-7 m. To prevent the injected steam from being short circuited, a steam trap is employed whereby the horizontal producer pressure is typically set 300-600 kPa lower than the injection pressure. Consequently, not all mobile fluids are produced from the reservoir; instead, some of the mobile fluids accumulate above and around the producer. By remaining inside the reservoir they contribute to convective heating ahead of the steam zone interface. Edmunds (1984) had

79

Production Forecast
Comparison
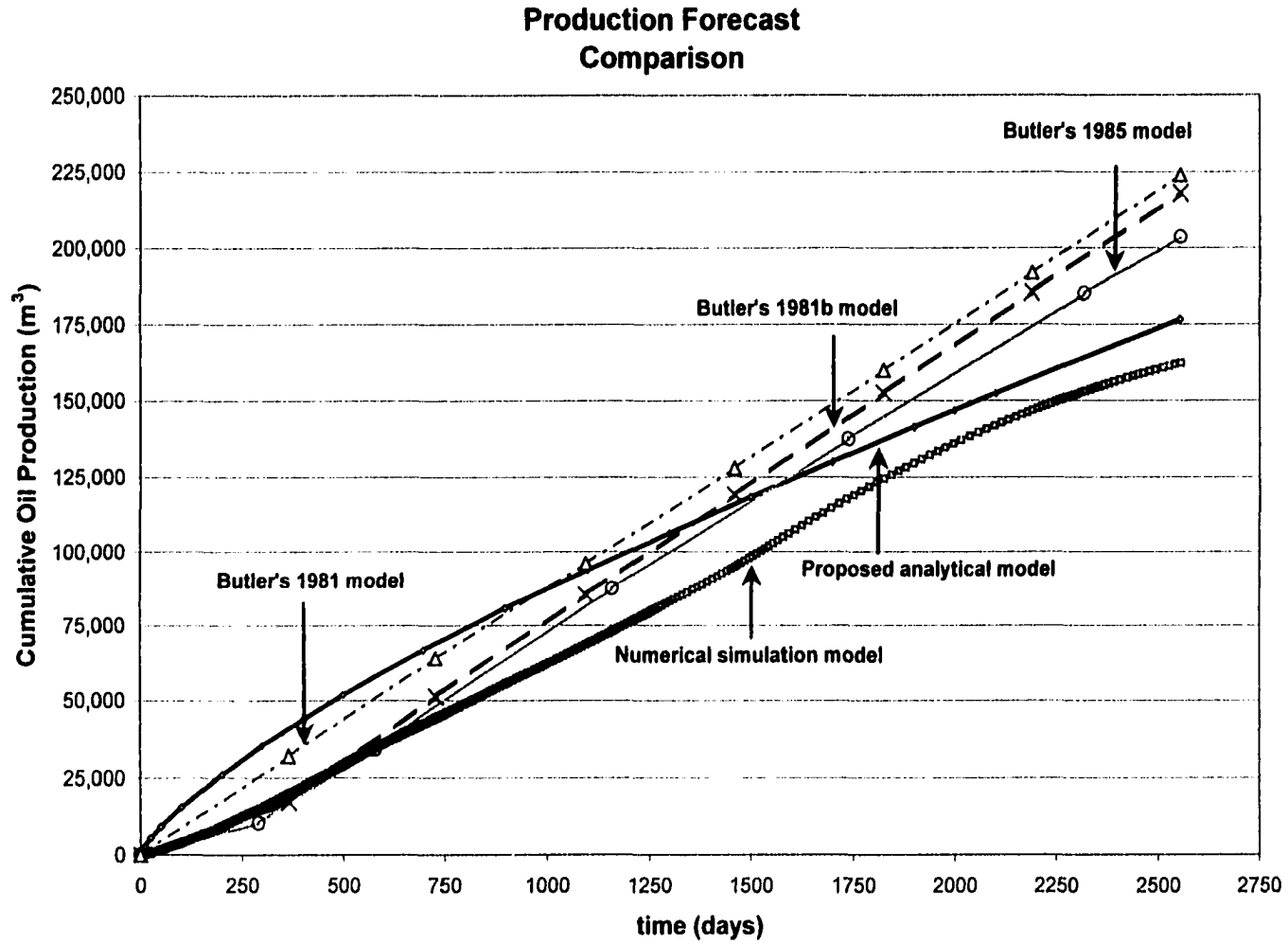
Figure 5.13: Comparison of Cumulative Oil Production Predicted by Butler et al.'s model (1981), TANDRAIN model, Butler's model (1985), STARS[TM] Simulator and New Analytical Model.

Interface Position During Constant Injection Period
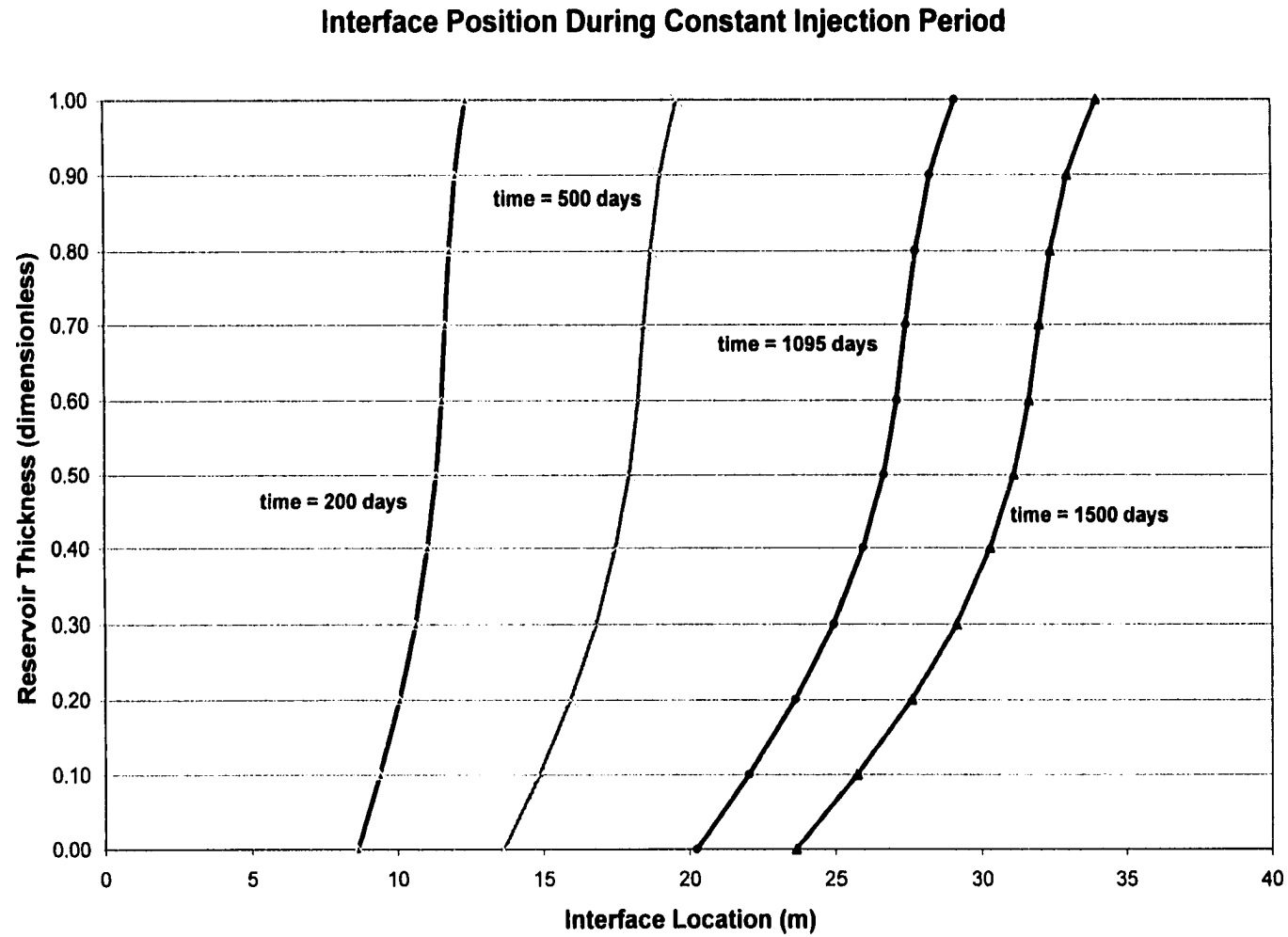
Figure 5.14: Position of Steam Zone Interface at Different Times, as Predicted by the New Analytical SAGD Model.

reported the presence of convective transport near the horizontal producer in SAGD process. Mandl and Volek (1969) had analyzed the importance of convective transfer in a steamflood, and pointed out the "flattened" temperature profile (i.e., (dT/dx) or slope of the temperature contour is close to 0). In view of Mandl and Volek's findings (1969), careful analysis of the temperature distribution around the SAGD horizontal producer (Figure 5.7) was made. It was noted that the width of the region containing the mobile and immobile oil saturation near the horizontal producer was larger than it was near the top of the reservoir. This observation was also true with the temperature profiles, i.e., the slope (dT/dx) was larger at the top than at the bottom of the reservoir. This observation was consistent with finding of convective transfer by Mandl and Volek (1969). It is reasonably safe, thus, to conclude that not all mobile fluids converge to the horizontal producer, where they were then produced.

The shape of the steam zone interface at the top of the reservoir is also of interest. As reasonably expected, it was dependent on the heat loss to the cap rock. An increase in heat loss to the cap rock would result in the position of the steam zone interface being "rolled back", i.e., the position of the interface at the top of the reservoir would be behind the furthest point of advancement of the interface in the reservoir. Conversely, if the heat loss to the cap rock were negligible, the position of the steam zone interface at the top of the reservoir would be expected to be the furthest point into the reservoir.

After 1000 days of steam injection, the steam zone interface position predicted from the new analytical model agrees closely with that determined by the STARS™ simulator. The new analytical model predicted the steam zone interface to be approximately 28 meters away from the well pair, at the top of the reservoir; the STARS™ simulator determined the interface to be about 30 meters from the well pair. The close agreement, however, deteriorated slightly near the production well.

In summary, it is seen from the above discussions that the new analytical model calculated steam zone interface position and velocity values in close agreement with results determined by Butler's LinDrain model (1994) and STARS™ reservoir simulator. The oil production rate determined by the new analytical model (75 m³/d) agreed quite closely with that obtained from the STARS™ simulator (70 m³/d) for the middle time period (between 500 days and 1000 days). Explanations are also provided for the poor match between simulated oil production rate (from STARS™ simulator) and rate predicted by the new analytical model. Even though the oil production rate profile predicted by the new analytical model declined at a steeper rate during the slope drainage period than those predicted by the TANDRAIN model and Butler's 1985 model, the three rates were generally within the same order of magnitude. The higher oil production rates predicted by the TANDRAIN model and Butler's 1985 model were probably due to no heat losses accounted for by both of these models.

82

5.4.2. Qualitative Comparison of Simulation Results and Selected Experimental Data for the SAGD Process

The following section is prepared for qualitative comparison of simulation results and selected experimental data for the SAGD process, and by extension qualitative comparison of results from the new analytical model with experimental data. Chung and Butler (1989) had compared the scaled up oil recovery from their experimental data for AOSTRA's UFT project with the rate predicted by Edmunds' simulation study (1987). The scaled up cumulative oil recovery was based on the assumption of a homogeneous (sandpack) reservoir having a permeability of 2.5 darcies. Two different cases were considered in Edmunds' study: i) isotropic reservoir, with permeability of 4 darcies, and ii) anisotropic reservoir, with vertical permeability of 1.0 darcy and horizontal permeability of 4 darcies. Figure 5.15 is reproduced from Figure 18 of their paper. Chung and Butler concluded that their scaled up experimental oil recovery was in general agreement with those predicted by the numerical simulation study, up to 2.5 years of production. Thereafter, the scaled up experimental oil recovery was less than that from the numerical simulator. It should be noted that, up to 2.5 years of production history, the scaled up experimental oil recovery curve stayed between the two simulation curves, i.e. it was less than the recovery curve for isotropic reservoir (case i) and larger than that for the anisotropic reservoir (case ii). Interestingly, the cumulative oil production was similar for these two cases of reservoir anisotropy at 4 years of production (approximately 110 m^3/meter of horizontal well length, compared with 90 m^3/meter of well length for the scaled up experimental production).

Chow and Butler (1996) used STARS™ simulator to history match scaled experimental data reported by Chung (1988). Two different well configurations were used to investigate the phenomena associated with the rising steam chamber phase, and the spreading steam chamber phase. The authors used linear relative permeability functions for oil and water (due to assumption of segregated flow of oil and water), with these functions being assumed independent of temperature. It was found that, despite reasonably good matches for the cumulative oil recovery and oil production rate, poor history match was obtained for the steam zone interface for the rising steam chamber phase. This poor match was believed to be due to the inability of the numerical simulator to simulate processes including emulsification and counter-current flow mechanism taking place during the rising steam chamber phase. Figure 5.16 is reproduced from Figure 5 of their paper, for the spreading steam chamber phase. In this case, the simulated temperature distribution inside the reservoir (represented by the position of the 100 °C isotherm at different times) was in good agreement with the measured position of the steam zone interface. Good agreement was also obtained for the predicted cumulative oil production curve and the experimental curve.
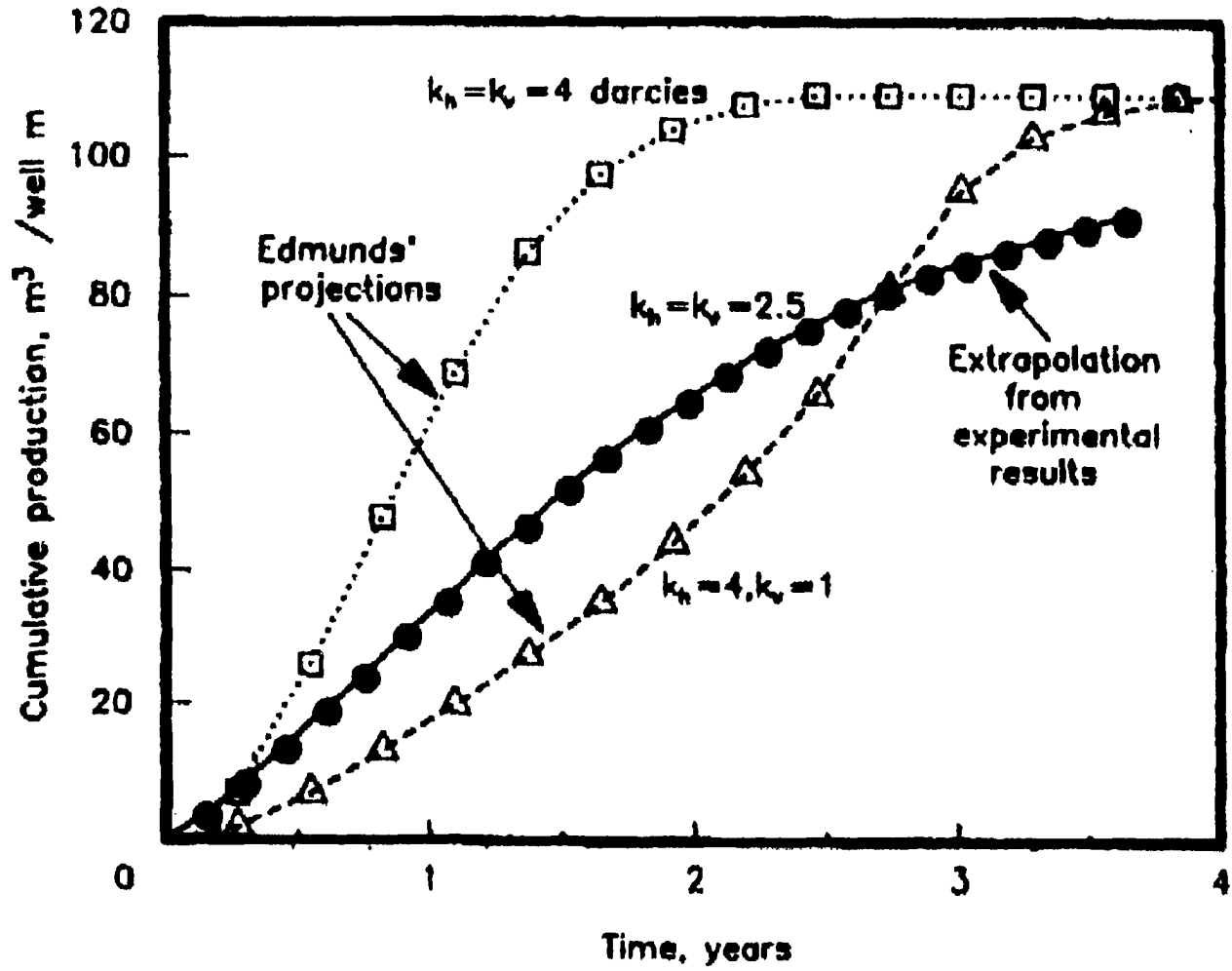
Figure 5.15: Comparison of Experimental Cumulative Production vs. Simulation Cumulative Production for UTF. (reproduced from Chung and Butler, 1989.)
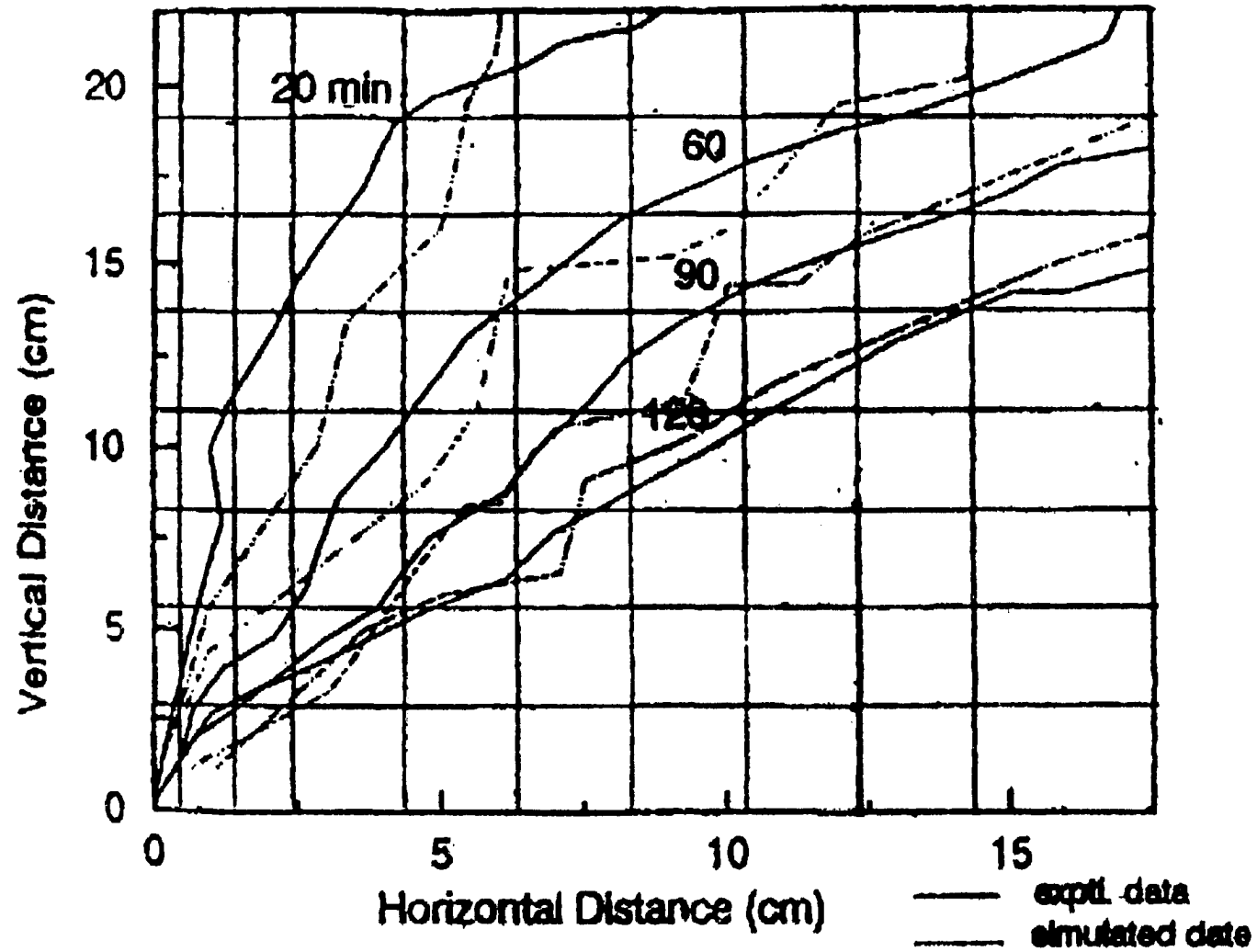
Figure 5.16: Comparison of Experimental Steam Zone Interface Position vs. Simulated Steam Zone Interface Position, at Different Times. (reproduced from Chow and Butler, 1996.)

Sasaki, Akibayashi, Yazawa, Doan and Farouq Ali (1999) carried out a systematic experimental and numerical investigation of the SAGD process. Different relative permeability functions were used in the history matching of experimental data. It was established that linear relative permeability functions with non-zero end-point saturations provided good history match for the steam chamber shape, while the match was poor for non-linear relative permeability functions. Good history matches were also obtained for the breakthrough time as a function of the vertical spacing between wells, cumulative oil recovery, oil production rate, and cumulative water production.

In summary, it can be seen from the above studies that numerical simulation can be used successfully to match experimental data for the SAGD process. As such, a reservoir simulator such as CMG's STARS™ could be used as an engineering tool to investigate different aspects of the SAGD process, including the temperature distribution inside the reservoir and the position of the steam zone interface at different times. In the absence of crucial experimental data – particularly heat losses from the reservoir and the relative permeabilities of the sandpack reservoir – in various experimental studies cited in this thesis, it was not practical to compare directly the results of the new analytical SAGD model (which accounts for heat losses) with these experimental data. At the same time, it must be said that there is close agreement between the steam zone interface position predicted by the new analytical model (28 meters at the end of 1000 days) and that from the STARS™ simulator (approximately 30 meters). This, coupled with the close agreement between the steam zone interface velocity predicted by this new analytical model and that calculated by Butler (1994) (as shown in Table 5.9), shows a good degree of validation for the new analytical model, and gives confidence in its predictive capability.

5.5. Parametric Study of New Analytical SAGD Model

The new analytical model was next used to carry out a parametric study to determine the effects of various parameters on its performance. The results of this study are presented in the following.

5.5.1. Effect of Production Potential

As shown in Chapter 4, fluid production rate is directly linked to the steam zone interface position via the mass and energy balance equation. In this section, the effect of fluid production rate on the position of the steam zone interface is studied. Figure 5.17 shows the position of the interface as a function of production potential (γ) at 1000 days. In this case, variables such as heat loss, thermal diffusivity, etc. were kept constant. Value for the variable (γ) ranges between 0.3 to 0.8. Clearly, the steam zone interface advanced the furthest into the reservoir with the lowest value of the production potential ($\gamma = 0.3$); conversely, when $\gamma = 0.8$, the steam zone interface trailed behind. These results show that higher fluid production volumes corresponded with higher flow potential. As such, more heat was produced (i.e., removed) from the reservoir with higher value for the production potential γ. Consequently, not enough energy was present in the reservoir to

86

Interface Position with Different Production Potential
1000 days
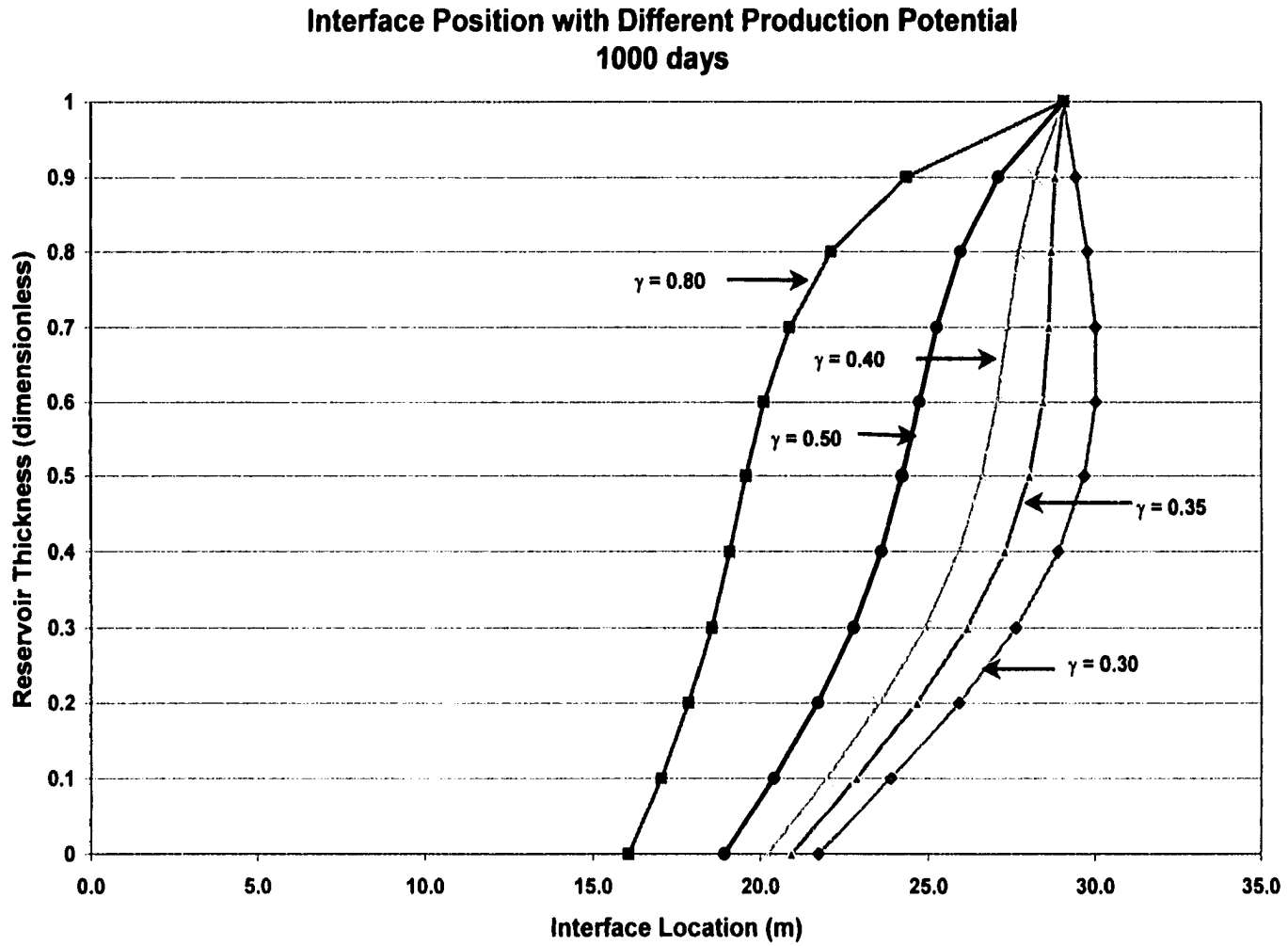
Figure 5.17: Effect of Flow Potential (γ) on Position and Profile of Steam Zone Interface, after 1000 Days.

promote further the growth of the steam zone (by convection). On the other hand, when value for γ was low, less heat was removed from the reservoir (due to lesser volume of fluids produced). As a result, the steam zone interface advanced further into the reservoir.

It was also noted that for $\gamma = 0.8$, the point of maximum penetration of the steam zone interface into Region 2 corresponded with a dimensionless height (y/h) of 0.7. For $\gamma = 0.3$, this point of maximum penetration of the steam zone interface into Region 2 corresponded with a dimensionless height (y/h) of 0.6. The reader is cautioned not to correlate the position of the steam zone interface with the volumes of oil displaced. In the development of this model, lower flow potential is associated with lower reservoir sand quality. Consequently, this lower flow potential limits the rate at which the reservoir could "deliver". It also limits steam injectivity (and hence, energy) into the reservoir. With lesser amount of energy injected into the reservoir, the position of the interface would not (surely) have advanced far into the reservoir. It was only for comparative purpose in Figure 5.17 that the energy and mass fluxes from Region 1 were maintained constant for the different cases shown in the figure. The fact that the steam zone interface had penetrated (advanced) further into the cold reservoir serves only to illustrate the relationship between the energy produced (removed) from the reservoir and the energy accumulated in the reservoir. As discussed in Section 5.3, this relationship had an impact on the mode of heat transfer in the reservoir, and the recovery performance of the SAGD process. Figure 5.18 shows the production rate at different times, for different values of the production potential. The results agree closely with those shown in Figure 5.17, as explained above.

5.5.2. Effect of Thermal Diffusivity

The effect of thermal diffusivity on the position of the steam zone interface is investigated in this section. Five different values of α, ranging from 0.01 to 0.06, were used in the investigation. Figure 5.19 presents the results for these different cases. It can be seen clearly that the position of the steam zone interface was influenced by the thermal diffusivity. Larger thermal diffusivity resulted in further advancement of steam zone interface into the reservoir. The steam zone advanced the least into the reservoir for $\alpha = 0.01$. These results point out that larger thermal diffusivity enables more heat to be transferred into the reservoir ahead of the moving steam zone interface. As a result, the steam zone advances further into the reservoir. Also, the slope of drainage was influenced by the thermal diffusivity: it was steeper for lower values of α, and more gradual for higher values of α.

Production Forecasts for Different Production Potential
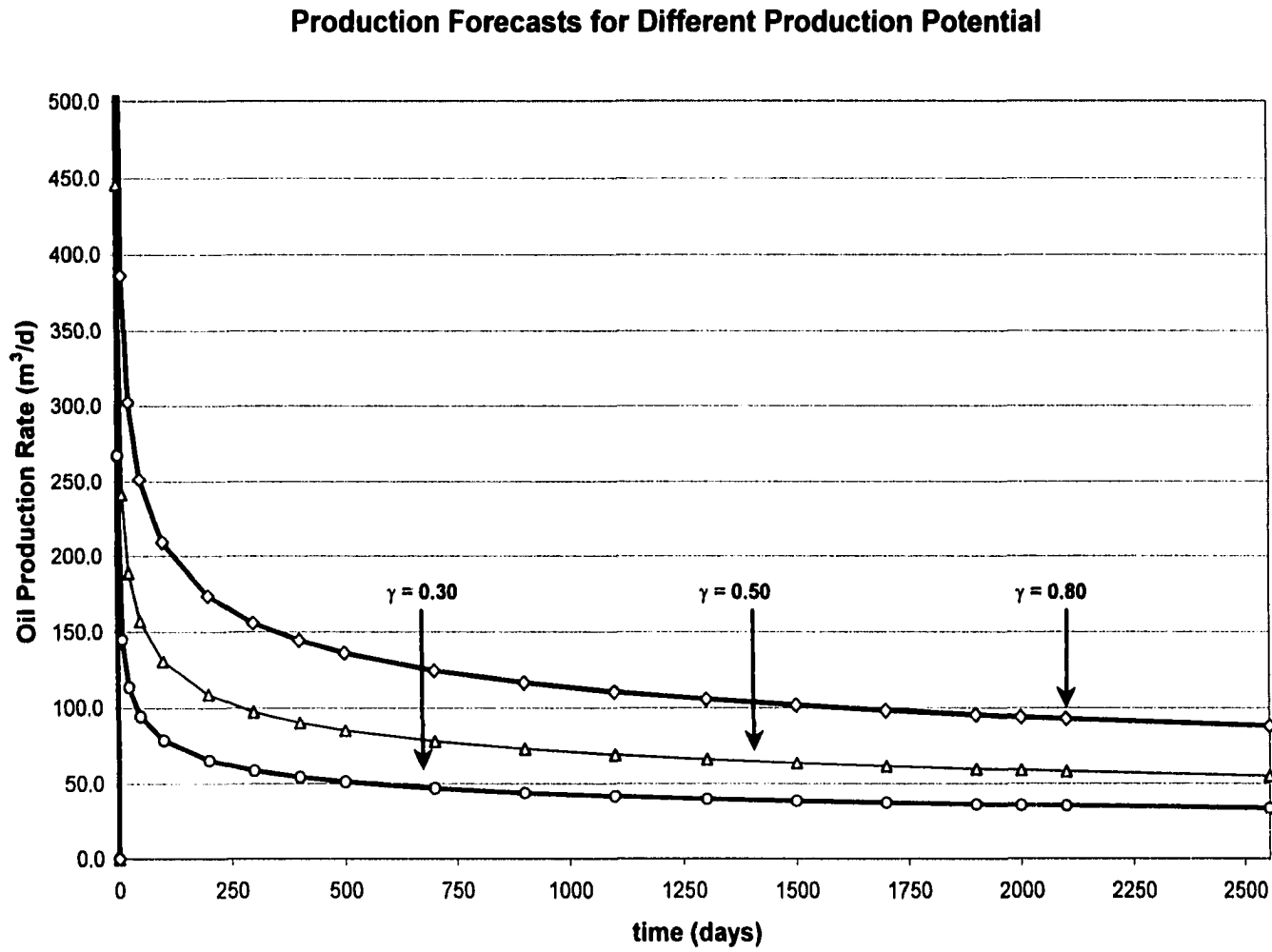
Figure 5.18: Effect of Production Potential on Oil Production Rate at Different Times, as Predicted by New Analytical Model.

Interface Position Having Different Thermal Diffusivity
1000 days
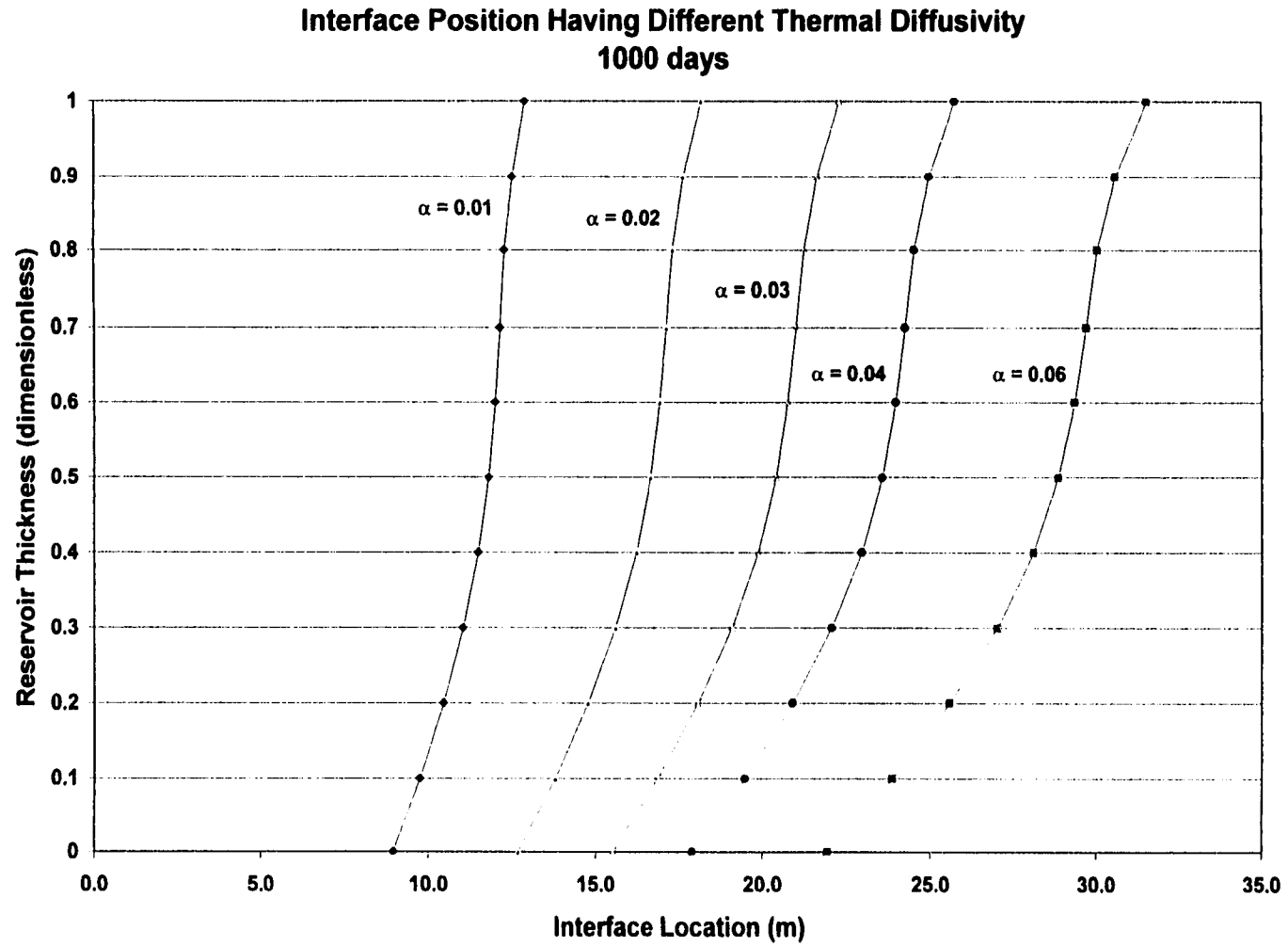
Figure 5.19: Effect of Thermal Diffusivity on Position and Profile of Steam Zone Interface, after 1000 Days.

5.6. SAGD Performance in Bottom-Water Reservoirs

5.6.1. Model Description

This numerical study was also conducted using CMG's STARS™ thermal simulator. The base case model represented half of an element of symmetry, and had a 20 x 5 x 18 grid matrix (giving an overall dimension of 43.5 m x 300.0 m x 27.25 m). A nine-point finite difference scheme was applied in the i,k (x- and z-) directions to ensure proper modeling of diagonal transmissibility. Smaller grid blocks were used around the horizontal injector and producer. The horizontal producer was placed 2 m above the base of the formation, and the horizontal injector 7.5 m above the producer. Table 5.5 shows the pertinent data that was used in the model. Figure 5.20 shows the grid used in this numerical study.

Steam injection rate was constrained at a bottom-hole pressure of 3.5 MPa (saturated steam temperature of 242.6°C) and at 90% steam quality. The steam trap was operated at 20°C below the saturation temperature with a maximum steam production rate of 5 m³/d (CWE). In modelling a reservoir in communication with a water sand (either above or below the oil pay), two or three additional grid layers were attached to the bottom or top of the base-case model – depending on the water sand thickness. The water sand was assumed 'static' in this study. However, the effect of increasing the areal coverage of the water sand on the recovery process was also considered. This increase in the areal extent of the 'thief' water zone roughly modelled a more active aquifer. In these runs, additional grid blocks were attached to the water sand extending along the x- and y- directions only. The length along the x-direction was extended by 152.0 m, while the length along the y-direction was extended by 300.0 m (150.0 m from the toe and heel of the horizontal well).

Horizontal permeability (k_h) and vertical permeability (k_y) of the reservoir rock were 5000 md and 1000 md, respectively. For a porosity value of 30% and oil saturation of 66.1%, the element of symmetry had 71.0 x10^3 m³ of original oil in place (OOIP) for the base case (142.0 x10^3 m³ for a full pattern). As in previous case, geomechanics was not modelled. The entire length of the horizontal well was assumed to be productive; wellbore hydraulics was ignored.

5.6.2. Discussion of Results

At the completion of the SAGD process large amounts of heat still remain in the reservoir. O'Rourke et al. (1997) indicated that after SAGD operation was terminated at UTF, about 70% of the injected heat still remained in the reservoir. Hence, some of the bitumen remaining in the reservoir was mobile. In thermal projects it is desirable to retain as much heat in the reservoir as possible. A thermal process is only efficient when the heat accumulated in the reservoir is larger than the heat produced and the heat loss combined (i.e., $Q_{accum} > (Q_{loss} + Q_{prod})$). The management of heat accumulated in the reservoir could provide additional recovery of oil in the

91

ROLE OF BOTTOM WATER ON SAGD PROCESS
C/C Heat Gain/Loss Rate (J/day) 2000-01-01   J layer: 1

File: Clm99-11a.txt.irf
User: Administrator
Date: 2000-07-28

Scale: 1:268.662607
Z/X: 1.00:1
Axis Units: m

0.00
0.00
0.00
0.00
0.00
0.00
0.00
0.00
0.00
0.00
0.00

0.00   10.00
0.00   6.00   10.00 m
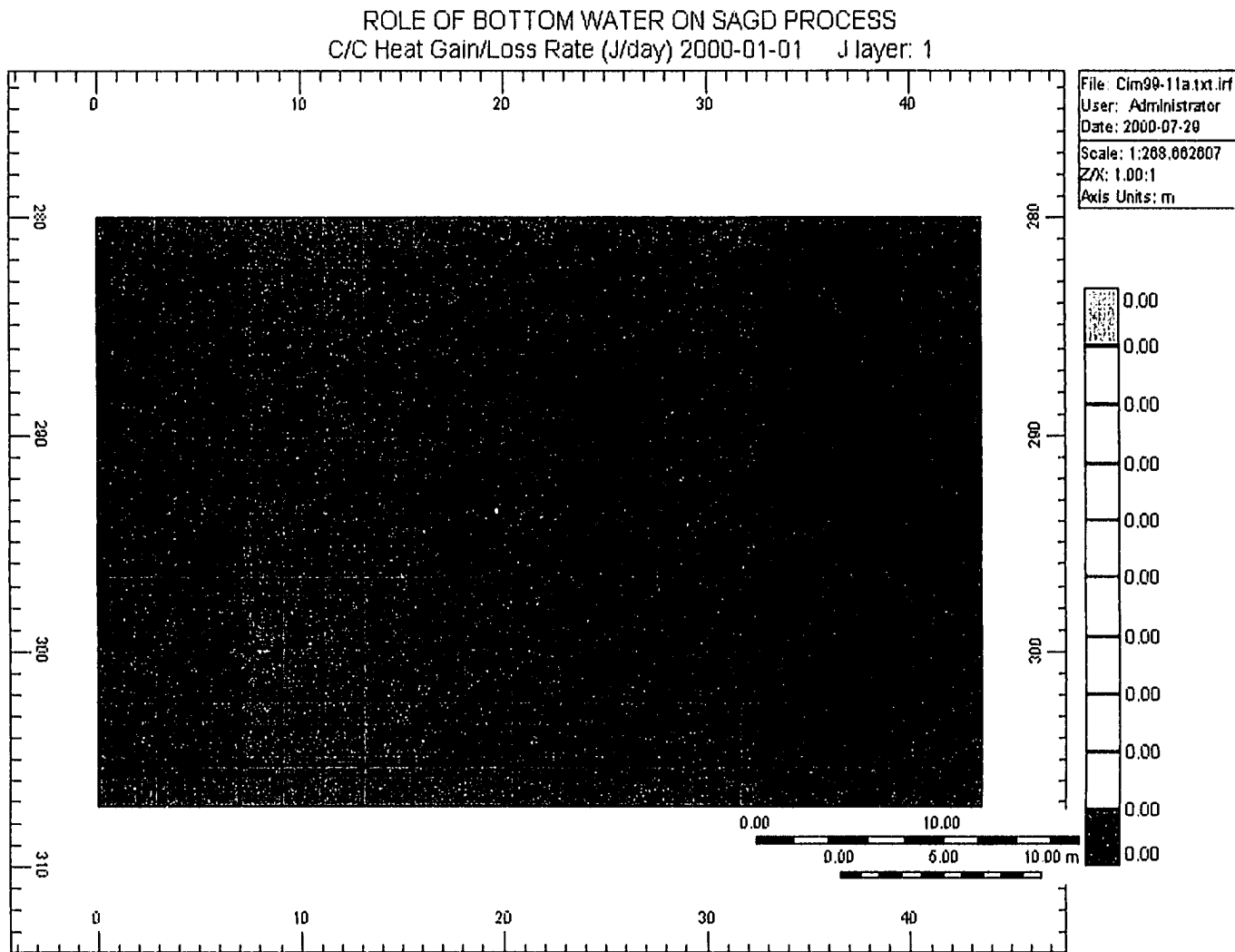
Figure 5.20: Grid Geometry for Simulation Studies of Role of Water Leg on SAGD Process, Base Case, STARS™ Simulator.

un-swept areas.

5.6.2. Base Case

Figure 5.21 shows the cumulative oil production and rate for the base case. The oil saturation profile is illustrated on Figure 5.22. The preheating period lasted 75 days before thermal communication was established between the horizontal injector and producer. The oil production rate – during the preheating period – was zero. As the temperature around the vicinity of the horizontal wells increased, the viscosity of bitumen decreased, and oil production rate increased. Steam injection rate also increased significantly as the viscosity of oil decreased. An average production rate of 80 m^3/d was maintained for 1400 days before rate decline was observed. With 335,500 m^3 (CWE) of steam injected, the resulting cumulative oil production was approximately 100,000 m^3, and the cumulative SOR ratio was 3.33 m^3/ m^3 (CWE). After 3288 days (9 years) of production, the recovery was 70% of the OOIP for this particular element of symmetry.

The ratio of volumes of steam injected (CWE) to the cumulative fluid produced at various time is illustrated on Figure 5.23. When the ratio was less than one (i.e., the cumulative injection was less than the cumulative production, it was inferred that the injected fluid was expanding; hence, steam expansion (drive) was present. This condition was seen to be present after 140 days of steam injection. When the ratio was greater than one, the injected fluid was a compressible fluid and a hot waterflood was present.

During the preheating period, approximately $4x10^8$ kJ of energy was injected. The average oil viscosity in the vicinity of the horizontal wellbore during this period was reduced to approximately 20 mPa.s. The cumulative heat loss to the cap and base rock, after 3288 days (9 years) of injection, was equal to $8.9x10^{10}$ kJ. The rate of heat loss to the cap rock was larger than base rock due to the larger temperature gradient present. From knowing the cumulative oil and water volumes produced along with their heat capacities, densities and temperatures, the heat produced from the reservoir was determined to be $3.7x10^{11}$ kJ. After 3288 days, the heat injected into the reservoir was $9.2x10^{11}$ kJ. From the heat balance equation, the heat accumulated in the reservoir was approximately $4.6x10^{11}$ kJ. Figure 5.24 shows the ratio of the heat that had accumulated in the reservoir, heat loss to cap rock and base rock, and heat produced as ratios of the heat injected. The recovery process was judged to be fairly efficient, as 50% of the injected energy was accumulated in the reservoir, with 10% lost to the cap rock and base rock, and 40% produced from the reservoir.

As steam was continuously injected into the reservoir, the ratio of heat accumulated to the heat injected in the reservoir decreased, which resulted in the formation of more condensate volumes. The increase in the condensate volumes led to a more important role played by convective heat and mass transfers in the reservoir.

93
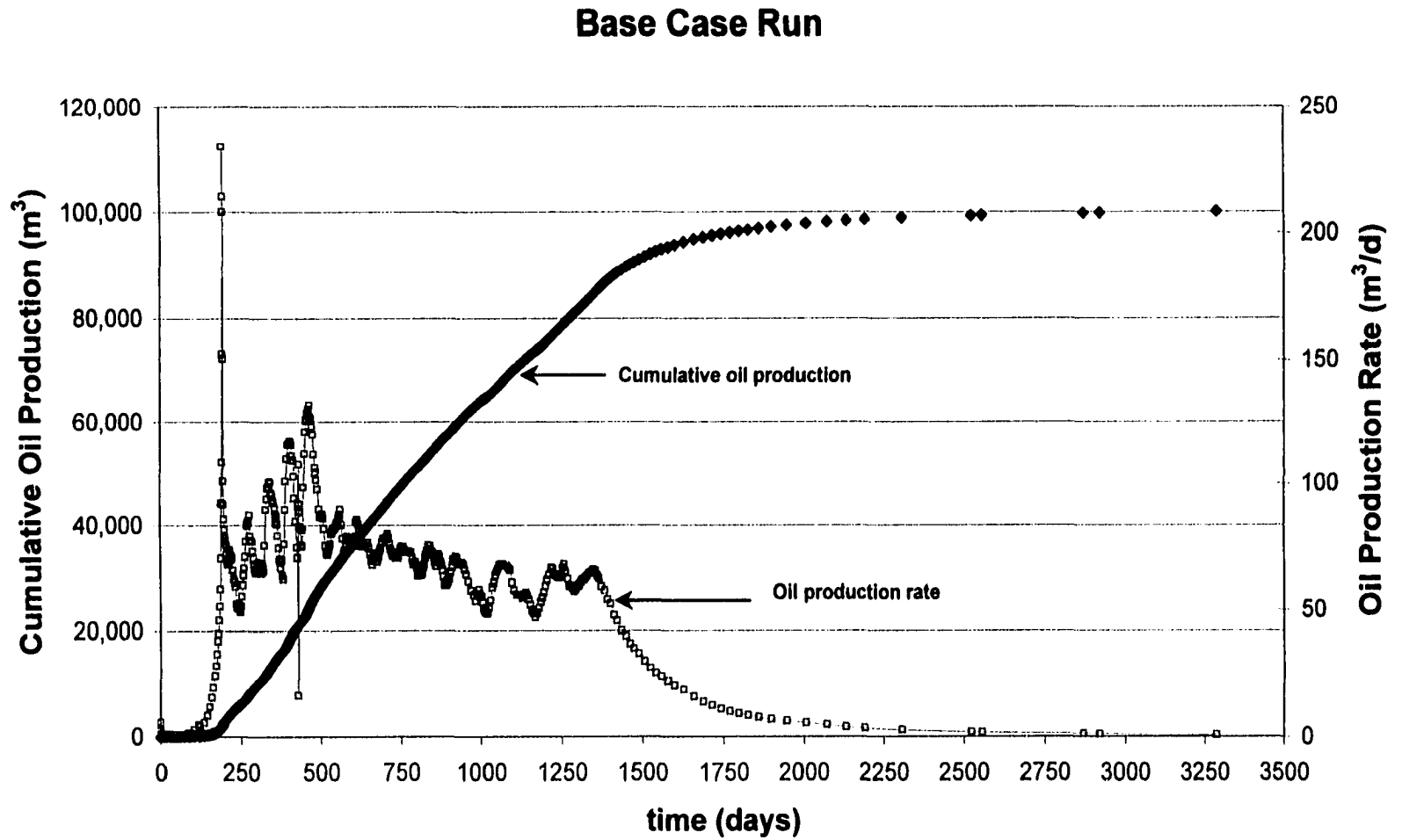
Base Case Run

Figure 5.21: Cumulative Oil Recovery and Oil Production Rate vs. Time, Base Case, STARS™ Simulator.
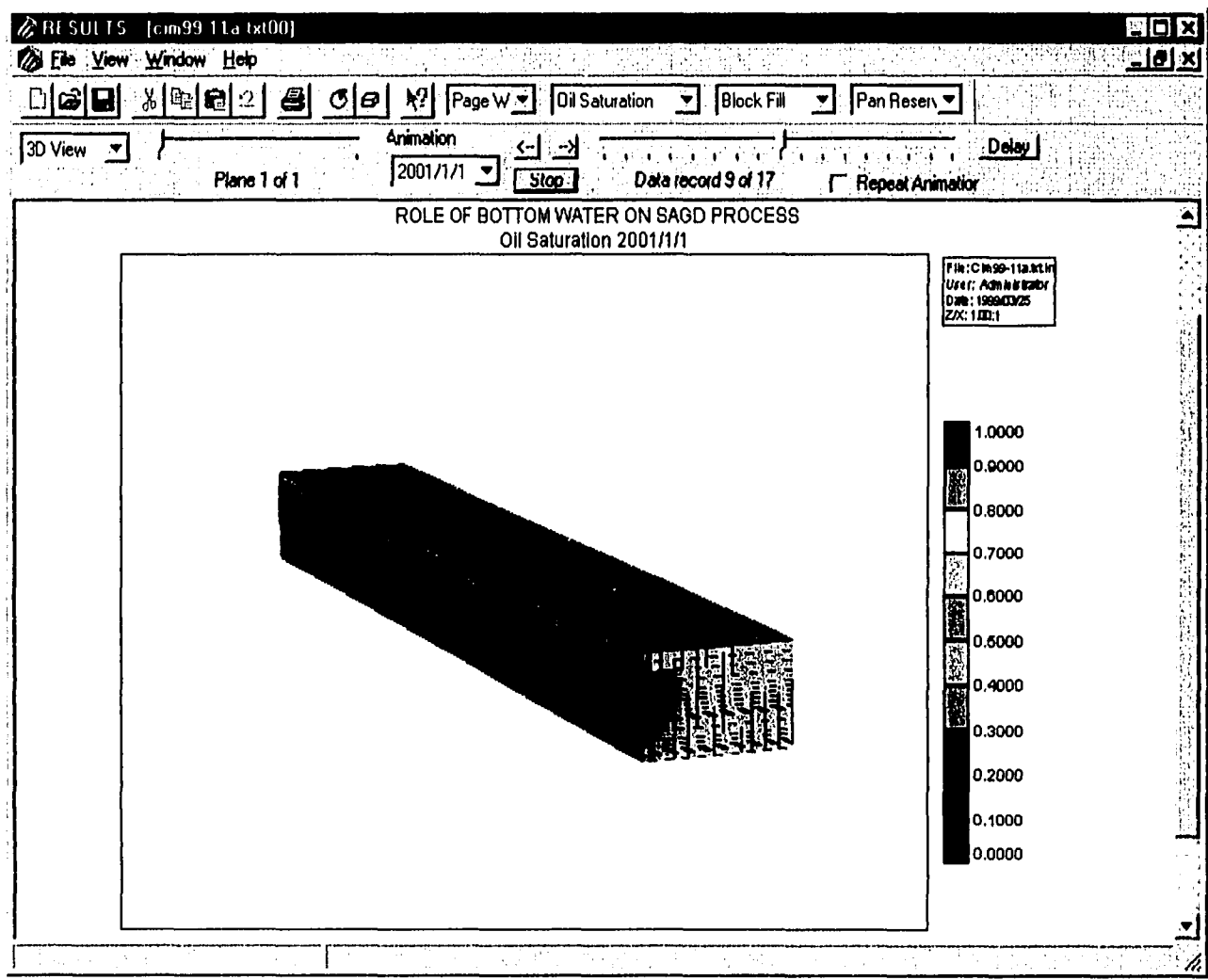
Figure 5.22: 3-D View of Oil Saturation Distribution, Base Case, STARS[TM] Simulator.
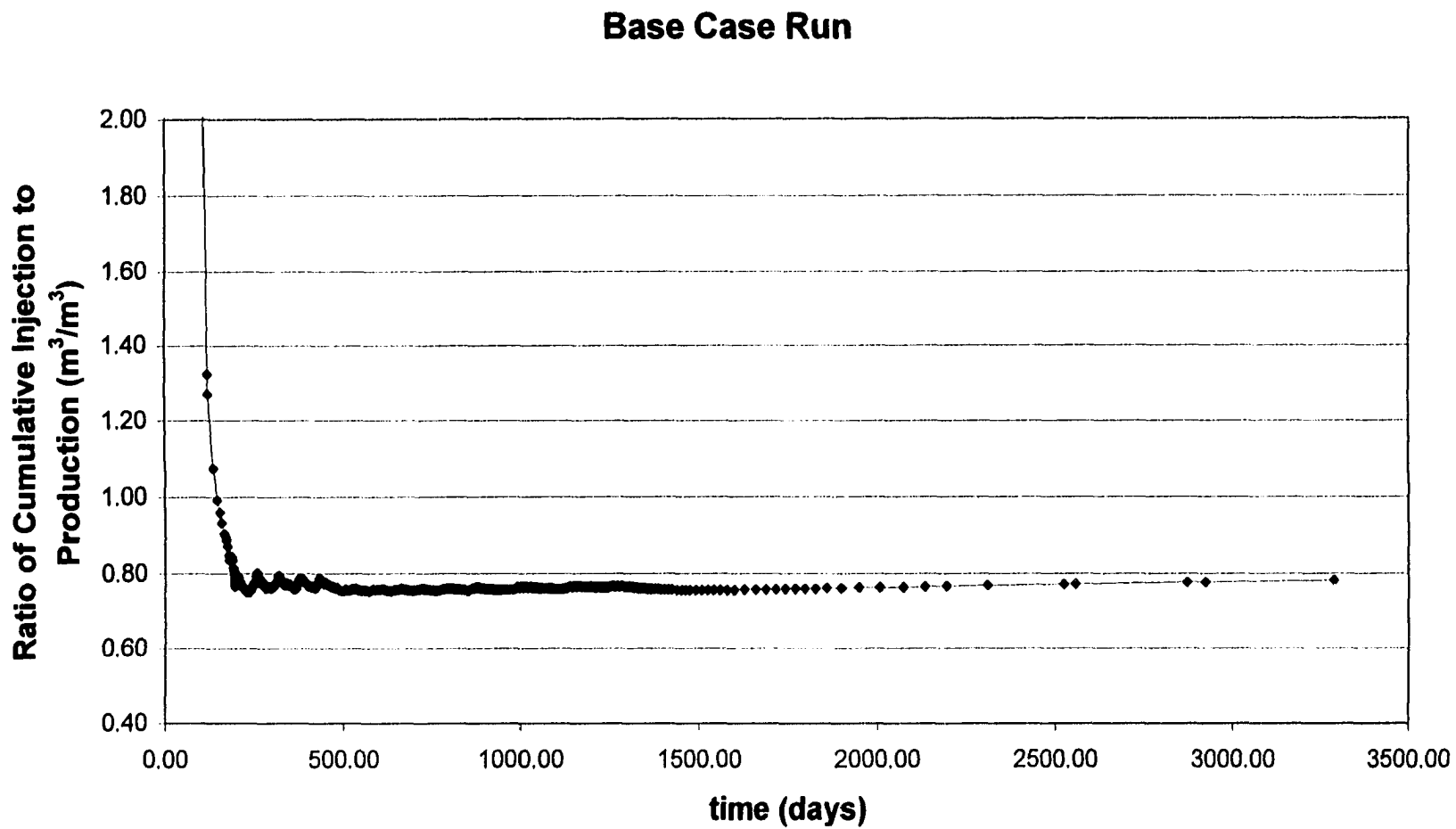
Base Case Run

Figure 5.23: Ratio of Cumulative Steam Injected to Cumulative Fluid Produced, Base Case, STARS™ Simulator.
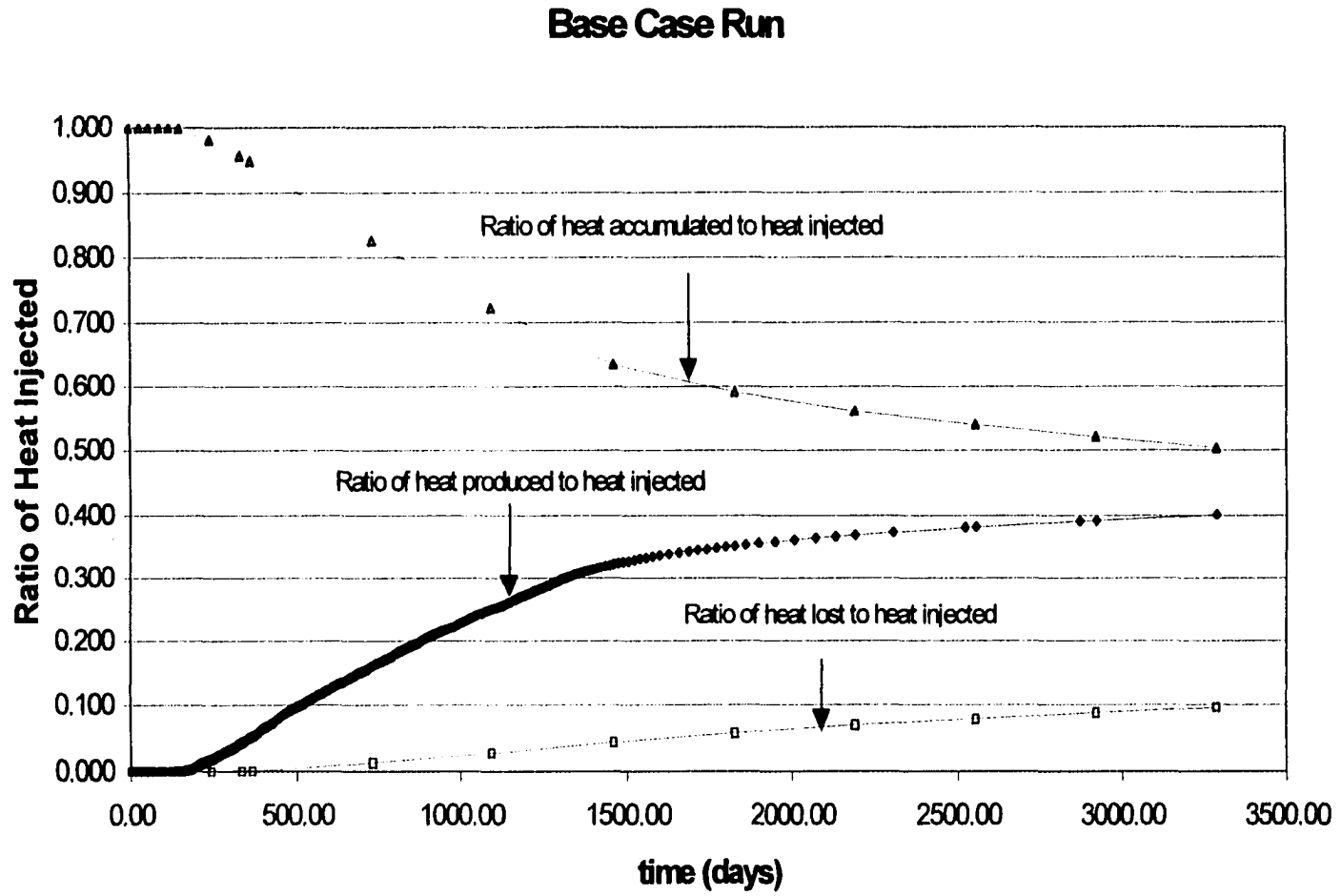
Base Case Run

Figure 5.24: Ratios of Heat Accumulated, Heat Loss (to Cap Rock and Base Rock), Heat Produced to Heat Injected, Base Case, STARS™ Simulator.

5.6.3. Presence of a Contiguous Water Sand

Depending on the oil density (°API gravity), the water sand could lie above or below the oil-bearing zone. The presence of both bottom water and overlying water sands was considered in this analysis. In addition, the effect of confinement (areal coverage of the water sand) was also evaluated. Altogether, six different scenarios were investigated:

a) confined bottom water sand (CBWL) – 6-m thick,

b) confined overlying water sand (COWL) – 6-m thick,

c) unconfined bottom water sand (UBWL) – 6-m thick,

d) unconfined overlying water sand (UOWL) – 6-m thick,

e) confined bottom water sand (CBWL) – 9-m thick,

f) unconfined overlying water sand (UOWL) – 9-m thick.

Comparisons between different scenarios were based on cumulative oil production for a given volume of steam injected (CWE) and the heat accumulated in the reservoir.

a) Confined Bottom – Overlying Water Sand – 6-m Thick

The effects of a confined bottom water sand (CBWL) and a confined overlying water sand (COWL) on the SAGD process were examined. Figure 5.25 shows the plot of cumulative oil production versus cumulative volume of steam injected for these two cases and the base case. After injecting 325,000 m^3 (CWE) of steam, cumulative oil production was 100,000 m^3 for the base case, and 92,600 m^3 for the other two cases. Hence, the presence of a water sand reduced the ultimate recovery by approximately 8% from the base case.

When an overlying water sand was present (case COWL), the heat that was injected into the reservoir was diverted to the overlying water zone. This resulted in the decrease in cumulative SOR at 500 days to 5.0 m^3/m^3 (CWE). Consequently, the recovery during this period of the steam injection process was lower. Because the water sand was confined, additional heat injected into the system provided sufficient heat to vaporize water into steam, which allowed the efficient gravity drainage of oil from the top of the reservoir. With this process, the SOR eventually reached 4.0 m^3/m^3 (CWE), and the recovery increased to 92,600 m^3 of oil, after 9 years (3288 days). Figure 5.26 shows a graph of the ratio of heat accumulated in the reservoir to the heat injected at various times. Initially, all of the energy that was injected accumulated in the reservoir; however, as steam injection continued, the steam chamber rose to the top of the formation, leading to heat loss to the cap rock. Also, the temperature of the produced fluid increased, which led to increased heat production from the reservoir. Subsequently, as expected, the ratio of heat accumulated in the reservoir to the heat injected decreased with time. From Figure 5.26, after

98

Confined Bottom and Overlying Water Sand - 6m Thick
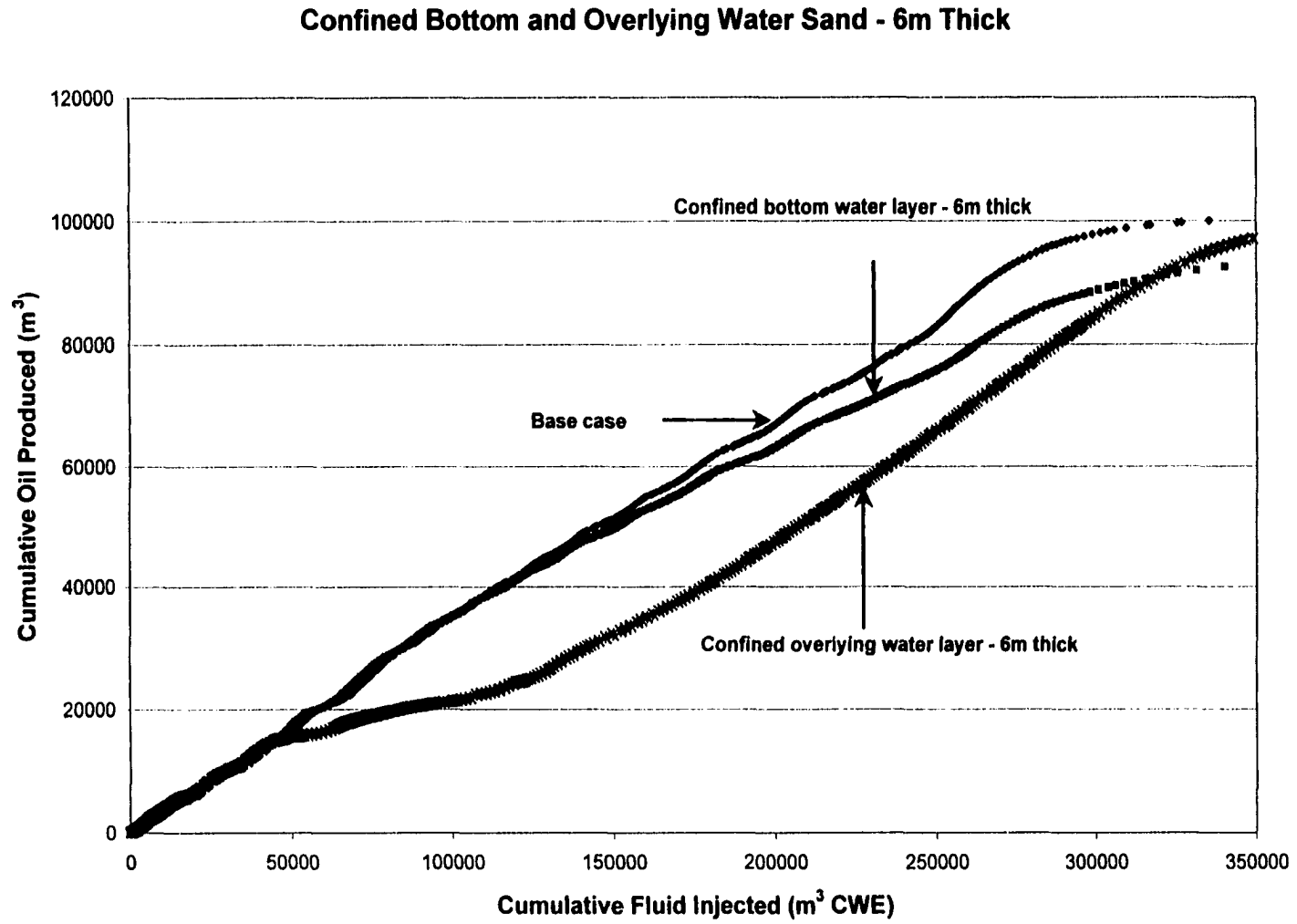
Figure 5.25: Cumulative Oil Recovery vs. Time, Confined Bottom Water Sand and Confined Overlying Water Sand – 6-m Thickness, STARS™ Simulator.

Comparison Between Confined Bottom and Overlaying Water Layer - 6m Thick
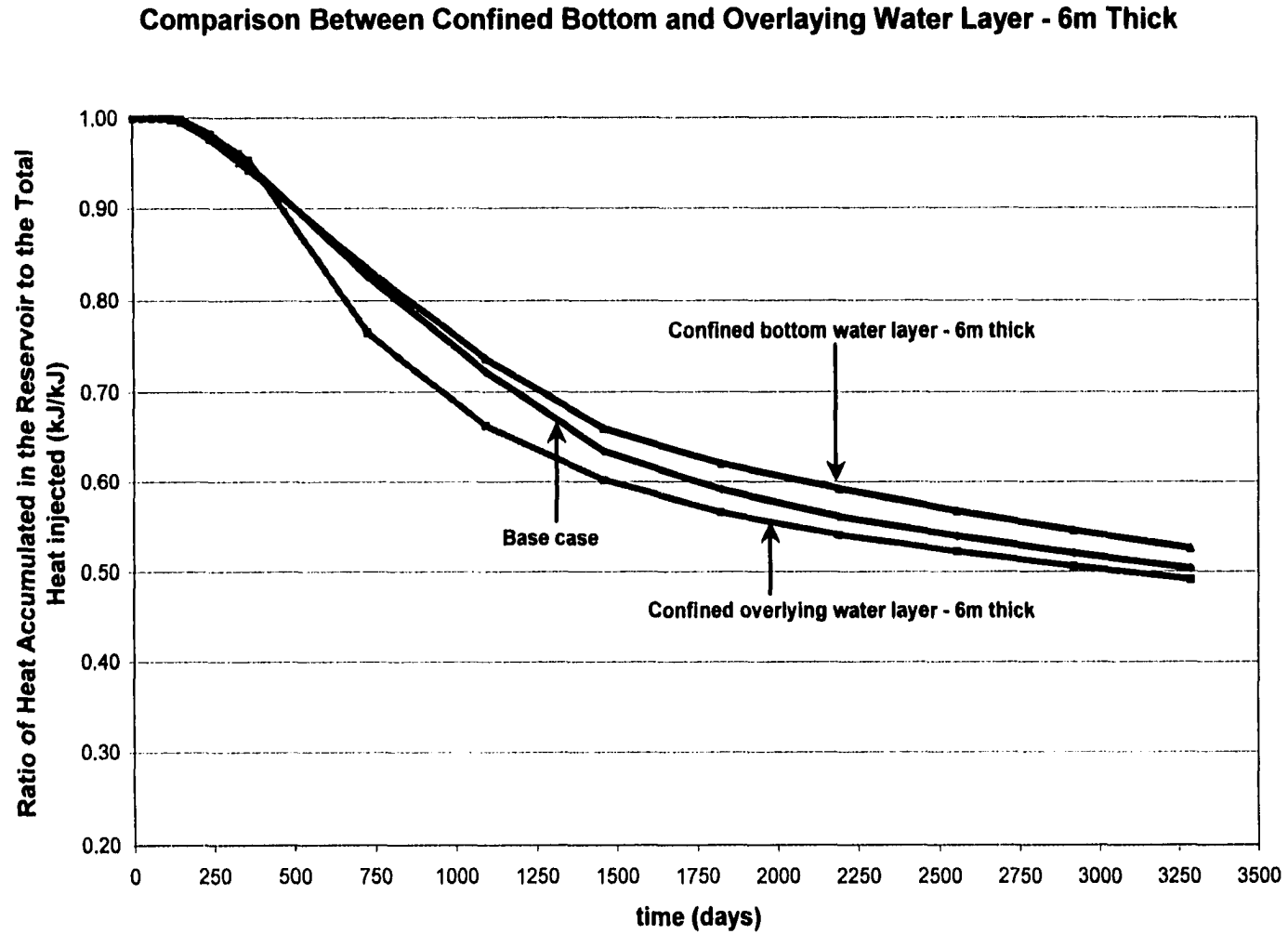
Figure 5.26: Ratio of Heat Accumulated to Heat Injected vs. Time, Confined Bottom Water Sand and Confined Overlying Water Sand – 6-m Thickness, STARS™ Simulator.

3288 days, the ratio of heat accumulated to the heat injected was the similar in all three cases. Overall, the process was considered efficient, because the $Q_{acc} > Q_{prod} + Q_{loss}$.

In the above discussion, an economic limit was not applied to the entire production history. In practice, the cumulative SOR, a common economic indicator, was chosen between 4.0 to 5.0 m^3/m^3 (CWE). When an economic SOR was taken at 5.0 m^3/m^3, the recovery for the case COWL was 28% (or 20,000 m^3 of oil). A similar economic SOR had not been observed in the case where confined bottom water sand (CBWL), 6m thick, was present.

b) Unconfined Bottom – Overlying Water Sand – 6-m Thick

The effect of unconfined water sand on recovery was extensively investigated. Simulation runs were performed to determine how the presence of an unconfined water sand (i.e. scenarios # 3 and # 4) could affect the heat distribution in the reservoir (including the water sand) and ultimate oil recovery.

Figure 5.27 shows the plot of cumulative oil produced versus cumulative volume of steam injected. Comparison of recovery efficiency between different scenarios must have common steam injection (hence heat) volume – taken at 325,000 m^3. After injecting 325,000 m^3 CWE of steam, approximately 88,500 m^3 of oil was produced (or 13% reduction in recovery from the base case) for the case UBWL, while for the case UOWL 69,900 m^3 of oil was produced (or 30% reduction in recovery from the base case). When an economic SOR of 5.0 m^3/m^3 was considered, the recovery for the case UOWL was 28% (or 20,000 m^3 of oil) of the OOIP (original oil in place). For the case UBWL – 6-m thick, an economic limit was never reached.

From Figure 5.27, the recovery for the base case was identical to the case UOWL – 6-m thick after approximately 50,000 m^3 (or approximately 1 year) of steam had been injected. As the steam chamber came into contact with the overlying water sand, heat was diverted away from the oil zone into the water sand, leading to the formation of condensate. The steam injected into the reservoir could not provide enough latent heat to maintain the steam chamber; consequently, recovery was severely reduced.

Significant reduction in recovery in the UOWL case was evident from the energy balance study. Figure 5.28 shows the ratio of heat accumulated to the heat injected into the reservoir at various times. At the completion of the run, the ratios of heat accumulated to heat injected in the reservoir for the UBWL and UOWL were 35% and 28%, respectively. Comparison of these results shows that unconfined overlying water sand significantly diverted heat away from the oil zone, causing steam to condense. As a result, large condensate volumes formed in the reservoir, which were subsequently produced. The ratio of heat produced to the heat injected for the UBWL and UOWL were 57% and 61%, respectively. Thus, the SAGD process was significantly inefficient when unconfined overlying water sand – 6-m thick – was present, as $Q_{acc} < Q_{prod} + Q_{loss}$.

101

Unconfined Bottom and Overlying Water Sand - 6m Thick
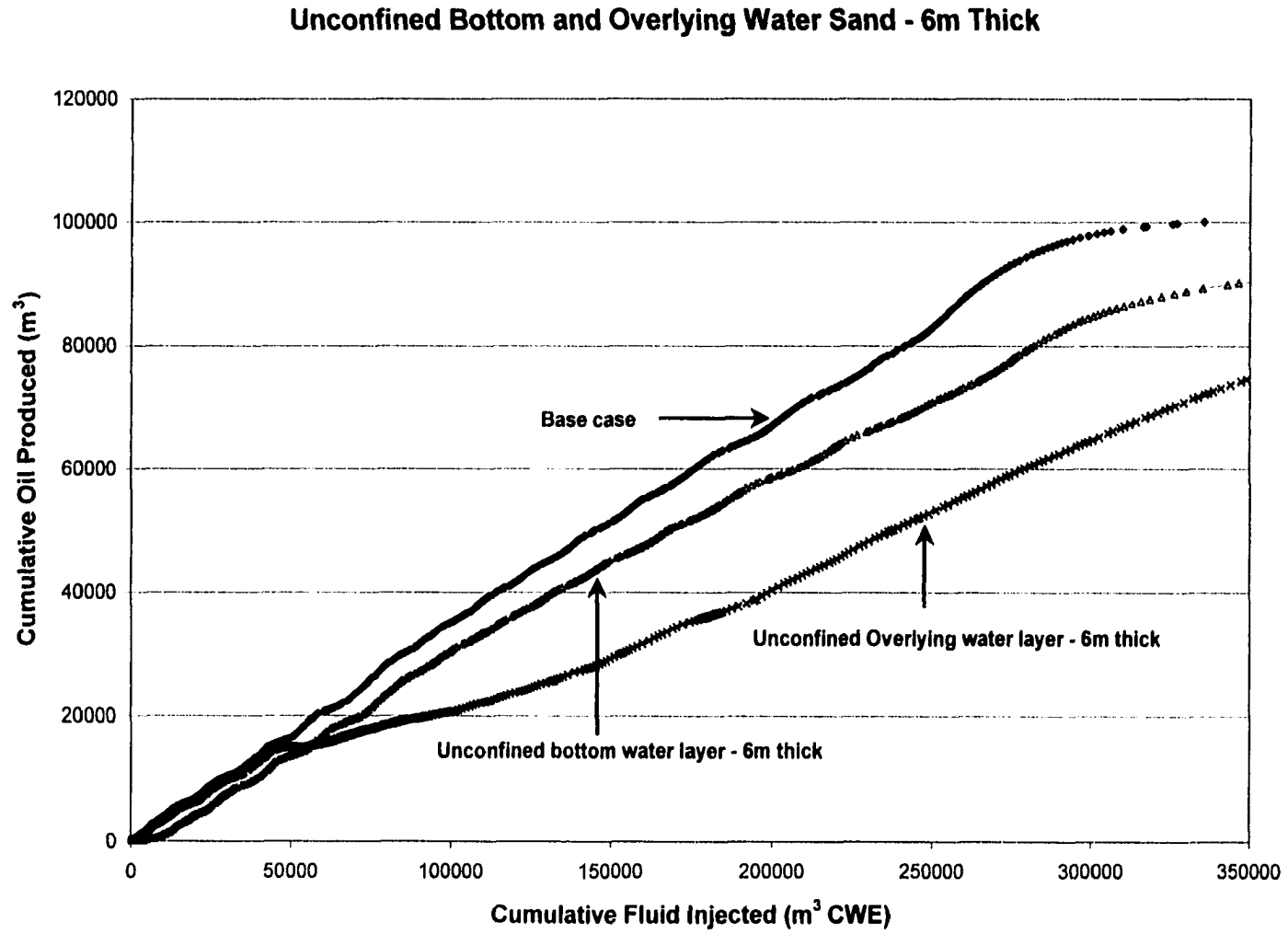
Figure 5.27: Cumulative Oil Recovery vs. Time, Unconfined Bottom Water Sand and Unconfined Overlying Water Sand – 6-m Thickness, STARS™ Simulator.

Comparison Between Unconfined Bottom and Overlaying Water Layer - 6m Thick
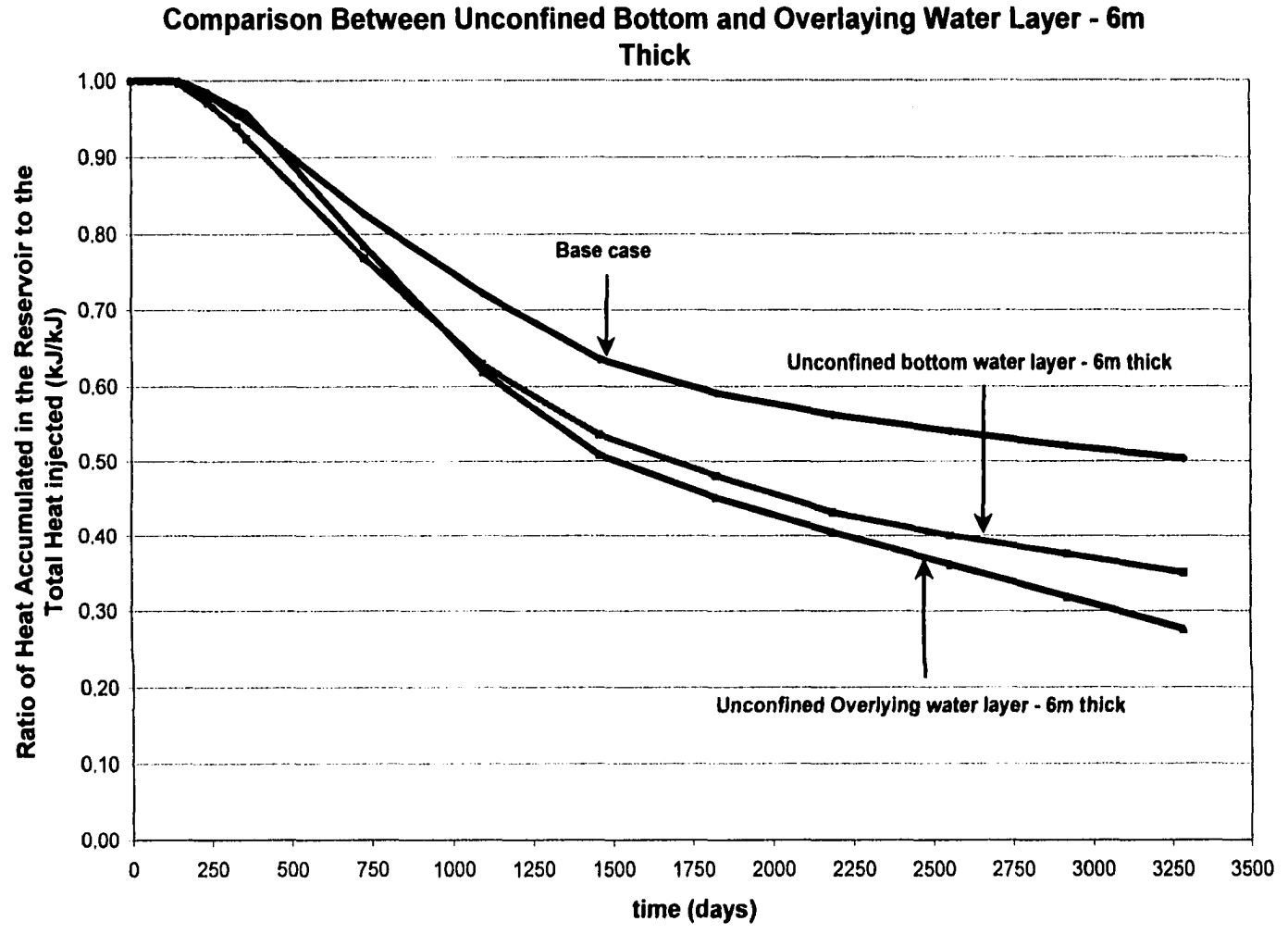
Figure 5.28: Ratio of Heat Accumulated to Heat Injected vs. Time, Unconfined Bottom Water Sand and Unconfined Overlying Water Sand – 6-m Thickness, STARS™ Simulator.

c) Unconfined and Confined Water Sand – 6-m Thick

The effect of confined and unconfined water sand (both bottom and overlying) on recovery was also extensively studied. Figure 5.29 compares the relationship between cumulative oil produced and fluid (steam) injected for the confined and unconfined water sand. The recovery was significantly reduced when overlying water sand was present, as compared to bottom water sand. Recovery was further reduced when unconfined water sand (both bottom water and overlying water) was present; however, the reduction in recovery was more significant for an overlying water sand as compared to a bottom water sand. The presence of an unconfined bottom water sand simply delayed (by approximately 150 days) the oil response from the case where the bottom water sand was confined.

d) Confined & Unconfined Overlying Water Sand – 9-m Thick

The effect of increasing the thickness (9 m) of the confined and unconfined overlying water sand on the recovery process was further investigated. Again, the plot of ratio of heat accumulated to the heat injected was generated. Figure 5.30 shows that when an unconfined overlying water sand (UOWL) of 9-m thickness was present, the heat accumulated in the reservoir was only 24% of the heat injected. Figure 5.31 shows that after 325,000 m^3 CWE of steam had been injected, about 43,500 m^3 of oil was produced (or 57% reduction in recovery from the base case). A comparison with the case where there was a confined overlying water sand (COWL) – of 9-m thickness shows that approximately 38% of the heat injected accumulated in the reservoir, and 84,000 m^3 of oil was produced (or 16% reduction in recovery from the base case).

When an economic SOR of 5.0 m^3/m^3 CWE was considered, the recovery for both cases UOWL – 9-m thick and COWL – 9-m thick were 28% of the OOIP (or 20,000 m^3 of oil). It was found that the thickness of the unconfined bottom water sand had only small influence on the recovery process, i.e. the economic SOR of 5.0 m^3/m^3 CWE was never reached.

5.7. Summary

In this chapter, results from Butler's models (original 1981000 model, and LinDrain model as discussed in 1994 Monograph), CMG's STARS™ simulator, and the new analytical model were presented. These results were analyzed carefully, first in checking for agreement (or disagreement) between them. Due to different assumptions behind Butler's models and the new analytical model, their results were not compared directly. However, the production rate predicted by the new analytical model agreed generally with that predicted by Butler's pseudo steady-state model. Additionally, the steam zone interface velocity calculated at different times were also within range of results from Butler's unsteady-state LinDrain model. This agreement is remarkable, in many respects, given the different treatments for the heat transfer inside the reservoir between the new analytical model (which incorporated transient convective transfers)

104

Unconfined and Confined Water Sand - 6m Thick
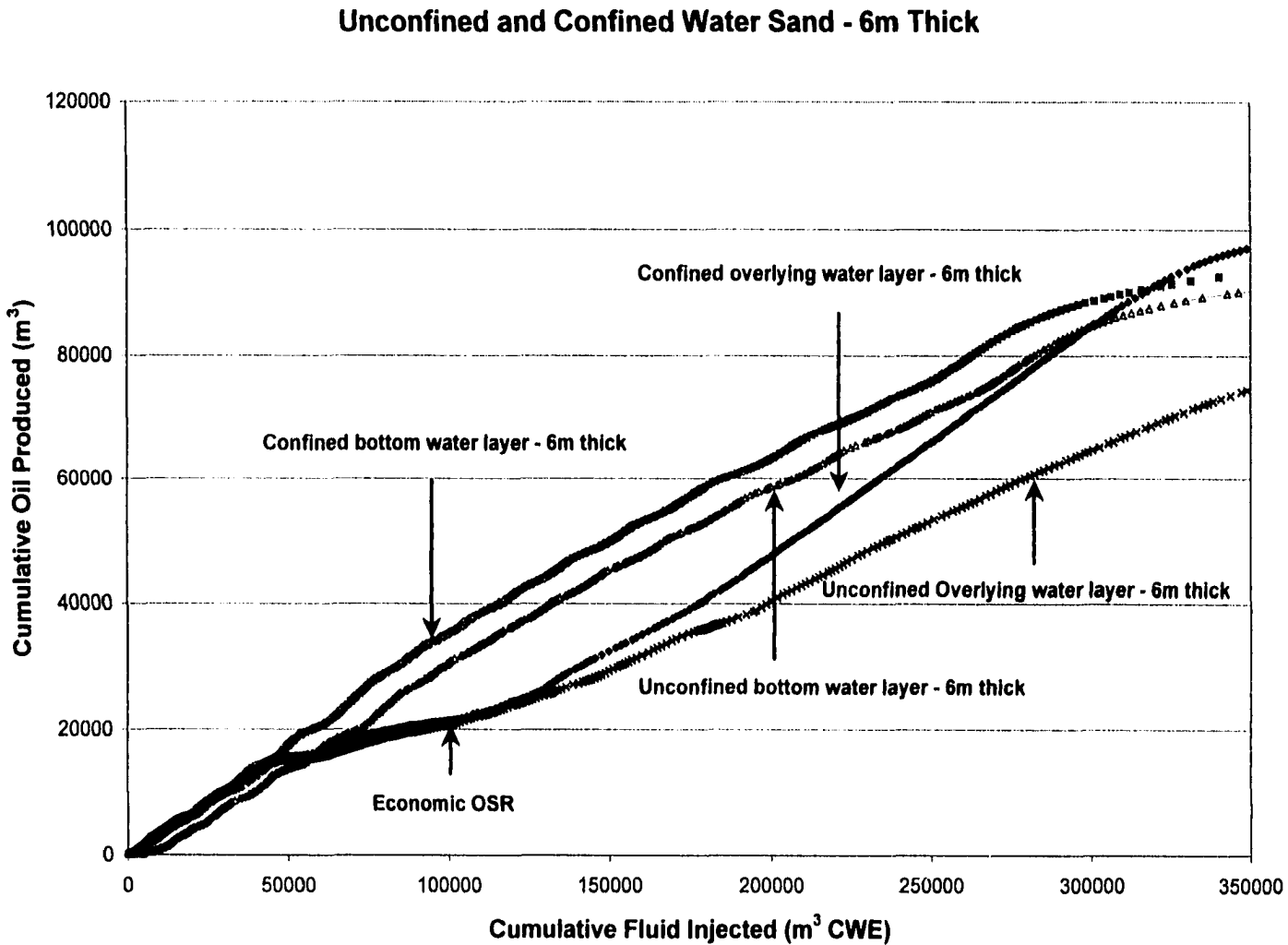
Figure 5.29: Cumulative Oil Recovery vs. Time, Confined vs. Unconfined Bottom Water Sand and Overlying Water Sand – 6-m Thickness, STARS™ Simulator.

Unconfined and Confined Overlaying Water Layer - 9m Thick
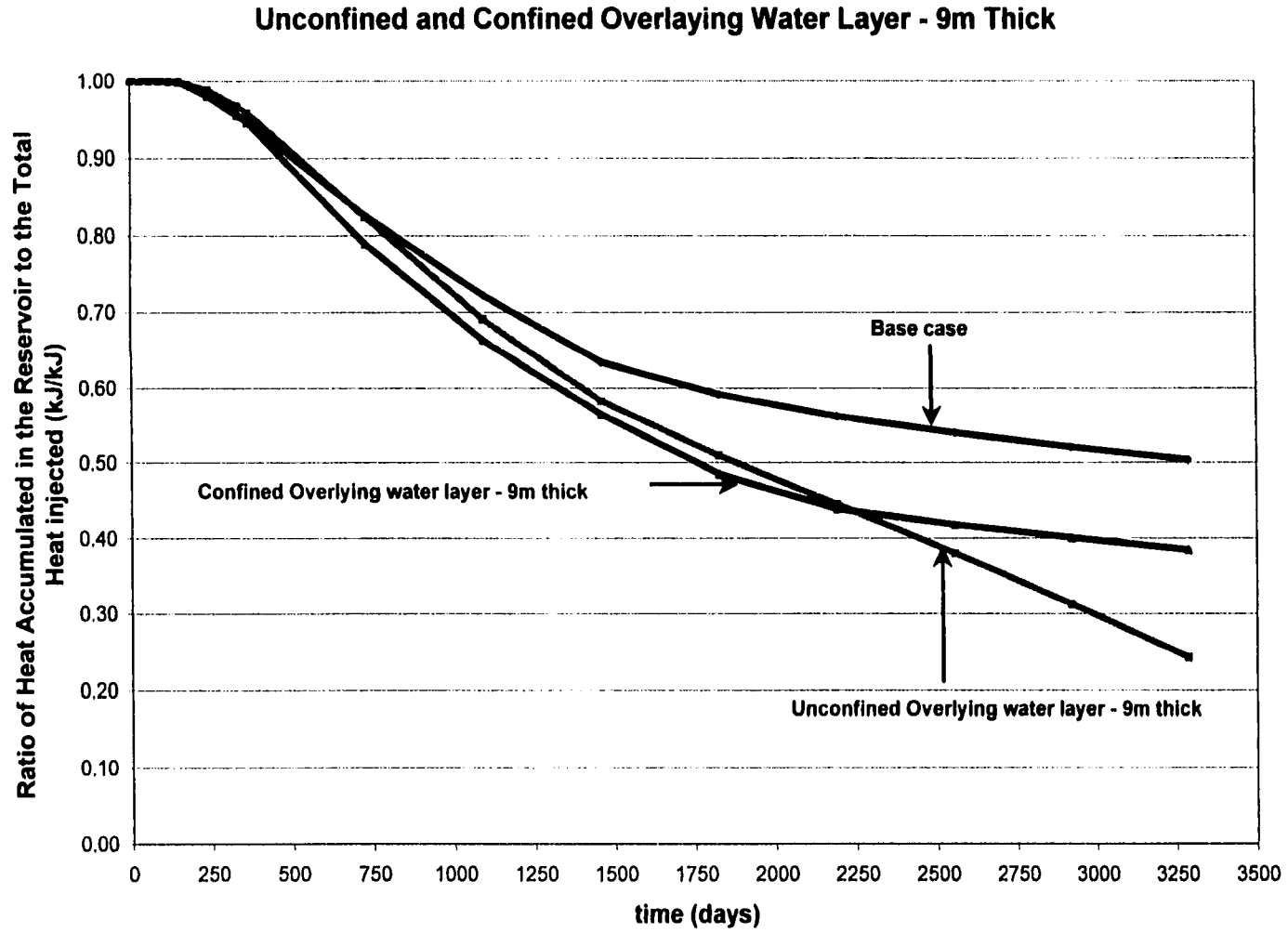
Figure 5.30: Ratio of Heat Accumulated to Heat Injected vs. Time, Confined vs. Unconfined Overlying Water Sand − 9-m Thickness, STARS™ Simulator.

Confined and Unconfined Overlying Water Sand - 9m Thick
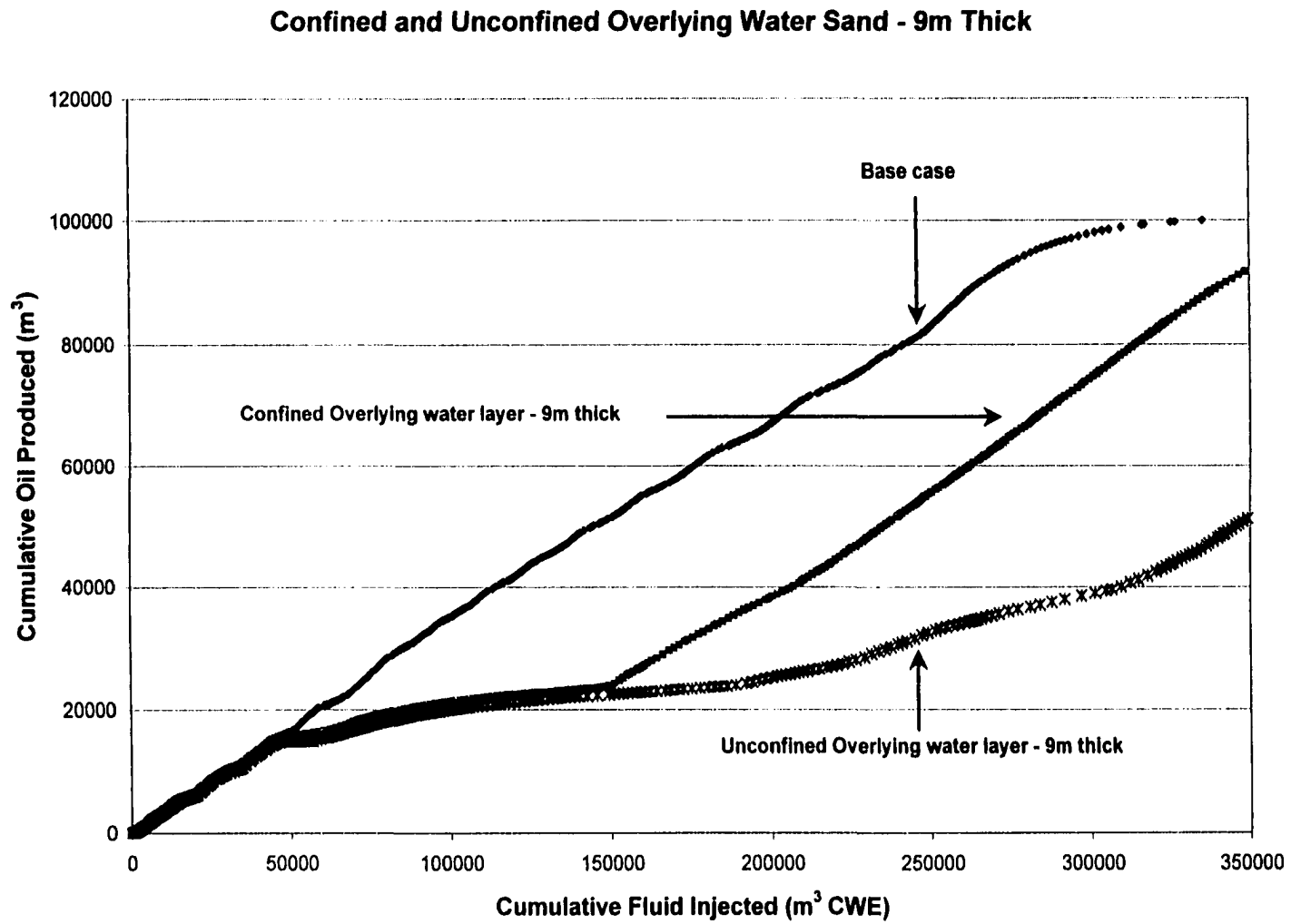
Figure 5.31: Cumulative Oil Recovery vs. Time, Confined vs. Unconfined Overlying Water Sand – 9-m Thickness, STARS™ Simulator.

and Butler's models (which assumed steady state heat conduction for temperature distribution in the reservoir ahead of the steam zone).

More importantly, values for the steam zone interface position and temperature distribution determined from the new analytical model agreed quite closely with results from the STARS™ simulator. Oil production rate and cumulative oil recovery for both the new analytical model and STARS™ simulator also agreed mostly with one another. The divergence in oil production rates from these models in the early and late time periods were logically explained.

108

Chapter 6 — Conclusions

The study presented in this thesis has been carried out to investigate several important aspects, especially the effects of convective transfers, on the transient performance of the steam-assisted gravity drainage (SAGD) process. On the basis of the work performed, the following conclusions are offered:

1. A new analytical model was developed to simulate the transient behaviour associated with an expanding steam zone in the SAGD process. This new analytical model was based mainly on the *Stefan Phase-Change problem*. Physically, the model simulated the dynamics associated with the expanding steam zone in the SAGD process by considering the mass and heat transfer across the moving steam zone interface. Additionally, convective heat transfers due to heat losses to the cap and base rock, and heat removed from the reservoir in the produced fluid stream were incorporated. A rigorous mathematical solution was obtained for this new analytical SAGD transient model, which enabled the steam zone interface position and velocity to be determined at different times.

2. Results from the new analytical SAGD transient model agreed mostly with results obtained from CMG's STARS™ thermal simulator. The agreement in the oil production rate between the new analytical model and STARS™ simulator was especially good for the middle-time period. Difference in the predicted oil production rates in the early time period was due to the use of steam trap control by the STARS™ simulator. Different external boundary conditions led to the difference in the predicted oil production rates for the new analytical model and the simulator in later time period. The steam zone interface position predicted by the new analytical model agreed with that determined by STARS™ simulator.

3. Selective results from the new analytical SAGD transient model agreed with results calculated from Butler's models. The steam zone interface velocity predicted by the new analytical model at different times agreed quite closely with those calculated by Butler's LinDrain model, with the agreement being closer in later-time periods. Oil production rate predicted by the new analytical model was less than those predicted by the TANDRAIN model, and Butler's 1985 model. The reason was believed to be due to the heat loss to cap rock and base rock, and due to heat removed due to fluid production from the reservoir; these losses are accounted for in the new analytical model.

4. The new analytical SAGD transient model was used to investigate the effects of flow potential and thermal diffusivity on the SAGD process. The results in these cases showed that the steam zone advanced further into the reservoir for low values of fluid production potential and high values of thermal diffusivity. In the first case, low fluid production potential resulted in

109

less heat being removed from the reservoir, and hence, more heat accumulated inside the reservoir and contributed to the forward movement of the steam zone. In the second case, high thermal diffusivity value promoted the expansion of the steam zone into the reservoir.

5. The effects of a water sand in communication with the oil reservoir on SAGD performance were also investigated. CMG's STARS™ was used in this investigation. The presence of a bottom water layer was determined to have a lesser impact on recovery than the overlying water layer case. In addition, oil recovery decreased with increasing water layer thickness. Increasing the areal coverage of the bottom water layer resulted in only a slightly reduced recovery as compared with the confined bottom water layer. However, increasing the areal coverage of the overlying water layer severely reduced the recovery efficiency of the process, as heat was diverted into the overlying water zone.

The principal contributions of this study include:

1. The formulation of a rigorous physical transient model to describe the expansion of a steam zone in the SAGD process, in particular the mass and heat convective fluxes from the steam zone into the reservoir, as well as convective transfers due to heat losses to the cap and base rock, and heat removed from the reservoir due to fluid production. This formulation did not rely on any assumption of steady state behaviour (such as temperature distribution) commonly used by other SAGD analytical models. Rather, it sought to determine the time-dependent position and velocity of the steam zone interface, as a function of parameters such as convective fluxes, convective heat transfers, and reservoir properties.

2. The new analytical model, as evidenced by the agreements between its results and other results from the STARS™ simulator and Butler's models, could be used as a predictive tool in evaluating recovery performance for a SAGD process under field conditions. Additionally, it could be used to estimate the contribution due to various mechanisms — including both conductive and convective transfers — to overall oil recovery performance, due to its formulation. This knowledge was of importance and would be of great utility, particularly in combination with heat balance calculations, in providing insights into the efficiency of the steam injection recovery process.

The contributions are pointed out in recognition of the limitations of the new analytical model, including its approach of modelling the 3-D flow in the reservoir as a pseudo 2-D problem.

110

Chapter 7 — Recommendations

On the basis of the work performed, the results obtained, and the discussion provided, in this study the following recommendations are offered.

1. The new analytical model should be modified to simulate heat losses to cap and base rock in an explicit manner. As discussed previously, the heat losses to cap and base rock depend on the contact area between the steam zone and the cap and base rock, as well as the thermal conductivity and temperature gradient across this contact area. The contact area could be estimated from the new analytical model presented in this thesis.

2. The new analytical model should also be modified to incorporate the effects of pressure (or potentials) on fluid stream lines at and around the steam zone interface. Such modifications should, if they were successful, help in describing more closely the effects of mobile fluid accumulation around the horizontal producer. In turn, the modified model would hopefully generate oil production rates in closer agreement with those predicted by thermal simulators (such as STARS™) in the early time period.

3. The new analytical model should be modified to simulate the dynamics of the steam zone itself. Such modification would help coupling the mass and heat fluxes between Region 1 (steam zone) and Region 2 (reservoir ahead of the steam zone) in a more rigorous and detailed way.

Appendix A

Derivation of Mass and Energy Balance at Steam Zone Interface

A.1. Energy Balance for General Transport Equation

The derivation of the energy balance equation, using Prats' (1982) terminology, is illustrated below.
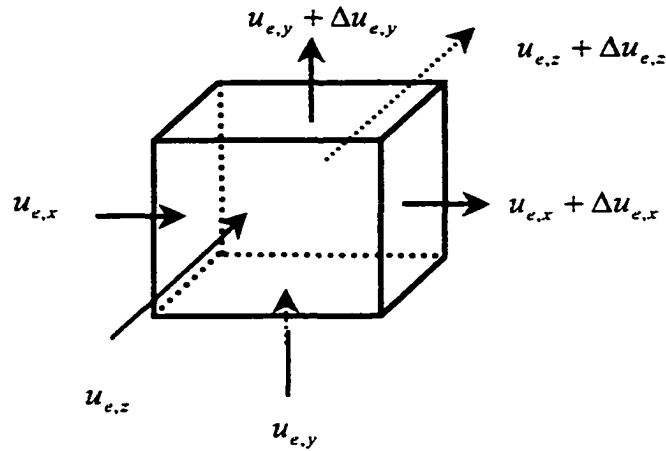
Figure A1: Volume element for derivation of energy balance

The differential equation describing the conservation of energy (or energy balance) for a volume element, illustrated in Figure A1, is

$$\frac{\partial u_{e,x}}{\partial x} + \frac{\partial u_{e,y}}{\partial y} + \frac{\partial u_{e,z}}{\partial z} = -\frac{\partial \rho e}{\partial t} + \dot{Q}$$

(A1)

where $u_{e,x}$ is the total energy flux in the x-direction; it is comprised of the conductive transport and convective transport (velocity is u_x), as shown in Equation (A2)

$$u_{e,x} = -k_{he} \frac{\partial T}{\partial x} + u_x \rho_f h_f$$

(A2)

As the heat capacity of a phase is not a strong function of temperature (except near the critical temperature), it is often convenient to express the enthalpy as,

112

$$h_f = C(T - T_r)$$

<div align="right">(A3)</div>

and internal energy as,

$$e = C_V(T - T_R)$$

<div align="right">(A4)</div>

By considering 1-D flow and no heat loss, the substitution of equations (A2)-(A4) into equations (A1) gives

$$k_{he} \frac{\partial^2 T}{\partial x^2} - u_f \rho_f C_f \frac{\partial T}{\partial x} - \rho C^* \frac{\partial T}{\partial t} = 0$$

<div align="right">(A5)</div>

Inclusion of the heat loss term would render the problem, described by Equation (A5) intractable, i.e., there would be no analytical. The de-coupled heat loss to the cap and base rock is coupled to the heat balance equation at the interface.

A.2. Material Balance at the Interface

The net convective transport present in the proposed model is derived below. The derivation is based on the material balance equation at the interface.

Steam Zone | **Oil Zone**

$\rho_{1,mf} u_1$ $\rho_{2,mf} u_2$

$\rho_{1,total}$ $\rho_{2,total}$

$\rho^*_{mf} u^*$
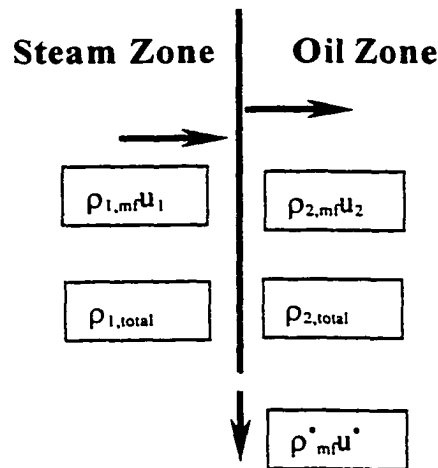
Figure A2: Material balance at the steam interface between Regions 1 and 2.

The material balance at the moving steam zone interface, as illustrated from Figure A2, as it moves a distance dX over a time interval dt is given by the following equation,

$$\left(\rho_{2,total} - \rho_{1,total}\right)\frac{dX}{dt} = \left(\rho_{2,mf}u_2 - \rho_{1,mf}u_1 + \rho_{mf}^{\bullet}u^{\bullet}\right)$$

(A6)

where the production flux is coupled to the moving steam zone interface, as shown in Equation (A7). Explanation for the production potential γ^* is given in Section A.4.

$$u^{\bullet} = \gamma^{\bullet} \cdot \frac{dX}{dt}$$

(A7)

The convective velocity from the expanding steam zone is coupled to the moving steam zone interface, as expressed in Equation (A8),

$$u_1 = \gamma_1 \frac{dX}{dt}$$

(A8)

The net convective transport into the oil zone (Region 2), which is represented by the bulk fluid movement, is thus given by Equation (A9)

$$u_2 = \frac{1}{\rho_{2,mf}}\left[\left(\rho_{2,total} - \rho_{1,total}\right) + \gamma_1\rho_{1,mf} - \gamma^{\bullet}\rho_{mf}^{\bullet}\right]\frac{dX}{dt}$$

(A9)

Introducing the following parameter relating the mobile fluid density between Regions 1 and 2,

$$\beta = \frac{\rho_1}{\rho_2}\bigg|_{mf}$$

(A10)

Substituting Equation (A10) into Equation (A8) and rearranging,

$$u_2\rho_{2,mf}C_{2,mf} = \Gamma\frac{dX}{dt}$$

(A11)

where

$$\Gamma = \left[1 + \beta(\gamma_1 - 1) - \frac{\rho_{mf}^{\bullet}\gamma^{\bullet}}{\rho_{2,mf}}\right]\frac{\left(\rho_{2,mf}C_{2,mf}\right)}{\left(\rho_{2,total}C_{2,total}\right)}$$

(A12)

The convective-conductive transport equation (i.e., Equation (A6)) becomes,

$$\alpha_2\frac{\partial^2 T_2}{\partial x^2} - \Gamma\left(\frac{dX}{dt}\right)\frac{\partial T_2}{\partial x} = \frac{\partial T_2}{\partial t}$$

(A13)

114

Equation (A13) is identical to Equation (4.26), which governs the temperature distribution inside Region 2 ahead of the moving steam zone interface. The velocity of the moving steam interface is (dX/dt).

A.3. Heat Balance across the Moving Steam Zone Interface

The presence of a mass flux into Region 2 is associated with an energy flux, which consists both conductive and convective heat transport. The energy balance at the interface corresponding with the mass balance at the interface is illustrated below.
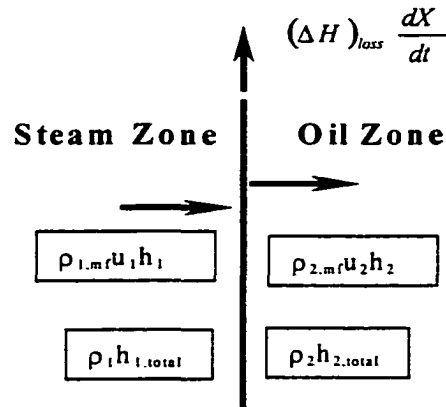
Figure A3: Energy balance at the steam interface between Regions 1 and 2.

The energy balance at the interface, as illustrated by Figure A3, is given by

$$\left(\rho_2 h_2 - \rho_1 h_1\right)\frac{dX}{dt} = \rho_{1,mf} u_1 h_1 - \left(\rho_{2,mf} u_2 h_2 - K_2 \frac{\partial T_2}{\partial x}\right) + \left(\Delta H\right)_{loss} \frac{dX}{dt}$$

(A14)

The two terms on the left hand side of Equation (A14) represents the the change in the enthalpy associated with the change in the position of the steam zone interface over a time step dt. The first term on the right hand side represents the convective transport from region 1. The second and the third terms on the right hand side represent the conductive and convective heat transport into Region 2. The last term on right hand side represents the total heat loss term $(\Delta H)_{loss}$ and is composed of the heat losses to cap and base rock. Due to the previously stated assumption regarding conditions for Region 1 (i.e., non-changing conditions inside the expanding steam

115

zone, with only changing parameter is its volume due to moving steam zone interface), the heat losses to cap and base rock are considered as sink term, and not explicitly defined.

Rearranging the above equation in the form,

$$-k_2 \frac{\partial T_2}{\partial x} = (\rho_1 h_1 - \rho_2 h_2)\frac{dX}{dt} + (\Delta H)_{loss}\frac{dX}{dt} - (\rho_{2,mf} u_2 h_2 - \rho_{1,mf} u_1 h_1)$$

(A15)

Equation (A15) is identical to Equation (4.22). The energy balance at the interface represents the boundary condition present on the moving boundary.

A.4. Production Potential

Calculation of oil production rate in the new analytical model is similar to approaches used by Butler et al. (1981), Butler (1985, 1994). The starting point in the development of an equation to predict the oil flow rate is Darcy's law for gravity drainage, given by Equation (A16)

$$dq = L\frac{kg}{v}dX$$

(A16)

Butler (1994) considered the material balance for an element of the moving steam zone interface. This led to the resulting equation,

$$\left(\frac{\partial x}{\partial t}\right)_y = -\frac{1}{L\phi\Delta S_o}\left(\frac{\partial q}{\partial y}\right)_t$$

(A17)

The above equation relates the interface velocity to the rate of drainage, which is varying along the vertical distance y. Noting the form of Equation (A17), differentiation of Equation (A16) with respect to y results in Equation (A18).

$$\frac{1}{L}\frac{\partial q}{\partial y} = \frac{kg}{v}\frac{\partial X}{\partial y}$$

(A18)

Recalling the assumption of fluid production taking place along the steam zone interface, i.e.,

$$u^\bullet = \gamma^\bullet \frac{\partial X}{\partial t}$$

(A19)

116

Consideration of Equations (A17), (A18) and (A19) gives the following expression,

$$\frac{kg}{v}\frac{\partial X}{\partial y} = \gamma \cdot \frac{\partial X}{\partial t}$$ (A20)

As such, the term (kg/v) represents the production potential associated with the SAGD process, and is defined by Equation (A21),

$$\frac{kg}{v} = \gamma$$ (A21)

Butler (1994) had suggested a function relating the steam zone interface position with reservoir height. For a given reservoir height and the corresponding position of the steam zone at this height, the right-hand-side of Equation (A18) is equal to a constant multiplied by the production potential.

The oil production rate is then given by,

$$q = \int_0^h \frac{dq}{dy}dy = L\int_0^h u^{\cdot} dy$$ (A22)

It can be seen from the discussion above that oil production rate is dependent on the production potential and the position of the moving steam zone interface. As the steam zone interface position changes with time, the oil production rate also changes correspondingly.

APPENDIX B

HEAT BALANCE CALCULATION

The following discussion examines the cumulative heat balance calculation. Applying heat conservation principle, the overall heat balance at any time t is given by

$$Q_{accum} = Q_{inj} - Q_{loss} - Q_{prod} \qquad (B1)$$

where,

Q_{accum} is heat accumulated in the reservoir

Q_{inj} is heat injected into the reservoir

Q_{loss} is heat lost to the cap and base rock

Q_{prod} is heat produced from the reservoir

The heat injected into the reservoir is given by:

$$Q_{inj} = \int_0^t i_{st} \left(h_{inj} - h_r + f_{st} L_v \right) dt \qquad (B2)$$

The heat removed from the reservoir due to cumulative fluid production is given by:

$$Q_{prod} = \sum_{i=1}^n \left(V_{w,i} C_{w,i} \rho_{w,i} + V_{o,i} C_{o,i} \rho o_{w,i} + V_{st,i} C_{st,i} \rho_{st,i} \right) \Delta T \qquad (B3)$$

The cumulative heat produced from the reservoir is determined incrementally from the production data including the volumes of fluid (oil, water, and steam) and their temperatures (compared to initial temperature) at different times i, where i = 1, 2, ..., n

The heat lost from the reservoir to cap and base rock is given by Fourier equation for conductive heat transfer, i.e.

$$Q^{\bullet} = -kA \left(\frac{dT}{dz} \right) \qquad (B4)$$

The cumulative heat loss to cap and base rock is therefore,

$$Q_{loss} = \int_0^t Q^{\bullet} dt \qquad (B5)$$

118

References

Adegbesan, K.O., R.P. Leaute, and D.E. Courtnage: "Performance of a Thermal Horizontal Well Pilot", SPE 22892, 1991 Annual Technical Conference and Exhibition of SPE, Dallas, Texas, Oct. 6-9, 1991.

Boberg, T.C. and R.B. Lanz: "Calculation of the Production Rate of a Thermally Stimulated Well", *Jour. of Pet. Tech.*, Dec. 1966, pp. 1613-23.

Britton, M.W., W.L. Martin, R.J. Leibrecht, and R.A. Harman: "The Street Ranch Pilot Test for Fracture-Assisted Steamflood Technology", *Jour. of Pet. Tech.*, March 1983, pp. 511-22.

Butler, R.M., G.S., McNab, and H.Y. Lo: "Theoretical Studies on the Gravity Drainage of Heavy Oil During In-Situ Steam Heating", *Canadian Journal of Chemical Engineering*, 1981, pp. 455-60.

Butler, R.M. and D.J. Stephens: "The Gravity Drainage of Steam-Heated Heavy Oil to Parallel Horizontal Wells", *Jour. of Can. Pet. Tech.*, 1981, 20, No.2, pp. 90-96.

Butler, R.M., D.J. Stephens, and M. Weiss: "The Vertical Growth of Steam Chambers in the In-situ Thermal Recovery of Heavy Oils", Proc. of the 3oth Canadian Chemical Engineering Conference, Edmonton, Alberta, October 19-22, 1980, Volume 4, pp. 1152-1167.

Butler, R.M.: "A New Approach to the Modelling of Steam-Assisted Gravity Drainage", *Jour. of Can. Pet. Tech.*, 1985, 24, No.3, 42-51.

Butler, R. M.: 'New Interpretation of the Meaning of the Exponent "m" in the Gravity Drainage Theory for Continuously Steamed Wells", *AOSTRA Journal of Research,* 1985, No 1 67-71.

Butler, R.M. and G. Petela: "Theoretical Estimation of Breakthrough Time and Instantaneous Shape of Steam Front During Vertical Steamflooding", *AOSTRA Journal of Research*, Volume 5, Number 4, Fall 1989, pp. 359-381.

Butler, R.M. and I.J. Mokrys: "Solvent Analog Model of Steam Assisted Gravity Drainage", AOSTRA Jour. of Research, Vol. 5, No. 1, 1989, pp. 17.

Butler, R.M.: Thermal Recovery of Oil and Bitumen, Prentice Hall Publishing Company, New Jersey, 1991.

Butler, R.M.: Horizontal Wells for the Recovery of Oil, Gas, and Bitumen, Petroleum Society of CIM, Monograph No.2, 1994.

Butler, R.M. and Q. Jiang: "Effect of Gravity on Movement of Water-Oil Interface for Bottom Water Driving Upwards to a Horizontal Well, JCPT, Sept. 1996, pp. 47-56.

Carslaw, H.S. and J.C. Jaeger: Conduction of Heat in Solids, 2nd ed., Oxford University Press, London, 1959.

Chan, M.Y.S., J. Fong, and T. Leshchyshyn: "Effects of Well Placement and Critical Operating Conditions on the Performance of Dual Well SAGD Well Pair in Heavy Oil Reservoir", SPE 39082, Fifth Latin American and Caribbean Petroleum Engineering Conference and Exhibition, Rio de Janeiro, Brazil, Aug. 20-Sept. 3, 1997.

Chang, H.L, S.M. Farouq Ali, and A.E. George: "Performance of Horizontal Vertical Well Combination for Stearflooding Bottom Water Formations", *Jour. of Canadian Pet. Tech.*, May 1992, pp. 41-51.

Chen, H.L. and N.D. Sylvester: "Appraisal of Analytical Stearnflood Models", SPE 20023, 60th California Regional Meeting of the SPE, Ventura, CA, April 4-6, 1990.

Chow, L. and R.M. Butler: "Numerical Simulation of the Steam-Assisted Gravity Drainage Process (SAGD)", *Jour. of Can. Pet. Tech.*, 1988, 35, No.6, pp. 55-62.

Chu, C.: "State-of-the-Art Review of Steamflood Field Projects", *Jour. of Pet. Tech.*, October 1984, pp. 1887-902.

Chung, K.H. and R.M. Butler: "Geometrical Effect of Steam Injection on the Formation of Emulsions in the Steam-Assisted Gravity Drainage Process", *Jour. of Can. Pet. Tech.*, 1988, 27, No.1, pp. 36-42.

Chung, K.H.: Heavy Oil Recovery by the Steam-assisted Gravity Drainage Process, Ph.D. thesis, University of Calgary, 1988.

Chung, K.H. and R.M. Butler: "A Theoretical and Experimental Study of Steam-Assisted Gravity Drainage Process", paper 89, Proc. of the Fourth UNITAR/UNDP Conference on Heavy Crude and Tar Sands, Edmonton, August 7-12, 1988.

Closmann, P.J. and R.A. Smith: "Temperature Observations and Steam-Zone Rise in the Vicinity of a Steam-Heated Fracture", *Jour. of Pet. Tech.*, Aug.1983, pp. 575-86.

Closmann, P.J., 1995: "A Simplified Gravity Drainage Oil Production Model for Mature Steam Drives", *SPE Reservoir Engineering*, May 1995, pp. 143-148.

Closmann, P.J., N.W. Ratliff, and N.E. Truitt: "A Steam-Soak Model for Depletion-Type Reservoirs", *Jour. of Pet. Tech.*, June 1970, pp. 757-70.

Combe, J., J. Burger, G. Renard, and E. Valentin: "New Technologies in Thermal Recovery: Contribution of Horizontal Wells", paper 117, Proc. of the Fourth UNITAR/UNDP Conference on Heavy Crude and Tar Sands, Edmonton, August 7-12, 1988.

Computer Modelling Group Ltd.: STARS™ User Manual, Computer Modelling Group Ltd., 1999.

Das, S.K. and R.M. Butler: "Countercurrent Extraction of Heavy Oil and Bitumen", SPE 37094, 1996 SPE International Conference on Horizontal Well Technology, Calgary, November 18-20, 1996.

Das, S.K.: "VAPEX: An Efficient Process for the Recovery of Heavy Oil and Bitumen", SPE Journal, September 1998, pp. 232-37.

de Haan, H.J. and L. van Lookeren: "Early Results of the First Large-scale Steam-Soak Project in the Tia Juana Field, Western Venezuela", *Jour. of Pet. Tech.*, Jan. 1969, pp. 101-110.

Denbina, E.S., T.C. Boberg, and M.B. Rotter: "Evaluation of Key Reservoir Drive Mechanisms in the Early Cycles of Steam Stimulation at Cold Lake", *SPE Reservoir Engineering*, May 1991, pp. 207-11.

Doan, Q., S.M. Farouq Ali, and A.E. George: "Scaling Criteria and Model Experiments for Horizontal Wells", *Jour. of Can. Pet. Tech.*, Vol. 31, No. 9, November 1992, pp. 57-65.

Doan, L.: Performance Prediction for Steamflooding Marginal Heavy Oil Reservoirs Using Horizontal Wells, M.Sc. thesis, University of Alberta, 1996.

Doan, L.T., H. Baird, Q.T. Doan, S.M. Farouq Ali: "Performance of The SAGD Process in The Presence of A Water Sand – A Preliminary Investigation", CIM 99-40, 1999 CSPG and Petroleum Society Joint Convention, Calgary, Canada, June 14-18/1999. {*in press* with the *Jour. of Can. Pet. Tech.*}

Donnelly, J.K. and M.J. Chmilar: "The Commercial Potential of Steam Assisted Gravity Drainage", SPE 30278, International Heavy Oil Symposium, Calgary, Canada, June 19-21, 1995.

Donnelly, J.K.: "Hilda Lake a Gravity Drainage Succes", SPE 54093, SPE International Thermal Operations and Heavy Oil Symposium, Bakersfield, CA, Mar. 17-19, 1999.

Doscher, T.M.: "Factors Influencing Success in Steam Soak Operations", Petroleum Industry Conference on Thermal Oil Recovery, June 6, 1966, pp. 76-80.

Dusseault, M.B., M.B. Geilikman, and T.J.T. Spanos: "Heavy Oil Production from Unconsolidated Sandstones Using Sand Production and SAGD", SPE 48890, 1998 SPE International Conference and Exhibition in China, Beijing, Nov. 2-6, 1998.

Edmunds, N.R.: "A Model of the Steam Drag Effect in Oil Sands", Jour. of Can. Pet. Tech., 1984, 23, No.5, pp. 34-9.

Edmunds, N.R., J.A. Haston, and D.A. Best: "Analysis and Implementation of the Steam Assisted Gravity Drainage Process at the AOSTRA UTF", paper no. 125, Proc. of the Fourth UNITAR/UNDP Conference on Heavy Crude and Tar Sands, Edmonton, August 7-12, 1988.

Edmunds, N.R. and S.D. Gittins: "Effective Application of Steam Assisted Gravity Drainage of Bitumen to Long Horizontal Well Pairs", Jour. of Can. Pet. Tech., June 1993, pp. 49-55.

Edmunds, N.R., J.A. Kovalsky, S.D. Gittins, and E.D. Pennacehioli: "Review of Phase A Steam Assisted Gravity Drainage Test", SPE Reservoir Engineering, May 1994, pp. 119-24.

Elliot, K.T. and A.R. Kovscek: "Simulation of Early-Time Response of Single-Well Steam Assisted Gravity Drainage (SW-SAGD)", SPE 54618, 1999 SPE Western Regional Meeting, Anchorage, Alaska, May 26-28, 1999.

Farouq Ali, S.M. and D.A. Redford: "Physical Modelling of In-Situ Recovery Methods of Oil Sands", Proc. of the Canada-Venezuela Oil Sands Symposium, Edmonton, Canada, CIM Special Volume No.17, pp. 319-326, 1977.

Farouq Ali, S.M.: "Steam Injection Theories - A Unified Approach", SPE 10746, 1982 SPE California Regional Meeting, San Francisco, March 24-26, 1982.

Farouq Ali, S.M.: "CSS - Canada's Superstrategy for Oil Sands", Jour. of Can. Pet. Tech., 1994, 33, No.9, pp. 16-19.

Farouq Ali, S.M.: "Current Status of Steam Injection as a Heavy Oil Recovery Method", Jour. of Can. Pet. Tech., Jan.-Mar. 1974, pp. 54-68.

Farouq Ali, S.M.: "Is There Life After SAGD?", Distinguished Authors Series, Jour. of Can. Pet. Tech., June 1997.

Fletcher, C.A.J.: Computational Techniques for Fluid Dynamics, Volume I: Fundamentals and General Techniques, Springer-Verlag, 1988.

Friedmann, F. and J.A. Jensen: "Some Factors Influencing the Formation and Propagation of Foams in Porous Media", SPE 15087, 56th California Regional Meeting of the SPE, Oakland, April 2-4, 1986.

Gomaa, E.E., J.H. Duerksen, and P.T. Woo: "Designing a Steamflood Pilot in the Thick Monarch Sand of the Midway-Sunset Field", Jour. of Pet. Tech., December 1977, pp. 1559-68.

Gomaa, E.E.: "Correlations for Predicting Oil Recovery by Steamflood", Jour. of Pet. Tech., February 1980, pp. 325-32.

Griffin, P.J. and P.N. Trofimenkoff: "Laboratories Studies of the Steam Assisted Gravity Drainage Process", AOSTRA 5th Annual 'Advances in Petroleum Recovery and Upgrading Technology' Conference, June 14-15, 1984, Calgary, Alberta.

Hamm, R.A. and T.S. Ong: "Enhanced Steam-Assisted Gravity Drainage: A New Horizontal Well Recovery Process for Peace River, Canada", Jour. of Can. Pet. Tech., 1995, 34, No.4, pp. 33-40.

Hong, K.C.: "Optimum Well Location for Steamflooding Steeply Dipping Reservoirs", SPE 21771, California Regional Meeting of SPE, Long Beach, CA, March 1991.

Huang, W.S. and M.A. Hight: "Evaluation of Steamflood Processes Using Horizontal Wells", SPE 14130, SPE 1986 Intl. Meeting on Petroleum Engineering, Beijing, China, March 17-20, 1986.

Huygen, H.H.A. and J.B. Black: "Steaming Through Horizontal Wells and Fractures – Scaled-Model Tests", Proc. of 2nd European Symposium on Enhance Oil Recovery, Paris, France, Nov.

8-10, 1982, 507-517.

Ito, Y. and S. Suzuki: "Numerical Simulation of the SAGD Process in the Hangingstone Oil Sands Reservoir", 96-57, 47th Annual Technical Meeting of the Petroleum Society of CIM, Calgary, Alberta, June 10-12, 1996; also *Jour. of Canadian Pet. Tech.*, September 1999, pp. 27-35.

Ito, Y., M. Ichikawa, and T. Hirata: "The Growth of the Steam Chamber During the Early Period of the UTF Phase B and Hangingstone Phase I Projects", 2000-05, Canadian International Petroleum Conference 2000, Petroleum Society of CIM, Calgary, June 4-8/2000.

Jain, S. and A. Khosla: "Predicting Steam Recovery of Athabasca Oil Through Horizontal Wells", CIM 85-36-28, 36th Annual Technical Meeting of the Petroleum Society of CIM, Edmonton, Alberta, June 2-5, 1985.

Jespersen, P.J. and T.J. Fontaine: "The Tangleflags North Pilot – A Horizontal Well Steamflood", 4th Petroleum Conference of South Saskatchewan Section, Petroleum Society of CIM, Regina, October 7-9, 1991.

Jones, J.: "Steam Drive Model for Hand-Held Programmable Calculator", *Jour. of Pet. Tech.*, September 1981, pp. 1583-98.

Joshi, S.D. and C.B. Threlkeld: "Laboratory Studies of Thermally Aided Gravity Drainage Using Horizontal Wells", *AOSTRA Journal of Research*, 1985, 2, No.1, pp. 11-19.

Kamath, V.A., S. Sinha, and D.G. Hatzignatiou: "Simulation Study of Steam-Assisted Gravity Drainage Process in Ugnu Tar Sand Reservoir", SPE 26075, Western Regional Meeting, Anchorage, Alaska, May 26-28, 1993.

Kasraie, M., A.K. Singhal, and Y. Ito: "Screening and Design Criteria for Tangleflags Type Reservoirs", SPE 37571, International Thermal Operations and Heavy Oil Symposium, Bakersfield, Feb. 10-12, 1997.

Kimber, K., S.M. Farouq Ali, S.M. and V.R. Puttagunta: "Verification of Scaling Approaches for Steam Injection Experiments", CIM 88-39-17, 39th Annual Technical Meeting of the Petroleum Society of CIM, Calgary, June 12-16, 1988.

Kimber, K.D., A.R. Deemer, T.H. Luce, and N.H. Sharpe: "A New Analytical Model for Assessing the Role of Steam Production in Mature Steamfloods", SPE 29657, 1995 Western Regional Meeting, Bakersfield, CA. March 8-10, 1995.

Kisman, K.E. and K.C. Yeung: "Numerical Study of the SAGD Process in the Brunt Lake Oil Sand Lease", SPE 30276, 1995 Intl. Heavy Oil Symposium, Calgary, AB, June 19-21.

Kumar, D., H.N. Patel, and E.S. Denbina: "Use of a Gravity Override Model of Steamflooding at Cold Lake", in *Canadian Heavy Oil Association Reservoir Handbook*, 1986, pp. 139-47.

Lauwerier, H.A.: "The Transport of Heat in an Oil Layer Caused by the Injection of Hot Fluid", Applied Science Research A, 1955, pp. 145-50.

Liebe, R.H. and R.M. Butler: "A Study of the Use of Vertical Steam Injectors in the Steam-Assisted Gravity Drainage Process", CIM 91-32, 1991 CIM Annual Technical Meeting, Banff, Alberta, April 21-24.

Luft, H.B., P.J. Pelensky, and G. Williams: "Thermal Performance of Insulated Concentric Coiled Tubing (ICCT) for Continuous Steam Injection in Heavy Oil Production", SPE 37534, 1997 SPE International Thermal Operations and Heavy Oil Symposium, Bakersfield, California, Feb. 10-12, 1997.

Mandl, G. and C.W. Volek: "Heat and Mass Transport in Steam Drive", Society of Petroleum Engineers Journal, March 1969, pp. 59-79.

Marx, J.W. and R.H. Langenheim: "Reservoir Heating by Hot Fluid Injection", Petroleum Transactions, AIME Volume 216, 1959, pp. 312-315.

Matthews, C.S.: "Steamflooding", *Jour. of Pet. Tech.*, March 1983, pp. 465-71.

Matthias, R.C.M., Q. Doan, S.M. Farouq Ali, and A.E. George: "Scale up of Horizontal Wells for Steamflooding a Bottom Water Reservoir", CIM 92-59, CIM Annual Technical Conference in Calgary, June 7-10, 1992.

Mendoza, H.A., J.J. Finol and R.M. Butler: "SAGD, Pilot Test in Venezuela", SPE 53687, 1999 SPE Latin American and Caribbean Petroleum Engineering Conference, Caracas, Venezuela, April 21-23, 1999.

Miller, M.A and W.K. Leung: "A Simple Gravity Override Model of Steamdrive", SPE 14241, 60th Annual Technical Conference, Las Vegas, September 22-25, 1985.

Mohammadi, S.S. and T.J. McCallum: "Steam-Foam Pilot Project in Guadalupe Field, California", *SPE Reservoir Engineering*, February 1989, pp. 17-23.

Moughamian, J.M., P.T. Woo, B.A. Dakessian, and J.G. Fitzgerald: "Simulation and Design of Steam Drive in a Vertical Reservoir", *Jour. of Pet. Tech.*, July 1982, pp. 1546-54.

Myhill, N.A. and G.L. Stegemeier: "Steam Drive Correlation and Prediction", *Jour. of Pet. Tech.*, February 1979, pp. 173-182.

Nikko, H. and P.J.P.M. Troost: "Experimental Investigation of the Steam-Soak Process in a Depletion-type Reservoir", *Jour. of Pet. Tech.*, August 1971, pp. 1006-14.

Neuman, C.H.: "A Gravity Override Model of Steamflood", *Jour. of Pet. Tech.*, January 1985, pp.163-169.

Neuman, C.H.: "A Mathematical Model of the Steam Drive Process – Applications", SPE 4757, 1975 SPE California Regional Meeting, Ventura, April 2-4, 1975.

O' Rourke, J.C., A.G. Begley, H.A. Boyle, C.T. Yee, J.I. Chambers, and R.W. Luhning: "UTF Project Status Update", *Jour. of Can. Pet. Tech.*, September 1999, pp. 44-53.

Oballa, V. and W.L. Buchanan: "Single Horizontal Well in Thermal Recovery Processes", SPE 37115, 1996 SPE International Conference on Horizontal Well Technology, Calgary, Canada, Nov. 18-20, 1996.

Ozisik, M.N., 1980: Heat Conduction, John Wiley and Sons Pub. Co., 1980.

Palmgren, C.T.S., J. Bruining, H.J. de Haan, H.J., F. Guemrah, and E.N. Biezen: "Water of Condensation and the Steam Condensation Front During Steam drive", Proc. of the 1991 European Symposium on Improved Oil Recovery, Stavanger, Norway, May 21 -23, 1991, pp. 863-872.

Palmgren, C.T.S. and J. Bruining: "An Interface Model To predict Vertical Sweep During Steamdrive", SPE 24077, 1992 Western Regional Meeting, Bakersfield, CA, March 30- April 1, 1992.

Patankar, S.V.: Numerical Heat Transfer and Fluid Flow, Hemisphere Pub. Co., Washington D.C., 1980.

Peake, W.T.: "Steamflood Material Balance Applications", *SPE Reservoir Engineering*, August 1989, pp. 357-362.

Prats, M.: Thermal Recovery, SPE Monograph 7, Society of Petroleum Engineers, 1982.

Pujol, L. and T.C. Boberg: "Scaling Accuracy of Laboratory Steam Flooding Model", SPE 4191, California Regional Meeting of the SPE, Bakersfield, November 8-10, 1972.

Reis, J.C.: "A Steam Assisted Gravity Drainage Model for Tar Sands: Radial Geometry", *Jour. of Can. Pet. Tech.*, 1993, 32, No.8, pp. 43-48.

Reis, J.C.: "A Steam-Assisted Gravity Drainage Model for Tar Sands: Linear Geometry", *Jour. of Can. Pet. Tech.*, 1992, 31, No.10, pp. 14-20.

Rial, R.M.: "3D Thermal Simulation Using a Horizontal Wellbore for Steamflooding", SPE 13076, 59th Annual Technical Conference and Exhibition of the Society of Petroleum Engineers, Houston, Texas, September 16-19, 1984.

Rubinstein, L.I.: The Stefan Problem, Trans. of Mathematical Monographs, Vol. 27, American Mathematical Society, 1971.

Sasaki, K., S. Akibayashi, N. Yazawa, Q. Doan, and S.M. Farouq Ali: "Numerical and Experimental Modelling of the SAGD Process", paper 99-21, 1999 CSPG and Petroleum Society Joint Convention, Calgary, Alberta, Canada, June 14-18, 1999. {accepted for publication in *Jour. of Can. Pet. Tech.*}

Sasaki, K., S. Akibayashi, N. Yazawa, Q. Doan, and S.M. Farouq Ali: "Experimental Modelling of the SAGD Process – Enhancing SAGD Performance with Periodic Stimulation of the Horizontal Producer", SPE 56544, 1999th Annual Technical Conference and Exhibition of the SPE, Houston, October 3-6, 1999. {accepted for publication in *Society of Petroleum Engineers Journal*}

Schild, A.: "A Theory for the Effect of Heating Oil-Producing Wells", Trans., AIME 1957, pp. 1-10.

Settary, A., P.R. Kry, and C.T. Yee: "Coupling of Fluid Flow and Soil Behaviour to Model Injection into Unconsolidated Oil Sands", paper 88-39-72, 39th Annual Technical Meeting of Petroleum Society of CIM, June 12-16, 1988.

Singhal, A.K., S.K. Das, S.M. Leggitt, M. Kasraie, and Y. Ito: "Screening of Reservoirs for Exploitation by Application of Steam Assisted Gravity Drainage/VAPEX Processes", SPE 37144, SPE Intl. Conference on Horizontal Well Technology, Calgary, Canada, Nov. 18-20, 1996.

Soni, Y. and R.A. Harman: "Simulation of Saner Ranch Fracture-Assisted Steamflood Technology", *Jour. of Can. Pet. Tech.*, January 1986, pp. 57-70.

Siu, A., L.X. Nghiem, S.D. Gittins, B.I. Nzekwu, and D.A. Redford: "Modelling Steam-Assisted Gravity Drainage Process in the UTF Pilot Project", SPE 22895, 66th Annual Technical Conference and Exhibition of the SPE, Dallas, October 6-9, 1991.

Stegemejer, G.L., D.D. Laumbach, D.D. and C.W. Volek: "Representing Steam Process with Vacuum Models", Society of Petroleum Engineering Journal, June 1980, pp. 151-174.

Sugianto, S. and R.M. Butler: "The Production of Conventional Heavy Oil Reservoirs with Bottom Water Using Steam Assisted Gravity Drainage", *Jour. of Canadian Pet. Tech.* March-April 1990, pp. 78-86.

Towson, D.E. and T.C. Boberg: "Gravity Drainage in Thermally Stimulated Wells", *Jour. of Can. Pet. Tech.*, 1967, 6, No.4, pp. 1-6.

Traverse, E.F., A.D. Deibert, and A.J. Sustek: "San Ardo – A Case History of a Successful Steamflood", SPE 11737, California Regional Meeting of the SPE, 1983.

van Lookeren, J.: "Calculation Methods for Linear and Radial Steam Flow in Oil Reservoirs", *Society of Petroleum Engineers Journal*, June 1983, pp. 427-39.

Vogel, J.H.: "Simplified Heat Calculations for Steamfloods", *Jour. of Pet. Tech.*, July 1984, pp. 1127-36.

Vogel, J.V.: "Gravity Drainage Vital Factor for Understanding Steam Floods", Oil and Gas Journal, Nov. 30 1992, pp. 42-47.

Yortsos, Y.C.: "A Theoretical Analysis of Vertical Flow Equilibrium", SPE 22612, Annual Technical Conference and Exhibition, Dallas, TX, Oct. 6-9, 1991.

Zhou, G., R. Zhang, D. Shen, and H. Pu: "Horizontal Well Application in High Viscous Oil Reservoir", SPE 30281, 1995 International Heavy Oil Symposium, Calgary, June 19-21, 1995.